INFORMATION PROTÉGÉE

[illegible]
April 29/92
AUTH[illegible]

ACTIVITÉS DE RECHERCHE ET DÉVELOPPEMENT DANS LA LIXIVIATION SOUTERRAINE ET IN-SITU DU CUIVRE ET DU MANGANÈSE

G. Deschênes
Laboratoire de Métallurgie Extractive

mars 1991

This document is an unedited interim report prepared primarily for discussion and internal reporting purposes. It does not represent a final expression of the opinion of the Canada Centre for Mineral and Energy Technology (CANMET)

Ce document est un rapport provisoire non révisé et rédigé principalement pour fin de discussion et de documentation interne. Il ne représente aucunement l'expression définitive de l'opinion du Centre canadien de la technologie des minéraux et de l'énergie (CANMET)

Projet: 30.52.99

Recouvrement des coûts

CONFIDENTIEL

Numéro de dossier: 50144
La lixiviation souterraine de l'or par la thiourée

LABORATOIRES DES SCIENCES MINÉRALES
RAPPORT DE DIVISION LSM 91-10 (RC)
105pp

MICROMEDIA

92-04589/

INFORMATION PROTÉGÉE

ACTIVITÉS DE RECHERCHE ET DÉVELOPPEMENT DANS LA LIXIVIATION SOUTERRAINE ET IN-SITU DU CUIVRE ET DU MANGANÈSE

par

G. Deschênes[1]

RÉSUMÉ

Ce rapport discute des principaux résultats des travaux de recherche et développement sur la lixiviation souterraine (in-site) du cuivre, sur la lixiviation in-situ du cuivre et sur la lixiviation in-situ du manganèse. Ces travaux ont été présentés dans le cadre de la Conférence Annuelle de SME de 1991.

De plus, les principales conférences reliées à la technologie de l'extraction de l'or sont également commentées.

Mots-clés: Lixiviation, souterraine, in-situ, cuivre, manganèse, or.

---

[1] Hydrométallurgiste

TRANSLATION
FROM FRENCH

i PROTECTED INFORMATION

RESEARCH AND DEVELOPMENT ACTIVITIES RELATING TO UNDERGROUND AND IN-SITU LEACHING OF COPPER AND MANGANESE

by

G Deschênes[1]

SUMMARY

This report discusses the principal results of research and development work on underground (in-situ) leaching of copper, in-situ leaching of copper and in-situ leaching of manganese. This work was presented as part of the 1991 annual SME* conference.

The principal papers on gold extraction technology are also commented on.

Key words: Leaching, underground, in-situ, copper, manganese, gold

---

* English term to be verified - Tr.

---

[1] Hydrometallurgist

1) INTRODUCTION

Le Congrès Annuel de la Société d'Ingénierie Minière, Métallurgique et d'Exploration (Society of Mining, Metallury, and Exploration Engineers) a eu lieu du 25 au 28 février 1991. Le programme de cette réunion était très élaboré.

Des symposiums sur: la gérance de l'environnement, l'évaluation et l'optimisation de la performance métallurgique et les opérateurs d'usines ont été organisés dans le cadre de cet événement. Parmi les nombreuses sessions incluses nous retrouvons: l'exploitation minière hydrologique, la géologie des métaux précieux, la géologie du cuivre, l'exploitation minière de surface, l'environnement, l'optimisation métallurgique, le traitement métallurgique lunaire, la minéralurgie appliquée, la pyrométallurgie, la flottation, les techniques géochimiques, la ventitation minière, la géomécanique des mines de charbon, la conception et pratique des nouvelles usines d'or, le contrôle avancé et les applications d'ordinateurs, la lixiviation en tas, la flocculation et la filtration, l'exploitation des mines de charbon, la biolixiviation, le traitement des résidus, le broyage et le concassage, l'automatisation, l'hydrométallurgie, l'électrochimie, la séparation gravimétrique, la géologie du diamant et des métaux spéciaux et l'entreposage des résidus nucléaires.

Ce congrès a mis un accent particulier sur l'exploitation in-situ qui est considérée comme une technologie de pointe, en croissance. En effet, un cours et deux sessions ont été préparés sur ce sujet. De plus quelques conférences en minéralurgie appliquée étaient aussi reliées à ce thème.

Les lixiviation in-situ et in-site possèdent certaines analogies par rapport à notre projet coopératif auquel participent LSM et la division Est Malartic de Minerais Lac. Ce projet concerne la lixiviation souterraine de l'or par la thiourée. Cette raison a incité ma participation à ce congrès pour connaître les derniers développements sur le sujet et évaluer leur incidence sur notre projet. De plus, le présent rapport contient des commentaires sur les conférences reliées à l'exploitation métallurgique de l'or, à titre d'information complémentaire.

La compagnie Codelco du Chili, le Bureau Américain des Mines, la Casa Grande de Cyprus Corporation et l'université d'Arizona sont les organisations impliquées dans le développement du domaine de la lixiviation in-situ.

Les pages suivantes discutent des différents projets rattachés à ces domaines.

2) DISCUSSION

2.1 Lixiviation souterraine (in-site)

Le projet de lixiviation souterraine de la division El Teniente , de la compagnie Codelco du Chili, a été présenté par R.A. Montoya. Ce projet vise à augmenter la production de cuivre de 25000 t/an. Pour se faire le minerai de basse teneur en cuivre (0.8-3 %), composé de 50 % chalcopyrite et de 50 % chalcocyte, sera miné et lixivié dans de grosse colonnes (stopes) de 200 pi de hauteur localisées dans la mine. Le lixiviation sera faite à l'acide sulfurique à un débit de 10 L/h/m^2. La durée de la lixiviation sera de 18 mois et la récupération du cuivre varie de 25 à 70 %. Le volume de solution récupéré est de 95 %. Le cuivre dissout sera réextrait par extraction liquide/liquide. Les essais dans le site de la mine ont été pilotés et correspondent aux résultats obtenus en laboratoire. L'opération industrielle est planifiée pour démarrer en 1993.

D. Borech, du Bureau américain des Mines, a présenté les travaux préliminaires de l'étude de caractérisation de la masse rocheuse dans le but de faire de la lixiviation souterraine en "stope". Cette étude de la masse rocheuse a pour but d'éviter la perte de métal entrainé par la perte de solution dans la roche ou encore d'éviter le problème de contamination du sous-sol par la solution. Cette étude est la pierre d'achoppement de tout projet de lixiviation en "stope". Les différentes techniques géologiques et géophysiques ont été vérifiées sur le champ dans une galerie de cette mine du Nevada et elles s'avèrent efficaces.

2.2 Lixiviation in-situ

Une étude de détermination dynamique des changement de perméabilité, durant la lixiviation in-situ, à la Casa Grande de Cyprus, a été présentée par Y. Zhao de l'université Tucson d'Arizona. La publication est incluse en annexe. Cette étude provient d'une compilation de données de l'opération industrielle. Il est démontré que la perméabilité de la roche exerce une influence majeure sur le contrôle de la solution servant à l'extraction du cuivre. Cette perméabilité est largement dépendante de la distribution et du développement d'ouvertures. Des déformations élastiques et plastiques des fractures se produisent lors de l'injection sous pression de la solution. Il est donc important de prévenir des pressions excessives qui créent de la canalisation. Cette canalisation détériore le rendement de lixiviation en compromettant la perméabilité.

J.R. Williams, de l'université d'Arizona a discuté des changements de microstructure lors de la lixiviation de minerais de cuivre. Les essais ont été faits en laboratoire sur des blocs (2x2 po) et sur des diques de minerais. L'examen, avec le microscope électronique à balayage, des échantillons lixiviés et non-lixiviés montrent que la lixiviation produit des ouvertures et des fractures dans le solide. De plus, les débit permissibles augmentent au fur et à mesure que la lixiviation progresse; le tout étant causé par la dissolution des minéraux solubles.

Ces changements de structure ont été caractérisés plus en détails par le travail de N.R. Sainath, de l'université d'Arizona, qui a étudié la perméabilité de ces minerais de cuivre lixiviés (rapport en annexe). La perméabilité et la porosité du minerai ont été évaluées en fonction du temps de la lixiviation du cuivre avec une solution d'acide sulfurique diluée. Il apparait que la perméabilité augmente à mesure que la lixiviation progresse; à cause de la dissolution des minéraux de cuivre le long des fractures qui s'élargissent progressivement. La porosité s'accroit également. Elle augmente lentement au départ puis plus rapidement par la suite. Ceci est également relié à la dissolution des minéraux. Toutefois, le taux de dissolution du cuivre qui est initialement élevé diminue avec la progression de la lixiviation.

M.J. Friedel, du Bureau américain des Mines, a discuté de l'effet de non-saturation sur l'hydrologie de la lixiviation du minerai de la Casa Grande. L'étude a été faite par diffusion du mercure. L'évaluation de la minéralogie, de la texture et l'évaluation de la distribution des pores sont également considérés. Les résultats de l'étude ont été modélisés (rétention d'eau, porosité). Les conditions de non-saturation (~95 % saturation) sont le facteur dominant le contrôle de l'écoulement de la solution (par les microfractures). La modélisation a démontré que la pénétration de la solution peut être réalisée, malgré la faible perméabilité associée aux conditions de non-saturation si les pressions et la durée sont suffisantes. L'injection de la solution, à une pression de 1500 psi, et l'opération de récupération de la solution par succion, contrairement à la pression naturelle qui est la pratique conventionnelle, s'avèrent être les conditions optimales pour récupérer 95 % de la solution (rapport en annexe).

Une évaluation des facteurs affectant la mesure de la solution, lors de la lixiviation in-situ du cuivre de la Casa Grande dans des condition de non-saturation, a été discutée par P.M. Jones du Bureau américain des Mines. L'étude a porté sur une période de 18 moins. Les mesures ont indiqué que seulement 24 % des pores de la zone géologique étaient saturées. Il a été conclu que la formation géologique ne laisse pas échapper de solution de lixiviation et que la différence entre le volume total de solution injectée et le volume récupéré résidait dans la solution résiduelle qui se déplace dans les fractures rocheuses.

D.C. Marozas, du Bureau américain des Mines, travaille sur l'élaboration d'une technique de lixiviation in-situ d'un minerai de manganèse avec le SO_2. L'étude a évalué: les mécanismes en cours lors de la lixiviation, la pétrologie (connaître la distribution du Mn et l'efficacité de la lixiviation), les charactéristiques de la formation géologique et les différents scénarios de lixiviation du Mn. Les essais de lixiviation ont été faits sur du matériel 3/4" + 1/2" dans des colonnes de 2 pi de haut. La récupération du Mn est de l'ordre de 97 % et elle est sélective (seulement 3 % Fe dissout). Le pH de la solution doit être maintenu en deçà de 2.5 pour que l'opération soit efficace. Par la suite, les essais de lixiviation ont été faits en traitant 4 colonnes en série et en mesurant le Mn dissout, le pH et

le potentiel rédox. Les résultats serviront à élaborer l'ingénierie de la lixiviation in-situ du Mn. (Le rapport est inclus en annexe).

En laboratoire, des essais de dynamitage de blocks de granite afin d'évaluer leur effet sur la perméabilité pour la lixiviation in-situ, ont été présentés par S.A. Rholl du Bureau Américain des Mines. Il a été démontré que de fortes charges d'explosif génèrent de nombreuses fractures radiales. La contrainte créée in-situ influence la densité de fractures et la distribution totale de ces fissures. L'étude conclue qu'un réseau de dynamitage avec des trous de 0.25 m, localisés à 12 m de distance, sont suffisants pour créer une modification de fracturation d'un dépôt de lixiviation in-situ jusqu'à 305 m de profondeur.

2.3 Commentaires généraux

La lixiviation souterraine (in-site) et la lixiviation in-situ sont des technologies de pointe, en voie de développement. Beaucoup de travaux sont en cours aux Etats-Unis pour améliorer l'exploitation in-situ du cuivre. Ces travaux sont principalement reliés à la Casa Grande de la compagnie Cyprus. De plus, des études sont en course pour développer l'exploitation de manganèse. Les résultats des études sur la fragmentation rocheuse par dynamitage, la perméabilité et la porosité, la rétention de solution et la dynamique de lixiviation dans des conditions de non-saturation fournissent des informations pertinantes à notre projet de lixiviation souterraine de l'or par la thiourée.

Dans un autre ordre d'idée, la lixiviation souterraine du cuivre est également à l'étude aux Etats-Unis et au Chili. Dans ce cas, les travaux ont atteint l'échelle de pilotage dans la mine. Cette technique est également appelée "lixiviation en stope". Elle est industriellement utilisée au Canada, à la Mine Denison, pour l'extraction de l'uranium.

La lixiviation pratiquée en stope, est un concept qui pourrait être appliqué à notre projet. Des travaux de la division El Teniente, du Chili, peuvent être tirées certaines analogies pertinantes. Le rapport de cette conférence n'était toutefois pas disponible. Les paramètres utilisés (granulométrie du minerai traité, composition du lixiviant) ne sont actuellement pas connus.

L'exploitation in-site ou in-situ des métaux précieux (Au, Ag) n'est pas pratiquéee industriellement; d'où la nécessité d'investir des efforts considérables au développement de ce concept.

Le projet de lixiviation souterraine de l'or du gisement Bousquet V, par la thiourée est actuellement à l'étape d'élaboration des paramètres de lixiviation. Ces travaux constituent l'étude de pré-faisabilité du circuit métallurgique. Advenant que le projet se poursuive, il sera nécessaire de réaliser les étapes suivantes:

- le choix du site
- une étude de pré-faisabilité des opérations souterraines
- une étude environnementale et
- une évaluation d'ensemble et une analyse de sensibilité

L'expérience acquise à Denison Mine peut également être mise à profit par un échange d'information. CANMET a participé à l'élaboration de ce concept de lixiviation souterraine utilisé par Denison.

3) TECHNOLOGIE DU TRAITEMENT DE L'OR

P.C. van Aswegen, de General Mining Metals and Minerals, d'Afrique du Sud a discuté des développements et des innovations de la lixiviation biologique des minerais d'or réfractaires. C'est en 1984 que cette compagnie a démarré des essais à l'échelle pilote (750 kg/J) pour le traitement par oxydation biologique d'une minerai d'or réfractaire de Fairview Mine (pyrite et arsénopyrite). Le circuit de traitement comprend les étapes de flottation, rebroyage, biolixiviation, épaississage, cyanuration de la sousverse de l'épaississeur, CEP élution du charbon et électrolyse de l'éluat. La récupération de l'or est de l'ordre de 97 %. La compagnie a construit une usine traitant 10 t/J de concentré d'or. Les efforts ont permi d'obtenir une meilleure performance. Les travaux d'amélioration du procédé de biolixiviation ont eu diverses répercussions: 1) une réduction du rapport S/L de 8:1 à 4:1; 2) une diminution du temps de rétention de 10 jours à 3 jours; 3) une augmentation de la température maximale d'oxydation de 40 °C à 45 °C; une diminution de

l'énergie de brassage (apport d'O_2) de 50 %; une diminution de la quantité de nutrients et une diminution de 30 % de la consommation de cyanure. Cette compagnie travaille actuellement à l'installation d'un circuite BIO^R à Sao Bento au Brézil. Cette technique va permettre d'augmenter le tonnage journalier de minerai d'or traité habituellement par oxydation sous pression et cyanuration. (Rapport en annexe).

R. Ott, de Newmont Gold Co., Nevada, a discuté du fondement d'utilisation du CEL (charbon-en-lixiviation). L'expérience de Newmont sur leurs usines #2 et #4 a montré qu'il devient avantageux d'utiliser le CEL, au détriment du CEP (charbon-en-pulpe) dans des conditions de traitement ordinaire. Ceci va à l'encontre de la philosophie classique qui stipule que le CEL doit être utilisé dans le cas où le minerai d'or à un comportement "preg robbing". Les nouvelles raisons de l'utilisation du CEL résident dans une diminution du coût en capital, une augmentation de la récupération de l'or et une diminution de l'inventaire d'or dans le circuit.

Deux conférences sur les opérations d'usines d'or ont été présentées par R.L. Beatty et P.A. Korpi. R.L. Beatty, de Bond Gold Bullfrog, a discuté des différents critères de sélection des tamis utilisés dans les circuits CEL/CEP. Il semble qu'il favorise le tamis NKM. (L'ensemble du contenu de sa conférence peut être retrouvé dans la dernière encyclopédie de Randol.) P.A. Korpi, de Newmont Gold Co., a discuté de l'équipement (loader, convoyeurs, concasseurs et SAG mill) utilisé dans la manutention de leur gisement de Gold Quarry Mining. Il a brièvement discuté des opérations de lixiviation en tas; mentionnant que les gicleurs avaient été remplacés par des tuyaux d'égouttement (drippers) et que le résultat était satisfaisant.

M.B. Schaflner, d'Echo Bay Mineral, a présenté une brève conférence sur l'utilisation de leurs 2 circuits Merrill-Crowe à leur opération de lixiviation en tas de McCoy/Cove. Une important problème d'obturation du circuit a été rencontré. Il s'avère que la cause de cette obturation des filtres réside dans la dissolution de la silice lors de la lixiviation de l'or. Ce problème, qui est soudainement survenu, provient du fait que cette opération a débuté le traitement d'un gisement de surface qui introduit du silicium dans la solution de lixiviation. Étant donné que la solution de lixiviation est recirculée, la concentration de silicum augmente

de 30 ppm jusqu'à 5000 ppm. La solution au problème réside dans le mélangeage du minerai de surface avec le minerai qui vient de la mine souterraine. Le minerai venant de la mine souterraine absorbe le silicium dissout et atténue la dissolution totale de la silice. De plus, Echo Bay va éliminer leur circuit Merrill-Crowe et utiliser du charbon activé.

F. Arslan, de l'université Columbia de New York, a discuté de ces travaux sur les mécanismes d'oxydation des minerais d'or réfractaires avec l'hypochlorite de sodium. L'hypochlorite de sodium est généré électrolytiquement à partir d'une solution de chlorure de sodium 10 % à 40 °C. Les minéraux réfractaires étudiés sont le carbone et la pyrite. La production électrolytique de l'hypochlorite de sodium est plus efficace lorsque le pH est contrôlé (pH 5-8). L'efficacité initiale de courant est de l'ordre de 100 % sur une pulpe à 5 % S/L. Le carbone et la pyrite sont efficacement oxydés. Toutefois la faible densité de pulpe n'est pas représentative d'un système économiquement viable (rapport en annexe).

J.B. Hiskey, de l'université d'Arizona a discuté des résultats de recherche sur l'électrochimie des composés d'or hallogénés (Cl, Br, I). Les cyclovoltagrammes des solutions d'or chlorées, bromées et iodées, à une concentration de 10^{-2}M, indiquent que les courants anodiques d'oxydation sont beaucoup plus grands pour la solution iodée que pour les deux autres solutions. De plus, à une faible concentration de NaI (3×10^{-3}M), deux paliers sont identifiés pour la polarisation; ce qui indique deux étapes d'oxydation du composé iode. Une seule étape d'oxydation du composé iodé est toutefois observée à de plus fortes concentrations. Ce pic d'oxydation est suivie d'une passivation.

Une conférence sur l'échantillonnage du charbon dans un circuit d'or a été présentée par T. Braington de Mine Developement Associates. D'après l'auteur, il est nécessaire de remplir 5 conditions, lors de l'échantillonnage, afin d'obtenir une estimée précise de l'inventaire d'or dans le circuit. Ces conditions sont: 1) l'échantillon prélevé doit avoir la même concentration de charbon que le réservoir, 2) la teneur en or de l'échantillon doit être représentative de la teneur en or du charbon du réservoir, 3) la préparation ne doit pas induire d'erreur, 4) la procédure d'analyse doit être appropriée, et 5) les échantillons doivent être prelevés au temps reflétant correctement la période de production. De plus, la précision de l'échantillonnage dépend de trois facteurs: 1) l'agitation et les caractéristiques de la pulpe

doivent être uniformes, 2) la méthodologie d'échantillonnage ne doit pas perturber l'agitation et 3) le volume d'échantillon doit être représentatif du réservoir. Lors de la préparation d'un échantillon de charbon pour l'analyse de l'or, ce denier doit être pulvérisé dans son entier avant d'être coupé. La précision analytique pour la détermination de l'or chargé sur le charbon est de l'ordre de 2 %. Les erreurs respectives attribuées à l'estimation de la concentration de charbon et à la préparation du charbon sont de 10 % et de 3 % (rapport en annexe). L'erreur analytique pour la détermination de l'or est de l'ordre de 7 %.

4) ANNEXE: RAPPORTS DE LA CONFÉRENCE

SOCIETY FOR MINING, METALLURGY, AND EXPLORATION, INC.

P.O. BOX 625002 • LITTLETON, COLORADO • 80162-5002

PREPRINT NUMBER

91-88

DETERMINATION OF DYNAMIC PERMEABILITY CHANGES DURING IN-SITU LEACHING AT CYPRUS CASA GRANDE OPERATION

Y. Zhao

Y. C. Kim

The University of Arizona
Tucson, Arizona

R. D. Schmidt

U. S. Bureau of Mines
Minneapolis, Minnesota

K. C. Behnke

Cyprus Casa Grande Corporation
Casa Grande, Arizona

For presentation at the 1991 SME Annual Meeting
Denver, Colorado - February 25-28, 1991

Permission is hereby given to publish with appropriate acknowledgments, excerpts or summaries not to exceed one-fourth of the entire text of the paper. Permission to print in more extended form subsequent to publication by the Society must be obtained from the Executive Director of the Society for Mining, Metallurgy, and Exploration, Inc.

If and when this paper is published by the Society for Mining, Metallurgy, and Exploration, Inc., it may embody certain changes made by agreement between the Technical Publications Committee and the author, so that the form in which it appears is not necessarily that in which it may be published later.

These preprints are available for sale. Mail orders to PREPRINTS, Society for Mining, Metallurgy, and Exploration, Inc., P.O. Box 625002, Littleton, Colorado 80162-5002.

PREPRINT AVAILABILITY LIST IS PUBLISHED PERIODICALLY IN MINING ENGINEERING

Abstract

Dynamic permeability is a significant hydrologic condition associated with in-situ leaching at the Cyprus Casa Grande operations. Several factors contribute to changes in the permeability conditions. They are: 1) hydraulically induced fracture development, 2) geochemical changes during leaching in the rock matrix, and 3) changes in the relative degree of saturation of the deposit.

Dynamic permeability conditions were evaluated using available pressure and flow rates from the 58 injection and recovery wells obtained over one year period. A finite element, 2-D hydrologic model called INVERT which is designed to estimate aquifer parameters under transient and steady state flow conditions was used for the investigation. The permeability conditions during 7 different steady state intervals throughout the one year time frame were determined. The results confirm that big changes in permeability occur as a function of time as well as a function of injection pressure condition.

Introduction

The process of in situ leach mining involves geologic, geochemical, hydrologic, geomechanical factors which need to be investigated in designing leaching operations. The permeability of the orebody to be leached is particularly important. The objective of this study is to investigate permeability conditions of the Cyprus Casa Grande mine in order to better understand the hydrologic behavior of the leaching process and to efficiently distribute leaching solution during leach operation. Through the cooperative research agreement between the Department of Mining and Geological Engineering, the University of Arizona, the Cyprus Casa Grande Corporation, and U.S. Bureau of Mines, we obtained all the data collected at the leaching site for over one year leaching operation. Based on the real data, estimations of the permeabilities are performed for seven individual intervals. The method adopted in the study is to solve the hydrologic inverse problem using the INVERT model which has the capability to estimate the hydrologic model parameters based on the known head and flow rate by utilizing the finite element approach and the maximum likelihood theory. The obtained results show the changes in permeability as a function of time as well as a function of injection pressure.

Description of the Cyprus Casa Grande Leaching Site

R. D. Schmidt and others (1990) in their paper entitled "Hydrologic Considerations of Underground In Situ Copper Leaching" gave a very detailed description of the Cyprus Casa Grande Leaching site. Some description of Casa Grande Mine can also be found in the same paper. The reader is referred to that paper for further details.

The deposit is primarily of granitic composition and contains zones of both oxide and sulfide mineralization. The sulfide ore zone is directly beneath the oxide ore zone. The oxide ore zone is overlain by 900 to 1500 feet (274 to 335 m) of Tertiary fanglomerate, a formation of cemented, unmineralized gravels. The oxide ore is intensively fractured, ganodiorite porphyry. Compared to the oxide ore zone, both the overlying fanglomerate and the underlying sulfide ore zone have much lower permeabilities. As a consequence, a 2-D flow condition can be reasonably assumed within the tabular oxide zone which is the focus of in-situ leaching.

Figure 1 shows the locations of the leaching wells along the hanging wall cross section, the 900 and 1100 level drifts, and the 5 panel drift. Figure 1 represents the actual distance of the wells as measured in a "flexible" plane on the hanging wall. A similar foot wall cross section can be made to represent the actual distance of the wells on the "flexible" plane along the foot wall. All the wells are drilled in the "tool crib" drift at angles ranging from 6 to 89 degree from the horizontal, and the wells range in length from 275 to 325 feet (84 to 99 m). As a result, the well locations on the hanging wall and the foot wall differ somewhat. However, the estimated permeabilities based on the hanging wall map and foot wall map are very close. The investigation of this study is done based the well locations of hanging wall as shown in figure 1. In figure 1, the vertical axis represents the actual distance along the hanging wall, and the horizontal axis represents the actual distance along the "tool crib" drift, where the 58 leaching wells were drilled.

A Brief Description of the INVERT Model

The solution of the groundwater flow governed by the diffusion-type equation (or Darcy's law) subject to the initial head condition and the certain boundary flux condition requires a knowledge of the "aquifer parameters" such as permeability, specific storage, sources or sink, and boundary head and boundary flux. Although some aquifer parameters can be measured in the field, such measurements are usually scarce and prone to error. Moreover, the measurements are generally taken on a scale much different from that required for modelling purpose. For a long time, many attempts have been made to determine the aquifer parameters from the field observed heads and flows. Carrera and Neuman (1986a) summarized the evolution of the concepts and development of the solution methods for the hydrologic inverse problem.

The 2-D hydrologic model called INVERT developed by the Department of Hydrology at the University of Arizona has the capability to estimate all the hydrologic model parameters by solving the inverse problem. The INVERT model formulates the hydrologic inverse problem into a nonlinear optimization problem by utilizing the concept of likelihood function. The optimum parameters estimated by the INVERT are taken to be those that maximize the probability with respect to the observed heads and flows. The primary idea of the INVERT model is to estimate the hydrological model parameters based on the available head and flow information by utilizing the finite element approach and the maximum likelihood theory. The detailed discussion of the algorithm of the INVERT model was given by Carrera and Neuman (1986a and b).

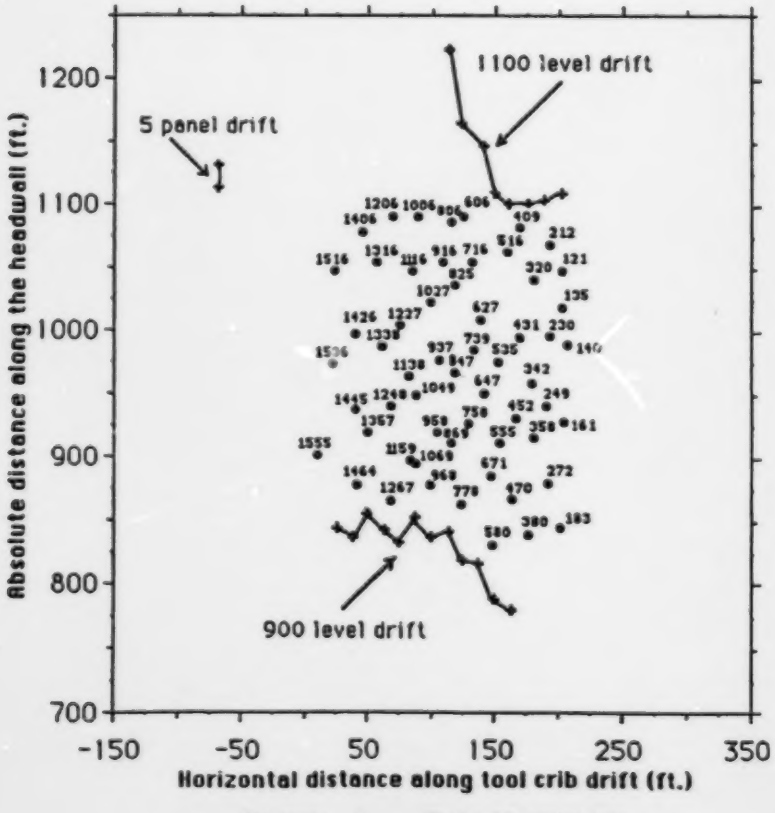

Figure 1. Vell locations

In the INVERT model, the problem is posed in the framework of nonlinear maximum likelihood (ML) estimation by means of minimizing the "log-likelihood" function which includes head measurements as well as prior information about the model parameters. If the true model parameters are designated by $\mathbf{p}$, and their prior estimates (or "measured" values) are designated by $\mathbf{p}^*$, the purpose of the INVERT model is to provide the improved estimates of $\mathbf{p}$, $\hat{\mathbf{p}}$, by relying on the head measurements, $\mathbf{h}^*$, obtained in a set of observation points at discrete time intervals. While the "true" heads at these observation points, $\mathbf{h}$, remain unknown, the inverse solution nevertheless yields a modified estimate of this quantity, $\hat{\mathbf{h}}$.

Since the statistics of the prior errors of both heads and flows are not known or not fully specified in practice, an iteration approach is required to minimize the log-likelihood function. In general, each iteration consists of the following steps:

1. Choose an initial set of parameters. $\mathbf{p}^k$, k=1.
2. Compute the heads, $\mathbf{h}=\mathbf{h}(\mathbf{p}^k)$, by the finite element approach and the value of the log-likelihood function.
3. Compute the updating direction for convergence, $\mathbf{d}^k$, by an appropriate formula.
4. Update the parameter estimates according to

$$\mathbf{p}^{k+1} = \mathbf{p}^k + \mathbf{b}^k\mathbf{d}^k,$$

where $\mathbf{b}^k$ is chosen so as to minimize the log-likelihood function with respect to $\mathbf{b}^k$.

5. If convergence has been achieved, stop; otherwise, set k=k+1 and return to step 2.

For the best results, the initial parameters, $\mathbf{p}^1$, is set equal to the best prior estimates, $\mathbf{p}^*$.

Raw data analysis

During the one year leaching operation, the operating modes of some wells were changed rather frequently from injection to recovery and vice versa. Also, the injection pressure ranged from 350 to 1400 psi. Seven (7) sets of data were extracted where the interval of each set was carefully selected such that, not only the operating mode of all the wells remained unchanged, but also the head conditions and flow rates remained fairly constant within that period. Therefore, each set of the data used for subsequent flow modeling can be reasonably assumed to represent a steady state flow condition. Table 1 gives the days of operation and the average injection pressure for each interval. The injection pressure of each well is obtained by gage pressure at the well collar plus the increment in head due to the solution filled in the well. The flow rate of each well is obtained by dividing the total flow rate of that well by its perforating length. Figure 2 shows the average flow rate for each interval and figure 3 shows the standard deviation of the flow rate.

Table 1. Intervals used in this study

Intervals	Days of operation	Ave. injection pressure (ft)
interval 1	80——90	1962
interval 2	136——139	2019
interval 3	182——187	1593
interval 4	234——249	1613
interval 5	300——307	3042
interval 6	351——355	2804
interval 7	362——366	955

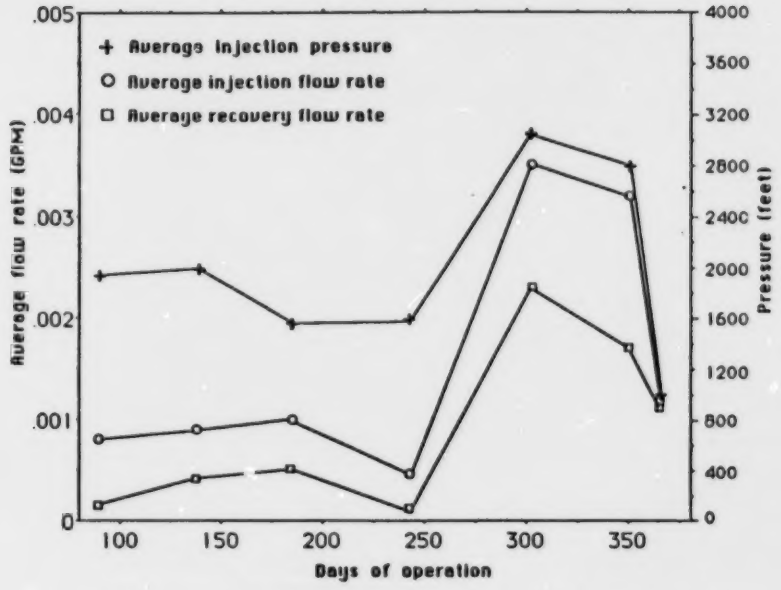

Figure 2. Average flow rates of seven intervals

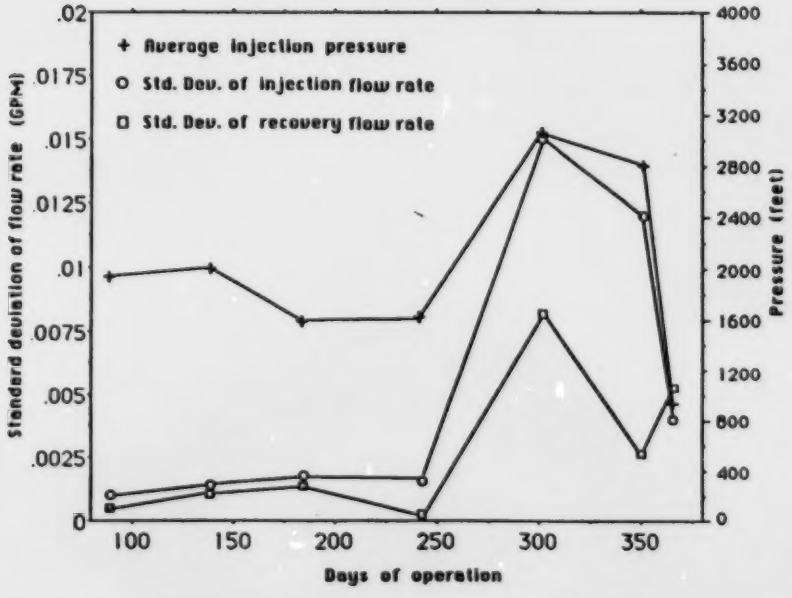

Figure 3. Standard deviation of flow rate

Three phenomena can be seen from figures 2 and 3: (1) flow rate increases dramatically when injection pressure is greater than 2,800 feet (853 m) water column; (2) both average injection and recovery flow rates have an increasing trend; and (3) the standard deviations of the flow rates are proportional to the flow rates themselves, particularly at high injection pressure. All the phenomena observed are reasonable and logical as can be seen from the following analysis.

The first phenomenon is mainly due to the hydrodilation which causes the existing fracture to be opened and/or propagated by high pressure injection of leach solution. When the injection pressure at a well is big enough to overcome the overburden pressure, the fractures intersecting the well may open, resulting an increase in the flow at the well. Since the ore body being leached is located 900 to 1000 feet (274 to 305 m) below the surface and the density of overlying rock mass is 2.7 times as big as that of water, one could expect that the injection pressure applied on the ore body must exceed 2700 feet (822 m) water column in order to overcome the overburden pressure and to open the existing fractures. Intervals 5 and 6 have the injection pressures greater than 2800 feet (853 m) water column, which have the possibility to overcome the total external stress by the fluid pressure. As expected, the flow rates at intervals 5 and 6 are much bigger than those of other intervals. Since the reduction of the injection pressure at interval 7 results in a decline in flow rate, the deformation of fracture due to high injection pressure can still be considered as elastic or partially elastic.

The second phenomenon can be attributed to the following processes which contribute to changes in permeability conditions during leaching: 1) geochemical effects of leaching to remove mineralization; 2) changes in the degree of saturation of the rock mass; and 3) fracture developments caused by weathering process of the leaching effect. The above processes make the overall permeability gradually getting bigger and bigger as leaching operation is going on. For instance, the average injection pressure at interval 7 is smaller than those of intervals 1, 2, 3 and 4, but the average flow rate at interval 7 is still bigger than those of the first four intervals. This phenomenon can be considered as a dynamic behavior of the permeability during leaching.

The third phenomenon can be explained by the fact that the incease in flow rate is more due to a small number of wells which are connected by the fractures instead of the evenly increasing in all the wells, particularly under high injection pressure. Because of the heterogeneities in the ore body, the average permeability is the combination of the intergranular pore network and the fractures. Since the fractures are much more efficient fluid conductors than rock matrix and the change in injection pressure causes a more sensitive response in the fractures than in the rock matrix, the fractures have a dominant influence on the overall permeability. Actually, more than 80 percent of the solution is controlled by less than 20 percent of the wells in all the intervals. Particularly when the injection pressure is big enough to open the existing fractures during intervals 5 and 6, the flow of the leach solution is mainly dominated by the fractures. In interval 5, 80 percent of the injection solution is attributed to only three injection wells (wells 212, 272, and 1049) and 80 percent of the recovery solution is returned by only four (4) recovery wells (wells 409, 671, 758, and 958). A similar result is also observed at interval 6. This clearly shows the fracture dominated behavior of the permeability of the orebody.

Input Data Preparation

Since the INVERT is a finite element program, a representative finite element mesh to the real problem must be prepared before running the program. The finite element layout consists of 147 irregular triangles connected by 227 segments between 86 nodal points as shown in figure 4. Basically, the location of each well is treated as a nodal point except well 1159 since it is very close to well 1069. 12 nodal points are chosen on 900 level drift, 8 nodal points on 1100 level drift and 2 nodal points on 5 panel drift. 7 other nodal points are chosen from the locations 150 feet away (46 m) from the ore body (see figure 4).

The entire area under consideration is divided into three permeability zones (see figure 5). Zone 1 denotes the middle main area of the ore body, which is not disturbed. Zones 2 and 3 are defined in the vicinities of the 900 and 1100 level drifts. The permeability characteristics of zones 2 and 3 may be different from that of zone 1 since these two zones are disturbed due to the following effects: 1) the stresses inside zones 2 and 3 may be relieved in some

degree because of the openings of the 900 and 1100 level drifts, and 2) some fractures may have been developed because of the openings of the drifts.

Although the INVERT program has the capability to estimate all the aquifer parameters such as permeability (or transmissivity), specific storage, boundary head, source and sink, the main interest of this study is only to estimate the average permeabilities for each of the three zones. Just like all other finite element programs, the INVERT program relies on the proper boundary specifications in order to yield the meaningful estimates.

Both head and flow rate information is available at each well, but only one of them, either head or flow rate, can be specified at each node since the LAPLACE equation used by INVERT program can not accept both head boundary and flow boundary at the same time.

Among all nodal points representing the wells, some nodes are subjected to a constant head condition and the others are subjected to a constant flow condition. Figure 6 is an example of the head and flow specifications. The nodes at which the head boundaries are specified should be selected such that they can best approximate the real head contours. The flow rate at the well location (or node) where it is already specified as the constant head condition is shifted to the nearby nodes with the same operating mode (injection or recovery). The constant head equal to atmospheric pressure is specified along the free openings of the 900, 1100 level drifts and the 5 panel drift. The head conditions at the nodes 150 feet (46 m) away from the ore body (see figure 4) are determined recursively by the INVERT program starting with the best guesses until they become stable. However in actuality, the estimates are not sensitive to the head boundaries specified at these nodes of approximately 150 feet (46 m) away from the ore body since they are relatively far away from the major area.

By comparing the total capacity of solution measured from all the injection wells with that measured from all the recovery wells, it is found that between 20 percent to 75 percent injected solution is returned from the recovery wells for the seven data sets used in the study. In other words, 25 percent to 80 percent of the injected solution is "missing". Actually, most of the "missing" solution is known to reach the 900 and 1100 level drifts, which are not measured. Since the INVERT program requires mass balance, the "missing" solution must be specified at the 900 and 1100 level drifts. Based on the best guesses, about 80 percent "missing" solution is assigned to the 900 level drift, and the remaining 20 percent "missing" solution is assigned to 1100 level drift.

Some assumptions are also made in running the INVERT program. These assumptions are:

1. The permeability characteristics of the ore body is isotropic.
2. The domain under consideration is saturated.
3. Steady state flow condition exists in each interval.

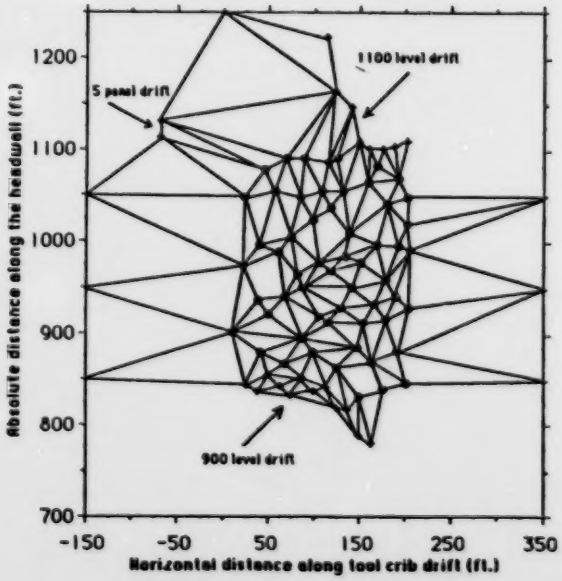

Figure 4. Finite element layout

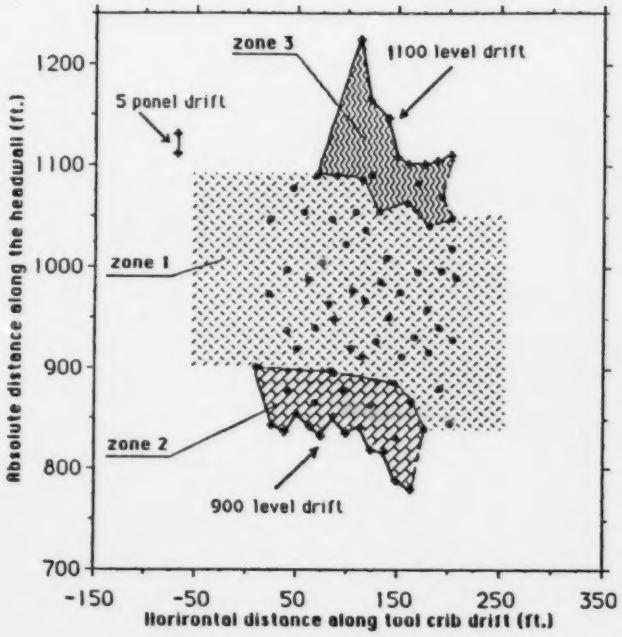

Figure 5. Three transmissivity zones

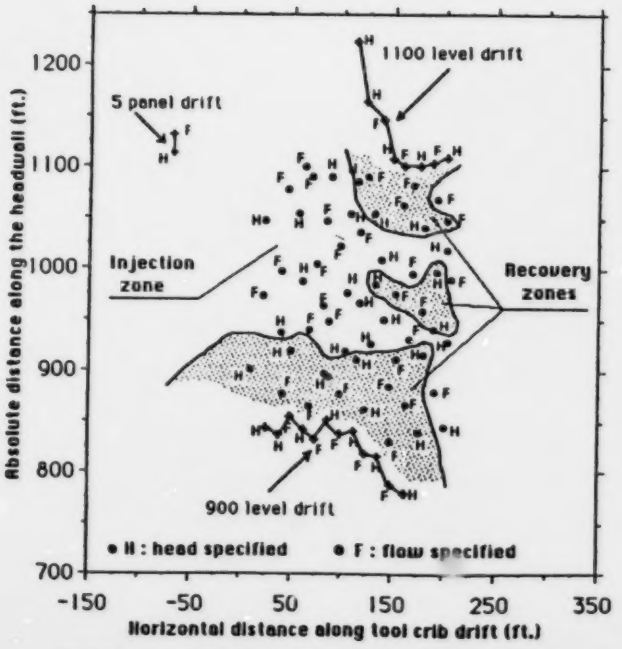

Figure 6. Head and flow boundaries specification

Output Analysis

The solution is sensitive to noise in the input head data as indicated by Carrera and Neuman (1986c). The speed of convergence also depends on the input data. For all the seven (7) cases in this study, the INVERT model converged within 100 iterations. The estimated permeabilities are relatively stable, particularly for zone 1.

Table 2 shows the sensitivity of the estimated permeabilities and the number of iterations with respect to the initial input permeabilities for interval 1 (days of operation 80 to 90). Four (4) runs were made for the sensitivity analysis. As it can be seen from table 2, if the initial input permeabilities are too large, the INVERT model will update them in the trend to make them smaller (see run 1). On the other hand, if the initial permeabilities are too small, the INVERT model will update them in reverse direction to make them larger (see run 3). When the initial inputs are very far off from the values they should be, the number of iterations needed will be very large (see run 1). As expected, when the initial permeabilities are very close to the values they should be, only several iterations are required (see run 4). Although the different permeabilities are obtained from different inputs, the estimated permeabilities are relatively stable. The differences of the input permeabilities are 2 orders of magnitude in the four runs, but the differences of the output permeabilities are still within one-half order of magnitude. In this case, the initial permeabilities of run 4 are considered as the best initial "guess", and the outputs of run 4 are considered as the best estimates of the "true" permeabilities.

From table 2, it can be seen that the estimated permeabilities of zone 1 are more stable than those of zones 2 and 3 with respect to the different initial inputs. In other words, the estimates of zones 2 and 3 are more sensitive to the initial inputs. The similar results are also observed in the estimates of the other 6 intervals. The possible reasons causing the above observations are: 1) Zone 1 has much more finite elements and covers more area than zones 2 and 3; 2) "Missing" solution, which is not exactly measured by gages, is assigned to the 900 and 1100 level drifts which are within zone 2 and zone 3. Consequently, the estimated permeabilities of zone 1 may be more reliable than those of zones 2 and 3.

Table 3 gives the summary of the estimated permeabilities for all the 7 intervals. Figures 7, 8 and 9 graphically show the changes in permeabilities as a function of time as well as a function of injection pressure for zones 1, 2 and 3, respectively. The increase of one and half order of magnitude in permeabilities of all three zones in intervals 5 and 6 are mainly attributed to the high injection pressures at these two intervals. The fact that the permeabilities of interval 7 are about half to one order magnitude larger than those of intervals 1, 2, 3, and 4, although interval 7 has the lowest injection pressure, indicates that the permeabilities have indeed increased due to one year's leaching operation.

Table 2. Sensitivity of the estimated permeabilities and the number of iterations to the initial input permeabilities (unit of permeability is millidarcy)

Number of runs	Zone	Initial Permeability	Estimated Permeability	Number of Iterations
1	zone 1	5.300	0.185	112
	zone 2	5.300	5.261	
	zone 3	5.300	1.058	
2	zone 1	0.530	0.185	35
	zone 2	0.530	1.106	
	zone 3	0.530	1.629	
3	zone 1	0.053	0.161	30
	zone 2	0.053	0.652	
	zone 3	0.053	1.350	
4	zone 1	0.170	0.185	3
	zone 2	1.700	1.720	
	zone 3	1.700	1.642	

Table 3. Estimated permeabilities

Days of operation	Ave. injection pressure (ft)	zone	Permeability (millidarcy)
80 — 90	1962	zone 1	0.188
		zone 2	0.528
		zone 3	1.633
136–139	2019	zone 1	0.357
		zone 2	2.204
		zone 3	1.522
102–107	1593	zone 1	0.220
		zone 2	5.300
		zone 3	5.300
234–249	1613	zone 1	0.271
		zone 2	2.838
		zone 3	2.917
300–307	3042	zone 1	2.711
		zone 2	23.09
		zone 3	30.26
351–355	2004	zone 1	3.741
		zone 2	36.57
		zone 3	24.15
362–366	955	zone 1	1.966
		zone 2	4.296
		zone 3	5.163

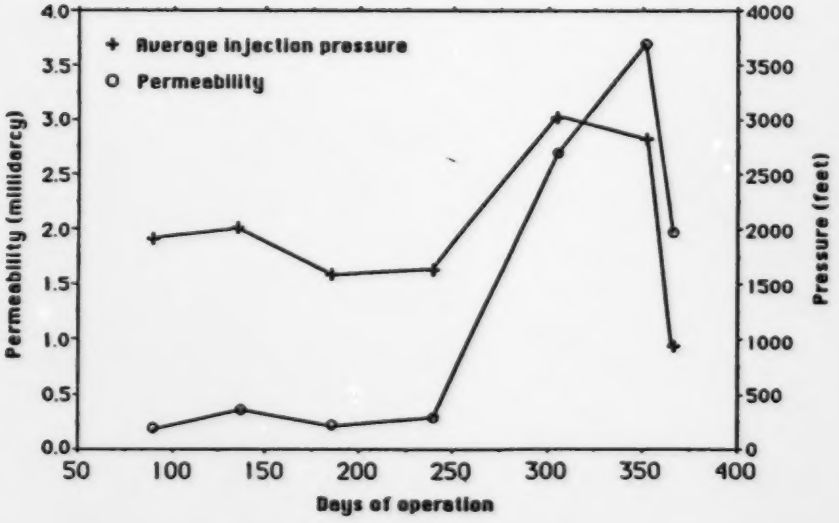

Figure 7. Estimated permeabilities of zone 1

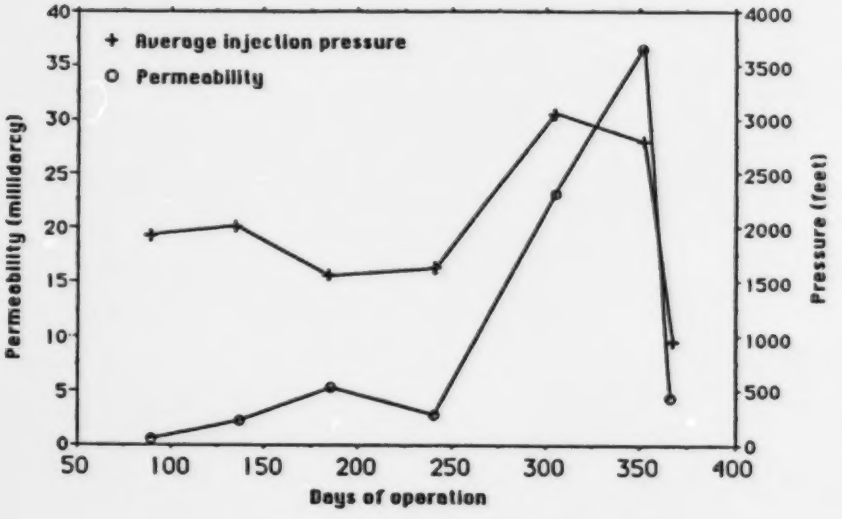

Figure 8. Estimated permeabilities of zone 2

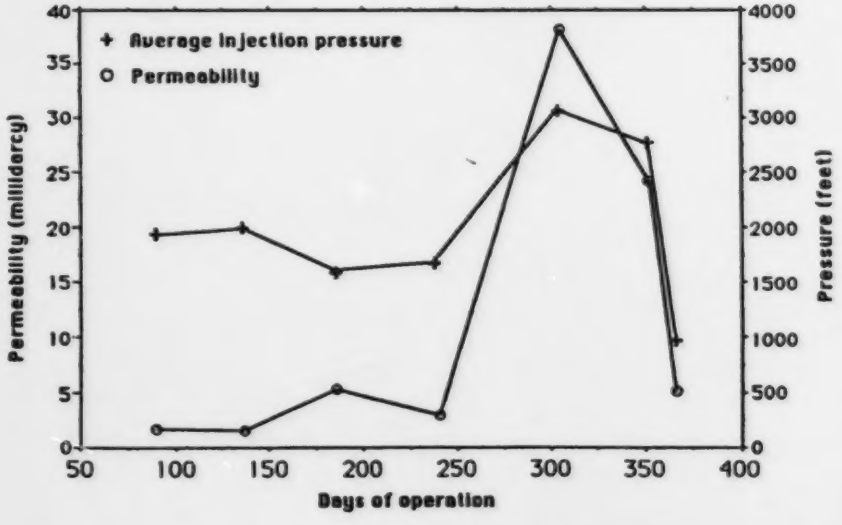

Figure 9. Estimated permeabilities of zone 3

In summary, the permeabilities at the three zones are increased by half to one order of magnitude during the leaching effect of one year period. As long as the injection pressure is not big enough to open the existing fractures (intervals 1, 2, 3, 4, and 7), the changes in permeabilities are slow and gradual. This type of changes may reflect the removal of mineralization in rock matrix by geochemical effect, fracture development by weathering process during leaching, and the changes in the degree of saturation. When the injection pressure is able to open the existing fractures, the changes in permeabilities are immediate and noticeable. In such a case, the increase in flow capacity is mainly due to some channels caused by hydrodilation, which will disappear or shrink when injection pressure is reduced. It must be emphasized that the permeabilities are dominated by the fractures although the estimated average permeabilities are the combination of the rock matrix and fractures.

Conclusion

Permeability exerts a dominant influence on the solution control and distribution concerns. In the copper ore body under investigation, permeability conditions are largely determined by the distribution and development of fracture openings. Elastic or plastic deformation of fractures may occur when injection pressure can overcome the overburden pressure. When fracture openings occur, most of the solution is distributed to a few wells connected by opening fractures. Therefore, the fracture deformation which may cause the channels should be prevented by controlling hydrodilation pressure to not exceed the overburden pressure.

Reference

Carrera, J., and S. P. Neuman, "Estimation of aquifer parameters under transient and steady state conditions, 1, Maximum likelihood method incorporating prior information", Water Resources Research, Vol. 22, No. 2, February 1986.

Carrera, J., and S. P. Neuman, "Estimation of aquifer parameters under transient and steady state conditions, 2, Uniqueness, stability, and solution algorithms", Water Resources Research, Vol. 22, No. 2, February 1986.

Carrera, J., and S. P. Neuman, "Estimation of aquifer parameters under transient and steady state conditions, 3, Application to synthetic and field data", Water Resources Research, Vol. 22, No. 2, February 1986.

Schmidt, R.D., Kermit, C.B., and J.F. Michael, "Hydrologic Considerations of underground in situ copper leaching", A paper presented at the SME annual meeting, Salt Lake City, Utah, February 26 - March 1, 1990.

Acknowledgements

The work described in this paper was partially funded by the Department of Interior's Mineral Institutes program administered by the Bureau of Mines under the allotment grant number G1194104. The authors wish to thank the director of Arizona Mining and Mineral Resources Research Institute, Dr. J. Brent Hisky, for his assistance throughout the duration of the project. The authors are grateful to the management of Cyprus Casa Grande Corporation for allowing us to publish this paper. Profs. Shlomo Neuman and Thomas Maddock III of Hydrology Dept, the University of Arizona are also acknowledged for making the INVERT computer program available for this work.

SOCIETY FOR MINING, METALLURGY, AND EXPLORATION, INC.

P O BOX 625002 • LITTLETON, COLORADO • 80162-5002

PREPRINT NUMBER

91-115

COMPUTERIZED ORE CONTROL PROCEDURES AT CYPRUS COPPERSTONE GOLD CORPORATION

S. Anderson

Cyprus Copperstone Gold Corporation
Parker, Arizona

R. Jerez

Cyprus Minerals Company
Englewood, Colorado

For presentation at the 1991 SME Annual Meeting
Denver, Colorado - February 25-28, 1991

Permission is hereby given to publish with appropriate acknowledgments, excerpts or summaries not to exceed one-fourth of the entire text of the paper. Permission to print in more extended form subsequent to publication by the Society must be obtained from the Executive Director of the Society for Mining, Metallurgy, and Exploration, Inc.

If and when this paper is published by the Society for Mining, Metallurgy, and Exploration, Inc., it may embody certain changes made by agreement between the Technical Publications Committee and the author, so that the form in which it appears is not necessarily that in which it may be published later.

These preprints are available for sale. Mail orders to PREPRINTS, Society for Mining, Metallurgy, and Exploration, Inc., P.O. Box 625002, Littleton, Colorado 80162-5002.

PREPRINT AVAILABILITY LIST IS PUBLISHED PERIODICALLY IN MINING ENGINEERING

Abstract. Advances in inexpensive computer automation led to the development and utilization of a computerized ore control system at Cyprus Copperstone Gold Mine near Parker, Arizona. These new ore control practices improved accuracy, performance, and productivity of the ore control effort.

An automated system for data collection, including bar coding of blast hole samples, laboratory analysis, data management, grade estimation, cut delineation, and ore zone stakeout, plays a major role in ore control practices. This is of particular interest because of the large amount of blast hole information being processed, analyzed, and reported daily.

Introduction

Copperstone Gold management has been, since start-up, progressive towards new efficient methods regarding ore reserve estimation, long term mine planning, short term mine planning, ore control, and surveying. Technological advances including powerful personal computers, applicable mine planning software, and surveying instrumentation have become readily available and affordable.

The computerized ore control procedures used at Copperstone, including sample data collection, laboratory automation and computerized data management, reduced the time to complete ore control on a blast pattern by 50 to 75 percent. The final product--ore control--is generated in a more timely and accurate manner.

This paper describes current ore control methods used at Cyprus Copperstone.

Mine History

The Copperstone Mine is located in La Paz County, Arizona. Copperstone, a wholly owned Cyprus Gold Corporation project, is comprised of federal unpatented mining claims and State of Arizona leases. The project is located in a comparatively flat desert environment at the northern edge of the Dome Mountains within the La Posa Plain. Figure 1 shows the location of the project 18 miles south of Parker, Arizona, and five miles west of U.S. Highway 95.

Cyprus Minerals Corporation acquired 100 percent working interest in 65 original Copperstone claims from local prospectors in 1980. Early exploration by other mining companies focused on the site as a porphyry copper target. Cyprus was the first mining company to recognize the gold potential.

Stripping began in mid 1987 and the carbon-in-pulp ((CIP) mill was commissioned later that fall. The mill has been in continuous operation ever since. Through 1989, 9.1 million BCY of alluvium, 7.9 million BCY of waste rock and 1.2 million BCY of ore have been mined since start-up. The life of mine stripping ratio is 10:1 (waste to ore).

The mining contractor, Morrison-Knudsen, under Cyprus' direction is responsible for all waste and ore mining. Waste rock is mined on twenty foot lifts and ore is mined in ten foot lifts. The ore is delivered to various stockpiles depending upon grade (high grade, leach grade, sub-leach grade).

The pit operates two (2) shifts per day, five (5) days per week. Major mobile mining equipment used at Copperstone includes one (1) Clark 380B tractor, three (3) Caterpillar 992C front-end loaders, one (1) Caterpillar 988B front-end loader, nine (9) Maxi-lights plants, one (1) Caterpillar 16G grader, one (1) Hydra P&H Omega Crane, one (1) Ingersoll Rand DM-25 drill, one (1) Ingersoll Rand DM 45-E drill, thirteen (13) Wabco Haulpak 120B trucks, one (1) International 50 ton truck, and various service, maintenance, and supervisor vehicles.

Current Ore Control Method at Cyprus Copperstone

The primary goal in ore control is to provide timely and accurate information to the mining team as to the location of ore and waste. Processing three to four hundred blast holes per day, the need for data accuracy and limited personnel led to the current computerized ore control procedures.

At Copperstone, the mining contractor designs the waste and ore patterns with guidance from the block model and historic blast hole data on the preceding benches. Ore patterns are drilled on a 13 foot by 13 foot staggered spacing with the waste patterns drilled on a 16 by 16 foot staggered spacing.

After the locations of the blast holes are measured and painted on the ground, the mining contractors' engineering technician numbers the locations of the holes in a logical sequence. These numbers are written on a six inch piece of lath and placed next to the painted drill hole location. This numbering sequence allows for efficient handling of the coordinate information in the ore control process. Copperstone staff receives a hand drawn sketch of the pattern, with the holes partially numbered, from the contractor.

Next, the Copperstone survey crew, consisting of an instrument man and a rodman, survey the corner holes and any odd holes of the pattern. This information is stored in a Lietz SDR-2 electronic field recorder. The SDR-2 is brought back to the engineering office and downloaded to a Compaq Deskpro 386 machine using Mintec's Survey Module.

Prior to the blast holes being drilled, bar codes are printed in the engineering office. Each drill receives a set of bar codes. The information on the bar code includes pattern, hole and interval, i.e., 880-101 10-20 (880 pattern, 101 blast hole, from 10 feet to 20 feet). This information is presented in both bar code (Code 39) and English.

Patterns are drilled in any order by drillers. The driller must locate the correct bar code and place it on a sample tag and drop the tag into a clear plastic sample bag with the blast hole sample. Samples are taken from the drill cuttings with a wedge cutter for each ten foot drilled. As a back-up, the driller writes the pattern, hole and interval information on the sample bag.

Blast hole samples are collected in the pit, brought to Copperstone's assay laboratory, and dropped off by the contractor's blasting crew. The blast hole samples are processed using a first in first out system but occasionally a priority system is used based on the need to

obtain assay information for a specific pattern.

Samples are processed at a normal rate of 125 samples per manshift. At two to three manshifts per day, the engineering office receives 250 to 375 assays per day.

In the laboratory, the samples are split, dried and pulverized. Approximately 400 grams of sample is stored for assay work with the remaining sample being wasted.

The sample preparation personnel uses a hand held laser scanner to record the pattern number, blast hole number and interval value from the bar code.

The scanner data is downloaded to the assay laboratory personal computer with a bar code initiated system. This procedure takes approximately two minutes and is dumped into a file named by the current date, i.e., MMDDYY.BAR. Pulverized samples are prepared for atomic absorption assaying using the standard hot cyanide process.

Next, the assay technician prepares the Perkin Elmer 2380 machine for assaying. The assay program is loaded using a "batch" command and is set up to accept the data from the Perkin Elmer. The file containing the pattern, hole, and interval is brought into the program and once assaying starts, the assay value is merged with the bar code information. Unique editing functions of this program allows the assay technician to reassay a sample while standards and zeros from the Perkin-Elmer are ignored. This file is closed and renamed to MMDDYY.ASY.

The file containing pattern, blast hole, interval, and gold assay is copied to a floppy disc and walked across the yard to the engineering office where the ore control technician takes the assay information and loads it to a menu driven data base.

While the laboratory is processing and assaying the blast hole samples, the ore control technician loads the surveyed pattern information into Mintec's Blast Hole Module interactive Survey Editor for generation of a grid file containing the northings and eastings of all the blast holes in the pattern. Both the Blast Hole Module and Medsystem are mine planning software products of Mintec, Inc., of Tucson, Arizona. This procedure can take 30 seconds to as much as 30 minutes depending on the complexity of the blast pattern and the training of the ore control technician.

Once the blast hole pattern has been plotted and checked against the contractor's hand drawn pattern, the ore grade technician downloads the pattern assay information from the data base. The file containing the sorted pattern assay information is checked for completeness. The assay information and grid information is merged into one file containing pushback, pattern, hole number, northing, easting, bench (elevation), interval (from/to), zone, and gold assay values. It is checked to assure no mistakes occurred in the merging process. The information is plotted and examined.

Depending on the area of the pit and apparent complexity of the ore zone, several blast patterns may be "added" together prior to cutting of the ore zone shapes. Our current revised edition of Mintec's Blast Hole Module will accommodate 1300 blast holes or five to six blast hole patterns.

The merged file is processed through a routine to generate another file to load into the Mintec's InterGraphics Planner Average program (IGPAVG) of the Blast Hole Module. The cut zones from surrounding, already cut, patterns are added to the screen to show trends and exact locations of other ore zones. The IGPAVG allows for an infinite number of trial cuts to be examined. Once the "correct" zone has been cut, it is selected and saved. Grade estimation of these zones is based on an arithmetic average of the blast hole assay values in the outlined or cut area.

The ore control technician plots the cut shapes. He then renumbers the plot and changes the SDR-2 file and plot file to allow for the ore to be staked-out more efficiently. Renumbering of the survey stake-out points is completed to accommodate the needs of the survey crew as several duplicate points are deleted.

Cut shapes are replotted and loaded into the SDR-2 for stake-out. The plot of the zones is photocopied and color coded and delivered to the contractor, loader operators, mine geologist, mine engineer, and to a permanent storage file. The color coding of the cut zones on the photocopy matches what is in the pit, i.e., blue represents ore while red and yellow represent leach and sub-leach.

Surveying at Copperstone Gold Mine is accomplished with a Leitz total station, a Leitz SDR-2 electronic field notebook and Mintec's Medsystem survey software, and a survey crew consisting of an instrument man and a rod man. This crew is capable of keeping up with the rigors of surveying patterns and progress, staking out ore zones, toes and crests, bench marks, and control points, and other work for exploration and development drilling projects.

The survey information is tagged to allow for ease of use by the surveyor in the field or by the mining engineer/ore control technician in the office.

Development of Computerized Ore Control Procedures at Copperstone

The old ore control system consisted of the following:

1. Contractor designs, places, and drills the blast pattern; delivers a hand drawn sketch of the pattern to Cyprus.
2. Cyprus processes and assays blast hole samples.
3. The ore control technician hand plots blast hole locations and grade (represented by colored shapes) on level maps.
4. Ore control technician examines possible ore zones.
5. Ore zone shape is finalized.
6. Average grade and bank cubic yards are hand calculated and recorded by the ore control technician by looking up and averaging the blast hole assays in the zone from the daily assay reports received from the laboratory.
7. Ore control technician digitizes the zones and loads them into the SDR-2.
8. Surveyors stake-out the ore.

Assaying to stake-out would take up to 5 working days. Possible data and information transposition and data entry errors were introduced by the contractor's technician, drillers, sample process technician, assay

technician and the ore control technician.

The major goal in the development of the new ore control system was to pinpoint reconciliation problems between laboratory, mine department and mill, and trace the origin of possible errors, and if possible, minimize the chance of errors on blast hole data entry, bag labeling, or laboratory analysis.

Technology advances were investigated to solve these problems:

1. Large amounts of blast hole samples being processed.
2. Easy to make a mistake at different data entry points.
3. Tedious data entry.
4. Key ore control personnel were involved in data entry.
5. Small staff to handle the overload of blast hole processing and surveying functions.

The second goal in development of the new ore control system was to expedite ore control. The available working faces in the pit area are being reduced as the pit deepens and almost immediate ore control is required after the pattern has been shot.

The first step in development of a computerized ore control system was to establish a rigorous data base system allowing ease of use and accurate data management. The data base chosen for this application was Rbase. Several problems were addressed including backup systems, various editing methods, report styles, data base management, and most of all, ease of use for the ore control technician.

Initially, the ore control technician was assigned the task of data entry of 300 to 400 assays per day; however, this introduced another source of transposition and data entry error.

Next, the most important portion of the ore control system was started--initiation and use of the Mintec's Blast Hole Module. After the software was received, several customized features were added to complement ore control at Copperstone.

Training of the ore grade technician on the Blast Hole Module took about six weeks. While the training occurred, the old method of hand plotting the assay information was maintained. This doubling of the work actually proved beneficial as we were able to check our work and make improvements by modifying the Blast Hole Module. The major improvement with the Blast Hole Module over the old method is recutting the zones to optimize the mineralization going to the various stockpiles.

Later on, the survey crew was trained in the use of the Blast Hole Module because of the close working arrangement of the ore control technician and surveying crew. Quite often, when the ore control technician is busy with other tasks, one of the surveyors assists with ore control in the engineering office.

The first step in the use of Blast Hole Module is to prepare blast hole data by converting blast hole coordinates from SDR-2 format to the standard blast hole/survey point file format. Next, a full grid of blast hole locations using the interactive Survey Editor routine is created followed by merging the blast hole coordinates with the laboratory assays to form the basic information for the pattern. At every step in blast hole preparation, information is either printed or plotted as a check and a reference. This data preparation process can be stopped and started at any point.

The IGPAVG or outline and average program is loaded with the individual blast holes. An arithmetic average of the blast hole assays is used to calculate the grade of each "trial" cut. If the average of all the values in the cut is above the ore cutoff, bank cubic yards and grade are reported in the ore category.

While the Blast Hole Module was being set up and training of the ore control technician continued, the mining contractor was introduced to our ideas for improving ore control: pattern layout, blast hole numbering and possible bar coding of samples.

Using the Rbase data base and Mintec's Blast Hole Module, data entry and plotting errors by the ore control technician were reduced. More important, the technician had the ability to "trial" cut zones before the optimal zone was cut and finalized. Time was saved by the ore control technician using the new system over the old system; more important, the ore control was greatly improved. Still, the largest stumbling block in the computerization of the ore control process is the capture of the large amount of assay data into a form that can be readily dumped into a data base and sorted.

After some research, we decided to use bar codes to capture and track the blast hole information from the pit through our assay laboratory to the engineering office.

Preprinted bar code samples from different vendors were examined. Concern for the bar code readability due to the bar code being in the sample drying oven (225 degrees Fahrenheit) from 1 to 24 hours. Several oven tests were completed on bar code samples obtained from different vendors. We even tested "thermo-transfer" type bar codes. Readability of the bar code under the worst possible condition was maintained.

Several vendors were contacted concerning possible purchase of pre-printed bar codes. Cost and the inability to have site specific bar code information on the bar code led to examination of in-house printing or generation of the bar codes. The features we wanted for bar code software include: ease of use, relatively inexpensive, menu driven, print on any media, print with dot matrix printer and capability of printing Code 39. Code 39 printing logic would be the most useful as it has variable length and supports 44 different characters: 10 digits, 26 letters, 8 graphic symbols.

Several different software packages were examined and EZBarcode II was purchased from Time Keeping Systems of Cleveland, Ohio, at a cost of $149.00. It can prepare a text file with database, spreadsheet, or word processing program and print the data as bar codes on dot matrix or laser printers.

Features of the EZBarcode include: interactive mode, keyboard entry, non-interactive mode (text file), printing from within a batch file or within another program; help commands; printing in Code 39, Interleaved Code 2 of 5 and UPC Version A.

Printing options on the EZBarcode include: number of copies, bar code type, bar code height, distance between, bar code passes, left margin, bar code width, text beneath, quotes in

text file, delimiter character, automatic incrementing or decrementing (can use alphanumeric digits), increment by, increment to, line counter, and new page at.

Use of the bar codes started immediately by the drillers. Originally, the driller placed one bar code on the outside of the plastic sample bag and drop a sample tag with an identical bar code in the bag. This duplicating of the bar codes was to assure the location information of the sample would not be lost. Problems with fine dust on the plastic bag caused the bar code not to stick, so the driller regressed to write the location information on the plastic bag while placing the bar code on a sample tag and dropping it in the sample bag.

No time savings were experienced by the drillers. However, sample duplicates and driller transposition errors were greatly reduced.

Some thought was given to exactly what instrument to use for recording the bar code information. Several devices exist for retrieving data from bar codes and they include plastic wands, metal wands, CCD scanners, and laser scanners.

The device purchased to record bar code information was a laser scanner, model LS-8560, manufactured by Symbol Technologies for $1750. The vendor was Innovative Products of Phoenix, Arizona. Also, a wedge was purchased from Innovative Products for $600. The wedge is used to connect the personal computer to the keyboard and the scanner through the same port.

The scanner has its own internal memory and does not have to be attached to the personal computer or power source when scanning data. The sample process technician uses a bar code initiated command to prepare and start the scanner to accept bar code information. The sample bags are scanned and downloaded to the laboratory personal computer with the bar code initiated command. He/she prints the bar code listing and checks the bar codes to assure all bar codes were scanned and processed properly.

This downloading and checking procedure saves each sample process technician 20 minutes per day over the old system. Again, transposition errors are greatly reduced.

The final step in completing the development of the ore control system was to develop an interface between the Perkin Elmer 2380 and a personal computer. The interface required the installation of a board in the instrument, communication software and some programming. The programming involved was to display on the screen of the personal computer the blast hole information together with the assay value being transferred. Other functions included in the software were editing commands, resampling and reporting capabilities. The assay technician checks the tube number with the sequence number of the bar code to assure proper matching of assays and location. The assay technician prints the assay file off for his records. No time savings were experienced by the assay technician; however, data entry errors were reduced.

Now, with the laboratory assay system operational and a data file containing laboratory assays being generated, data entry by the ore control technician in the engineering office is limited to loading the assay date file to Rbase. This activity saves the ore control technician 2 (two) to 4 (four) hours of work per day and, again, data entry errors were reduced.

Surveying methods and procedures were not changed.

To review the current ore control system used at Copperstone:

1. Contractor designs and paints the blast hole pattern in the pit.
2. Cyprus prints and delivers bar codes containing pattern, hole number and interval to the contractor.
3. The contractor drills the pattern and places the correct bar code in the sample bag with the sample.
4. Cyprus processes the sample.
5. Cyprus sample process personnel scans the pulverized samples and dumps the information to the laboratory personal computer. He/she prints the bar code information and checks to assure no samples were missed.
6. Samples are prepared for assay.
7. Perkin-Elmer 2380 is activated, the assay program loaded, bar code file opened and assaying commences.
8. Laboratory assays are downloaded to a floppy and brought to the engineering office.
9. Ore control technician loads the laboratory assays to Rbase.
10. Grid file, merged file, cut zones, and SDR-2 files are generated with the Blast Hole Module.
11. Surveyors receive the SDR-2 file and stake out the ore.

Conclusions

Computerized ore control methods improved accuracy, performance, and productivity of the ore control team at Copperstone. Data and information reliability increased while time required to complete ore control was decreased.

The technology used in the modernization of the ore control effort at Copperstone existed prior to development of this system. Affordability and ease of use of the technology made the conversion to our new method relatively easy for all involved.

An additional benefit of developing the computerizing ore control system at Copperstone is the integration of short term mine planning and daily ore control. This allows for improved ore grade prediction to the mill and improved scheduling of both waste and ore.

Acknowledgments

The authors would like to thank Cyprus Copperstone Gold Corporation and Cyprus Minerals Company for permission to publish this paper.

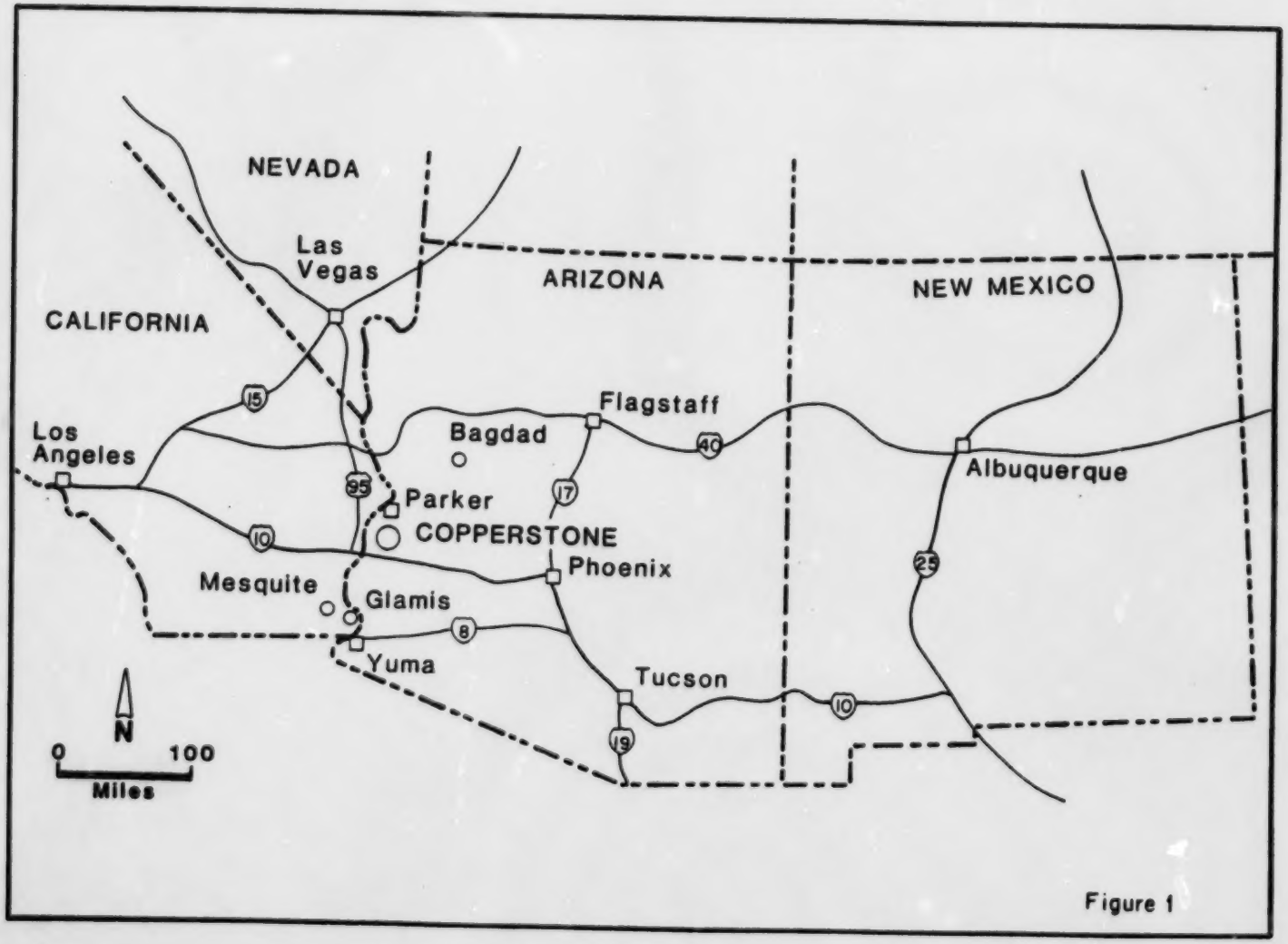
NEVADA
Las Vegas
ARIZONA
NEW MEXICO
CALIFORNIA
15
Flagstaff
Los Angeles
Bagdad
40
Albuquerque
95
17
Parker
COPPERSTONE
10
Phoenix
25
Mesquite
Glamis
8
Yuma
Tucson
10
19
N
0
100
Miles

Figure 1

Enhanced recovery of gold from a refratory sulfidic - carbonaceous ore using bacterial pretreatment and tu extr

J.A. Bierley
R.Y. Wan

Gold'90 Feb 26 - March 1, 1990
Salt Lake City (AIME)

SOCIETY FOR MINING, METALLURGY, AND EXPLORATION, INC.

P.O. BOX 625002 • LITTLETON, COLORADO • 80162-5002

PREPRINT NUMBER

91-58

EFFECT OF LEACHING ON PERMEABILITY OF COPPER ORES

N. R. Sainath

S. Harpalani

University of Arizona
Tucson, Arizona

For presentation at the 1991 SME Annual Meeting
Denver, Colorado - February 25-28, 1991

Permission is hereby given to publish with appropriate acknowledgments, excerpts or summaries not to exceed one-fourth of the entire text of the paper. Permission to print in more extended form subsequent to publication by the Society must be obtained from the Executive Director of the Society for Mining, Metallurgy, and Exploration, Inc.

If and when this paper is published by the Society for Mining, Metallurgy, and Exploration, Inc., it may embody certain changes made by agreement between the Technical Publications Committee and the author, so that the form in which it appears is not necessarily that in which it may be published later.

These preprints are available for sale. Mail orders to PREPRINTS, Society for Mining, Metallurgy, and Exploration, Inc., P.O. Box 625002, Littleton, Colorado 80162-5002.

PREPRINT AVAILABILITY LIST IS PUBLISHED PERIODICALLY IN MINING ENGINEERING

ABSTRACT. This paper discusses the results of a laboratory investigation carried out to study the microscale flow characteristics of copper ores and the variation in flow behavior resulting from flow of leach solution. Fractures in 1.5 and 4 inch diameter cores were mapped by visual inspection. The cores were stressed in a triaxial stress field representative of *in situ* conditions. The permeability of the samples to water was then estimated. The samples were exposed to 20 g/l sulfuric acid and the experiment repeated. The permeability of unleached samples ranges from 10^{-16} to 10^{-19} m^2 and it increases as leaching progresses. The porosity variation and the rate of recovery of copper from the specimen during leaching were also studied.

Introduction

With fluctuating copper prices, the need to develop a low-cost, environmentally sound technology to mine copper is gaining importance. Presently, *in situ* leaching is being looked upon as a viable alternative to conventional methods of copper mining. This technique offers several advantages over conventional mining. The process requires less capital investment (Pugliese, 1989) and the start-up time for production is reduced considerably. The method also eliminates the process of extraction, crushing and milling thereby reducing the production costs. Additional advantage is that miners are not exposed to the hazards of underground mining resulting in fewer health and safety risks. The technique disrupts the environment significantly less than conventional mining as the process only removes the target metals from the ground. Also the site is easily reclaimed to its original condition by treating the groundwater, capping the wells, and dismantling the processing plant.

In spite of these advantages, *in situ* leaching technique has certain drawbacks which make it unattractive to the domestic copper producers. In the past, experimental programs involving *in situ* leach mining were carried out at a number of sites to determine the feasibility of a commercial operation. The results of these tests were not very encouraging. Problems encountered were, and to some extent still are, low rates of leach solution recovery (D'Andrea et al. 1977), low copper content of pregnant leach solution, and containtment of the leach solution within the orebody (Ahlness et al. 1983). The flow of solution in the orebody depends on a number of factors like porosity and permeability of the rock matrix, permeability of the fractures, size and density of the fractures. Most of these factors vary continuously over the life of an orebody depending upon mineral dissolution, precipitation, clay hydration, and physical sedimentation. Knowledge of the trends in the variations of the above factors is essential before any model for flow of leach solution in ore body can be developed.

In order to estimate the variations in porosity, permeability, and the resulting changes in the flow characteristics of copper bearing ore deposit as the mineral is depleted, an experimental investigation is currently underway at the University of Arizona. This paper discusses the experimental work completed so far and a preliminary analysis of the results.

Background

In situ leaching has tremendous potential and seems to be the technology of tomorrow. The process is unique where chemicals are the miners deciding what to take and what to leave behind in the ground. The mechanics of leaching involves flow of a solution through the orebody to dissolve the required mineral and recovery of this solution with dissolved mineral to a collecting system. For copper recovery, oxide ores can be leached using a dilute acid. An oxide copper ore is a rock containing a combination of oxide, carbonate, silicate or sulfate copper minerals that can be dissolved in a short period of time using a weak acid like dilute sulfuric acid (Hardwick, 1967). Copper from sulfide copper minerals cannot be easily dissolved within a short time using dilute acid, thus making *in situ* leaching of sulfide copper minerals difficult. If an oxide deposit contains some pyrite or sulfide minerals, water alone without any sulfuric acid may be used as the leach solution, since pyrite in the presence of oxygen forms sulfuric acid.

A typical *in situ* leaching project involves a system of vertical wells through which the orebody is leached. The solution is forced down the injection wells and the leachant with dissolved metals is recovered through the recovery wells. Extraction of the metal from the leachant and the treatment of the leachant for reuse is done at the processing plant. The effectiveness and the efficiency of an *in situ* leaching system depends on a large number of variables which can be classified into two categories.

1) Chemical solution characteristics, injection pressure, and injection rate, etc
2) Orebody - rock characteristics

The variables in the first category can be easily controlled during the process of leaching. But the orebody characteristics are a function of the *in situ* conditions and cannot be controlled significantly. The variations in the rock characteristics with time, as leaching progresses need to be studied in detail and the results incorporated in modeling the flow behavior within the orebody in order to predict long-term production rates.

Laboratory core leaching experiments on granodiorite porphyry that contained chrysocolla and quartz monzonite containing atacamite copper mineral were carried out in the past (Paulson and Kuhlman, 1989; Cook, 1987) to study the copper recovery, acid consumption and permeability changes. In the study, permeability increases during leaching ranged from 4 to 110 times the initial value in case of granodiorite porphyry and by 100 to 1300 times in case of quartz monzonite ores. In ores where most of the mineralization is along the fractures, permeability increased considerably during the course of leaching.

An actual *in situ* leaching field investigation to carry out flow behavior and modeling studies is being conducted jointly by the Cyprus Casa Grande Corporation and the U.S. Bureau of Mines at Cyprus Casa Grande. The pressure and the flow data from the injection and recovery wells is being used to statistically model the flow of solution in the orebody (Schmidt, et al. 1990). This statistical modeling combines hydrologic modeling with statistical testing using the available pressure and flow data to generate permeability estimates of the orebody.

In the present work being carried out at the University of Arizona, laboratory core leaching experiments are being performed to study the variations in the orebody characteristics during the leaching process. Experimental work of this nature is an inexpensive and easy way to gain qualitative information regarding the changes taking place while leaching an ore deposit, although values of permeability variations obtained from core leaching experiments cannot be easily scaled to apply to the entire orebody, since the field permeability of a particular ore deposit will most certainly be quite different from that measured using core samples. This is due to the impact of large fractures and other preferential flow paths occuring in a deposit. However, correlation of permeability changes during the experiments with data on the fluid chemistry yields information that is useful for determining the potential impact of these mechanisms during actual *in situ* mining in the field.

Experimental Work

Specimen Preparation

For the experimental work, tactite copper ore samples were obtained from the Cyprus Casa Grande Mine in Arizona. Lumps of ore were brought from the mine site. 1.5 and 4 inch diameter cores were prepared using a coring machine. The ends of these specimens were ground parallel using a surface grinder. In accordance with the International society of Rock Mechanics (ISRM) testing procedures (Obert and Duvall, 1967) effort was made to keep the length of the specimen twice the diameter. The length of 1.5 inch diameter samples therefore varied from 3 to 4 inches. The length of the 4 inch samples, however, ranged from 6 to 8 inches due to difficulty in preparing longer specimens. Cylindrical specimens were used instead of powdered samples primarily for two reasons. Firstly, the core leaching experiments simulate the solution/rock interface *in situ* better than the powdered samples; this is particularly important since most of the mineralization in the ore occurs along the fractures and pore spaces. Also, the solution flow along the fractures in core leaching represents more realistically the flow characteristics taking place in the field during leaching. Secondly, core specimens allow for an estimation of the effective porosity and permeability of the samples during the course of leaching. This makes it possible to study the variation of porosity and permeability with time during a leaching operation.

As a part of the initial specimen characterization, fractures on the specimens were mapped on a matt acetate sheet. Most of the copper mineralization occurs along the fractures. This was done by wrapping the matt acetate sheet around the specimen and carefully marking the paths of the fractures on the surface of the specimen. Figure 1 shows the mapped fractures on the surface of one specimen. This figure indicates the approximate nature and extent of fractures on the surface of the specimen used for experimental work. The distribution appears to be quite random. However, since most of the flow in a core specimen is expected to take place along the fractures, it is important to know the extent of the fractures in the specimens. It was found that the permeability of the specimens generally increased with increase in the extent of the fracture network visible on the surface of specimen. But in certain cases, specimens with very few fractures had relatively high permeabilities. This might be due to the large widths of the fractures, or the fracture distribution within the specimen. With continued leaching, most specimens eventually cracked open along these fractures as the copper mineralization along the fractures was dissolved by the acid.

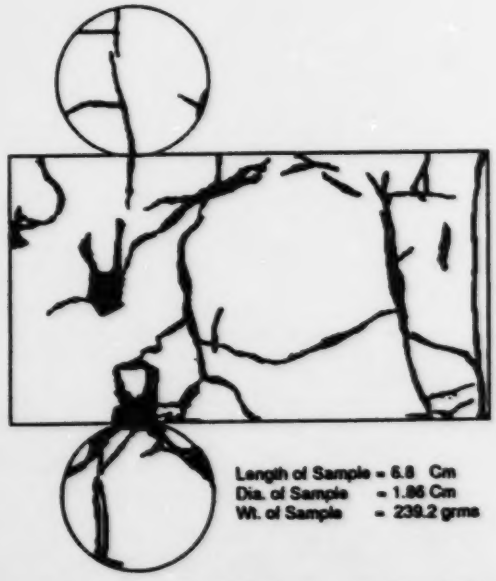

Figure 1. Map of the visible fractures on the surface of the specimen.

Sequence of Experiments

The following experiments were performed on each specimen.

1) After the specimen was prepared, its was in the oven at 105 °c till its weight stabilized; the specimen was then weighed.
2) The permeability of the specimen was measured using helium (dry specimens were used for testing).
3) The specimen was then placed in water until it was completely saturated and the volume of water in the specimen at saturation was measured. Porosity of the specimen was thus calculated using the bulk volume, dry weight, and the water content of the specimen at saturation.
4) The specimen was immersed in a beaker containing the raffinate obtained from Cyprus Casa Grande Mine. This solution contains 20 g/l of sulfuric acid. The specimen was leached for varying intervals of time.
5) At the end of the leaching period, the copper content of the raffinate was measured to estimate the rate of copper recovery from the specimen.
6) After the leaching process, the specimen was dried, weighed and the permeability of the dry sample was measured. The sample was then saturated with water to estimate the pore volume in the sample and its porosity was calculated.

The above sequence of experiments was repeated on each specimen to obtain the porosity and permeability of the sample at various intervals of time during the leaching process.

Porosity Measurements

The water saturation method was used to measure the effective porosity of the specimens. This is a simple and easy method to estimate the effective porosity of the specimen although errors in the results might be expected due to the entrapped air in the specimen. Sometimes the error in the estimate of effective porosity with this method can be as high as 10% (Koorevaar et al. 1983). But since the possibility of air entrapment also exists in the field, the effective porosity estimated by this method is fairly representative of the effective porosity in the field. To estimate the porosity by this method, the specimens were oven dried at 105 °C until their weight stabilized. After drying, each sample was weighed. These samples were then water saturated by placing them in beakers containing water. The saturation curves - weight of the sample vs time were drawn for each sample. The volume of water in the saturated specimen was estimated by using the density of water as 1 g/ml. The volume of water in the specimen thus gave the pore volume or the effective porosity, which is an estimate of the interconnected voids in the specimen. The bulk volume of the specimen was calculated by measuring the dimensions of the sample. The effective porosity of the samples was, therefore, calculated using the standard expression

$$\text{Eff. porosity} = \frac{\text{Wt. of the sat. sample - Wt.of the dry sample}}{\text{Bulk volume of the sample}} \quad (1)$$

Permeability Experiments

The primary objective of this experimental study was to study the variation of permeability with time during a leaching operation. Due to the low permeabilities of the specimens before leaching, it was extremely difficult to estimate the permeability of the specimens using water. Therefore, recourse had to be taken to estimate the permeability of the specimens using a gas. Helium was used for testing the permeability since it does not get adsorbed on the surface of the rock, and also because the small molecular diameter and light weight ensures maximum penetration and flow through the microfractures. The permeability experiments were carried out with the specimen stressed triaxially to simulate *in situ* conditions. An experimental setup which permitted simultaneous control and measurement of applied stresses, applied gas pressure, and flowrate through the specimen was designed. The setup consisted of a triaxial cell, modified to provide gas inlet and exit ports through the upper and lower platens. The cell was connected to a hydraulic pump with a gauge to apply the confining stress. The axial stress was applied by placing the cell in a load frame. The specimen to be tested was inserted into the cell and the steel perforated discs (to distribute and collect the gas) were placed at the two ends of the specimen inside the cell. Platens were then inserted into the ends of the cell. A hydrostatic stress of 1000 psi was applied to the sample. The flowrate through the specimen was measured using a soap bubble meter. Helium gas was supplied via a regulator and pressure gauge to the top of the cell and was led away from the lower end of the specimen to the flowmeter. A vacuum pump was used to dry any water vapor present in the setup before performing permeability experiments using helium gas. Figure 2 shows the schematic of the experimental setup that was used for permeability testing. Helium at 50 psi was applied at the upper end of the specimen using a regulator and the flowrate at the lower end was measured at 30 minute intervals until three consecutive measurements were similar to ensure that steady state flow conditions were reached. Once this occured, the gas pressure at the upper end of the specimen was increased in increments of 50 psi up to 300 psi and the procedure repeated.

The permeability of the specimen for each pressure gradient was calculated using Darcy's law. Darcy's law for steady state flow of fluids through porous media (Carman, 1956) is given as:

$$Q = \frac{k\,\mu\,\Delta P}{A\,\Delta L} \qquad (2)$$

$$\text{or, } k = \frac{Q\,\mu\,\Delta L}{A\,\Delta P} \qquad (3)$$

where, k is the permeability of the media (m^2), A is the area of the cross section of the specimen (m^2), μ is the viscosity of the fluid (NS/m^2), $\Delta P/\Delta L$ is the pressure gradient ($N/m^2 - m$), Q is the volumetric flow rate at the outlet (m^3/s). For flow of compressible fluids, this equation is modified to give

$$k = \frac{Q\,\mu\,\Delta L\,P_o}{A\,\Delta P\,P_m} \qquad (4)$$

where, P_o is the pressure at the downstream end (N/m^2), P_i is the pressure at the inlet end (N/m^2), P_m is the mean gas pressure(N/m^2) and is equal to $(P_o + P_i)/2$.

It was shown by Klinkenberg (Klinkenberg, 1941) that

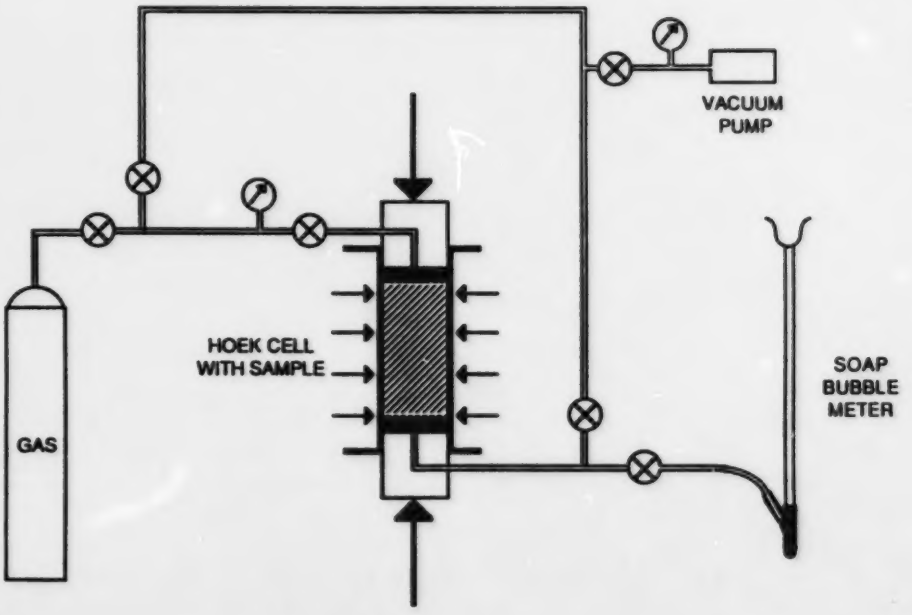

Figure 2. Schematic of the experimental setup used to measure permeability of a rock sample using a gas.

permeability determined using a gas is not the same as the permeability of the medium to a liquid. Permeability to gas is a function of the mean free path of the gas molecules, and thus depends on factors which influence the mean free path, such as pressure, temperature, and the nature of the gas. Figure 3 shows a plot of observed permeability of a porous medium as determined at various mean gas pressures using hydrogen, nitrogen, and carbon dioxide as flowing fluids. The linear relationship between the observed permeability and the reciprocal of mean pressure is expressed as:

$$k = \frac{k_o}{(1 + b/P_m)} \qquad (5)$$

$$\text{or, } k = k_o - m/P_m \qquad (6)$$

where, k is the permeability of the medium to a single phase liquid completely filling the pores of the medium, k_o is the observed permeability to gas, b is a constant for a given gas in a given medium, and m is the slope of the line which is a function of the gas. From the equation it can be seen that $k = k_o$ when $1/Pm = 0$, or at infinite mean pressure. Therefore the plot of observed permeabilities as a function of reciprocal mean pressure of the test, when extrapolated to infinite mean pressure (1/mean pressure = 0), gives the equivalent liquid permeability of the medium. This technique of estimating permeability of a sample to a liquid has been shown to be accurate (Stormont, 1990).

Estimation of Copper Recovery Rate

The rate of copper recovery from the specimen during leaching was measured by estimating the copper content of the leach solution at the end of each leaching period. An atomic adsorption spectrometer was used to estimate the copper content in the leachant. The atomic adsorbtion spectrometer measures accurately upto 10 mg/l of copper in the solution. The pregnant leach solutions with dissolved copper, therefore had to be diluted to measure their copper content. Using this measured concentration and the quantity of leachant used to leach the specimen, the amount of copper recovered was estimated. Evaporation of the leachant during leaching was minimized by covering the beakers containing the specimen and the leachant with aluminum foil.

Results and Discussion

Variation in Porosity

The saturation curve for each specimen was drawn for a period of 400 hours. Figure 4 shows the saturation curve for one specimen. From the figure, it can be seen that there is very little increase in the volume of water absorbed by the specimen after 72 hours. The effective porosity of the specimen after each leaching cycle was, therefore estimated by measuring the amount of water absorbed by the dry specimen during the 72 hours after immersion in the beaker containing water. The effective porosity of the specimen increased with the amount of leaching. The variation in the observed porosity of the specimen, measured as a ratio of initial porosity is shown in figure 5. After an initial slow rate of increase, the porosity of the specimen increases rapidly and continuously as leaching progresses. Over a 45 day period, the effective porosity increased by over 30%. This clearly suggests formation of a void space as soluble material dissolves in the acid and is removed.

Variation in permeability

Figure 6 shows the observed permeability of the specimen measured at each pressure gradient plotted as a function of the reciprocal mean pressure applied during the test. The linear relationship between the observed permeability and the reciprocal mean pressure applied during the test, suggests a clear Klinkenberg effect. The equivalent liquid permeability was estimated by extrapolating this linear relationship to infinite mean pressure (reciprocal of mean pressure = 0).

The variation of the equivalent liquid permeability of

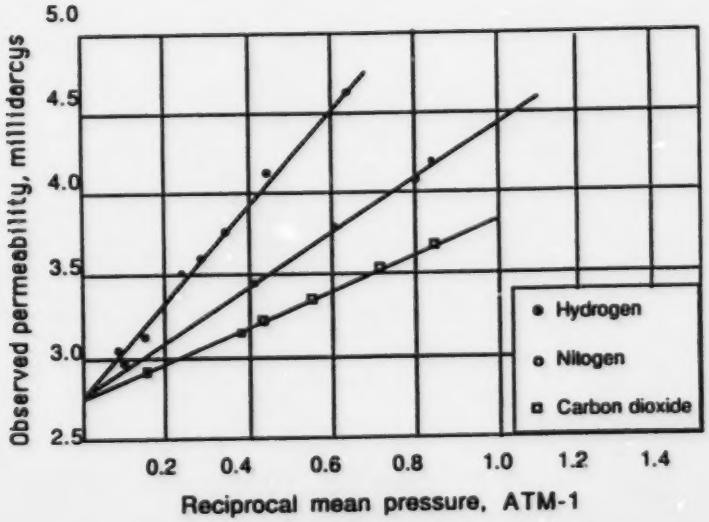

Figure 3. Permeability of a core sample to hydrogen, nitrogen, and carbon dioxide at different pressures (From Klinkenberg, 1941).

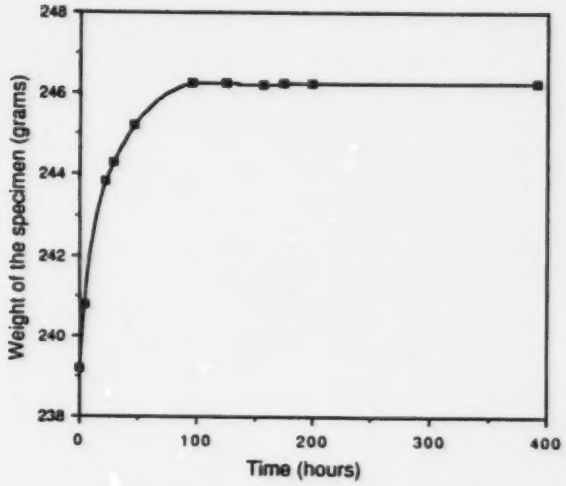

Figure 4. Saturation curve of the specimen.

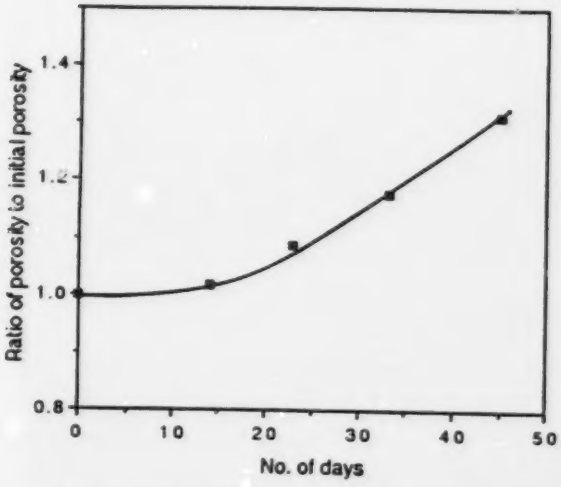

Figure 5. Variation in porosity with time as leaching progresses.

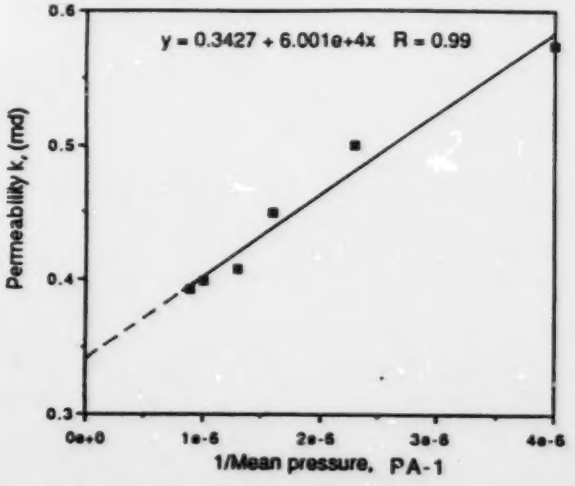

Figure 6. Permeability at various pressure gradients as a function of reciprocal of mean pressure.

the specimen as leaching progresses is shown in figure 7. There is a definite and continuous increase in the permeability of the specimen with leaching. As shown in the figure a near linear relationship exists between permeability and the number of days the specimen was leached. From this relationship, it is seen that the permeability of the specimen increased at an average rate of 0.0366 md per day. The permeability increased by 1.647 pmd over a 45 day period.

Variation in Copper Recovery Rate

The total copper recovered from the specimen as a function of time is shown in figure 8. The flattening of this curve indicates that after an initial high rate of copper recovery, it gradually reduces as the copper in the specimen is depleted. This effect can be seen more prominently in figure 9 which shows the variation in the amount of copper recovered per day of leaching. As leaching progresses and the copper in the specimen is depleted, the amount of copper recovered per day of leaching decreases.

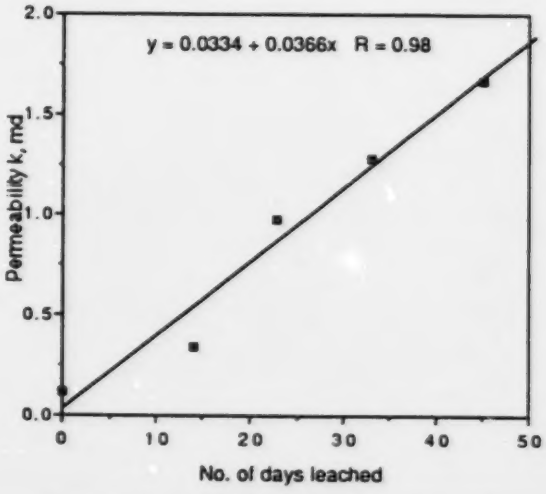

Figure 7. Variation of permeability of the specimen during leaching.

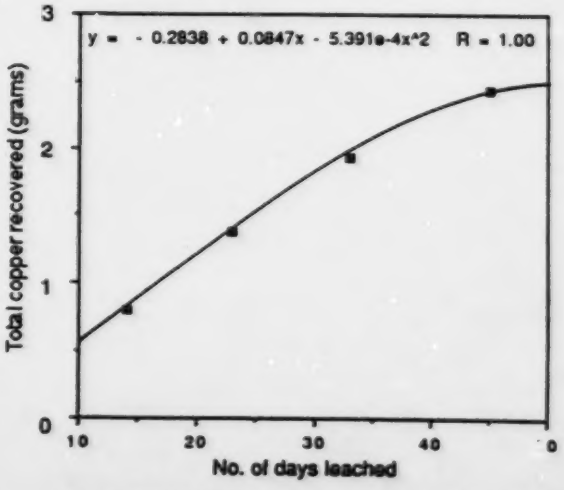

Figure 8. Total copper recovered from the specimen as leaching progresses.

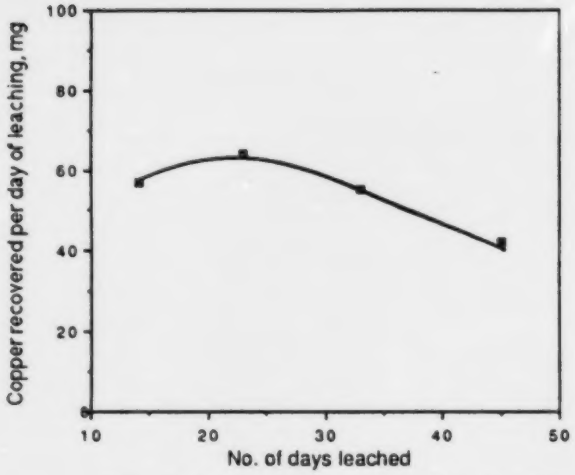

Figure 9. Amount of copper recovered per day of leaching expressed in milligrams.

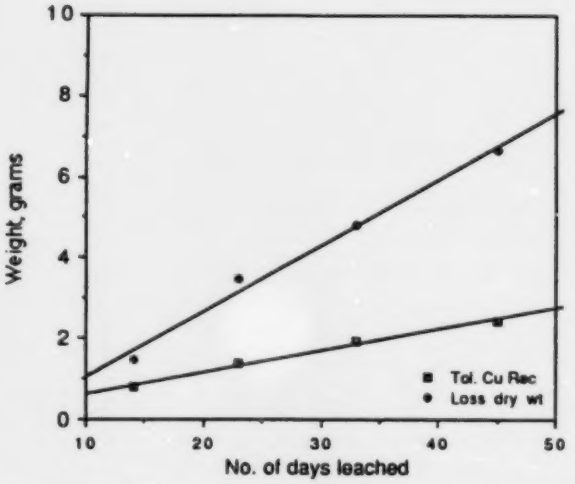

Figure 10. Loss in weight of the dry specimen and the total copper recovered from the specimen.

Figure 10 shows the loss in the weight of the dry specimen and the total copper recovered from the specimen. Initially 70% of the material dissolved by the leach solution is copper. This is perhaps due to the fact that copper oxide which is mostly present along the fractures of the specimen, is more easily accessible to the leach solution. But, once this copper oxide present along the fractures is depleted, more of the other minerals present in the rock matrix dissolve in the acid. At the end of 45 days of leaching, copper forms only 37% of the total material dissolved from the specimen, although there is an increase in the overall material dissolved by the raffinate.

Conclusions

Based on the preliminary work performed so far, the following conclusions can be made.

1) There is a definite increase in permeability as leaching progresses. This is primarily due to the dissolution of copper mineral(s) along the fractures, thus widening the fracture aperture. This was confirmed when most specimens broke along fractures after leaching for a couple of months.
2) The effective porosity of the core samples increases with leaching. The rate of increase in porosity is slow initially, followed by a relatively rapid rate. This is, once again, due to dissolution of soluble material in the sample and confirms the effect mentioned above (in 1), although this could also be due to matrix flow - which is significantly slower.
3) The rate of copper recovery is high initially and reduces as leaching progresses. With continued leaching, there is substantial amount of non-copper material being removed from the core. This is either due to depletion of copper along fractures, or because of increased flow through the matrix.

Acknowledgements

This research was carried out as a part of the project funded by the Department of Defense through the Arizona Copper Research Center. The authors wish to thank these organizations for their support. Also, thanks are due to Cyprus Casa Grande management, in particular to Mr. K. Behnke and Mr. P. K. Medhi for providing the samples, raffinate and constant guidance, and Mr. J. Williams of University of Arizona for assisting in designing and construction of the experimental setup.

References

Ahlness, J. K., and Pojar, M. G., 1983, " In Situ Copper Leaching in the United States: Case Histories of Operations," IC 8961, 1983, BuMines, pp. 10-15.

Carman, P. C., 1956, Flow of gases Through Porous Media, Butlerworths Scientific Publications, London.

Cook, S. S., 1987, "Petrologic Analysis of Laboratory core Leaching Experiments," Proceedings, In Situ Recovery of Minerals, Eng. Found. Conf., Santa Barbara, CA, pp. 81-97.

D'Andrea, D. V., Larson, W. C., Fletcher, L. R., Chamberlain, P. G., and Engelmann, W. H., 1977, " In Situ Leaching Research in a Copper Deposit at the Emerald Isle Mine," RI 8236, 1983, BuMines, pp. 41.

Hardwick, W. R., 1967, "Fracturing A Deposit with Nuclear Explosives and Recovering Copper by the In Situ Leaching Method," RI 6996, 1967, BuMines, pp. 11-12.

Klinkenberg, L. J., 1941, "The Permeability of Porous Media to Liquids And Gases," Drilling and Production Practices, American Petroleum Institute, pp. 200-213.

Koorevaar, P., Menelik, G., and Dirksen, C., 1983, " Static Equilibrium in Soils," Elements of Soil Physics, 3 rd ed, Elsevier, New York, pp. 72.

Obert, L., and Duvall, W. I., 1967, Rock Mechanics and Design of Structures in Rock, John Wiley and Sons, Inc., New York, pp. 333.

Paulson, S. E., and Kuhlman, H. L., 1989, "Laboratory Core-Leaching and Petrologic Studies to Evaluate Oxide Copper Ores for In Situ Leach Mining," Proceedings, In Situ Leach Mining, BuMines Technology Transfer Seminar, Phoneix, AZ, pp. 28; 35.

Pugiliese, J. M., 1989, " Generic Design Manual : Cost Model for In Situ Copper Mining," Proceedings, In Situ Leach Mining, BuMines Technology Transfer Seminar, Phoneix, AZ, pp. 11.

Schimdt, R. D., Behnke, K. C., and Friedel, M. J., 1990, "Hydrologic Considerations of Underground In Situ Copper Leaching," 1990, Soc. Min. Eng., AIME Preprint.

Stormont, J. C., 1990, " The Permeability Changes in Rock Salt During Deformation," Ph.D Dissertation, University of Arizona, Tucson, AZ.

SOCIETY FOR
MINING, METALLURGY, AND
EXPLORATION, INC.

P.O. BOX 625002 • LITTLETON, COLORADO • 80162-5002

PREPRINT
NUMBER
(Assigned when paper is received at SME Headquarters.)

EFFECT OF AN UNSATURATED SETTING ON THE HYDROLOGY OF IN SITU COPPER LEACHING

91 161

Michael J. Friedel
Hydrologist

Robert D. Schmidt
Supervisory Hydrologist

Twin Cities Research Center
Bureau of Mines
U.S. Department of the Interior
Minneapolis, Minnesota

For Presentation at the 1991 SME Annual Meeting
Denver, Colorado, February 25-28, 1991

Permission is hereby given to publish with appropriate acknowledgments, excerpts or summaries not to exceed one-fourth of the entire text of the paper. Permission to print in more extended form subsequent to publication by the Society must be obtained from the Executive Director of the Society for Mining, Metallurgy, and Exploration, Inc.

If and when this paper is published by the Society for Mining, Metallurgy, and Exploration, Inc., it may embody certain changes made by agreement between the Technical Publications Committee and the author, so that the form in which it appears is not necessarily that in which it may be published later.

These preprints are available for sale. Mail orders to PREPRINTS, Society for Mining, Metallurgy, and Exploration, Inc., P.O. Box 625002, Littleton, Colorado 80162-5002

PREPRINT AVAILABILITY LIST IS PUBLISHED PERIODICALLY IN MINING ENGINEERING

Abstract. The permeability and flow capacity in unsaturated media is investigated by the Bureau of Mines for application to in situ copper leach mining at the Cyprus Casa Grande mine site. Moisture retention properties are derived and combined with scanning electron microprobe data to characterize the mineralogy, texture, pore size, distribution, and permeability of the host rock. Finite element modeling is used to derive a saturated permeability, ambient degree of saturation, and assess various injection-recovery schemes. Recommended design modifications for optimization of solution distribution and maximum recovery from the rock matrix requires either (1) the injection pressures on the order of 1500 psi and recovery wells operating in a suction mode, or (2) performing permeability enhancement, through rubblization. By producing a maximum block diameter of 4 m, injection pressures can be reduced to 500 psi with improved recovery and containment of solutions.

Introduction

Hydraulic properties and characteristics of copper ore associated with the Casa Grande deposit at the Casa Grande mine are investigated by the Bureau of Mines to assess permeability and its impact on flow capacity during in-place, copper leaching operation. The copper ore is a heterogeneous, unsaturated, and fractured medium in which the permeability is dominated by a network of macrofractures, defining blocks of rock of various sizes. Upon saturating the macrofractures, these act as a network of distributed sources and sinks for flow of solution into and out of the rock matrix. Since copper is disseminated throughout the rock matrix, understanding and exploiting permeability conditions is essential for successful leaching operations in both the matrix and fracture system. This study provides insight into fluid flow behavior within the rock blocks, following saturation of macrofractures.

In general, it is difficult to quantify unsaturated flow in a heterogeneous rock mass. Moreover, few direct measurements of permeability and flow characteristics have been made. One problem hindering direct measurement is associated with the excessive time involved (months or years). Another stems from limitations in test equipment.

The approach used to assess transient migration of fluids at the Casa Grande mine site first estimated hydraulic properties indirectly, using models that account for dependence of saturation on water pressure head (also known as matric potential, capillary pressure, and suction head). Empirical relationships associated with retention properties of the porous medium are then combined with theoretical models of unsaturated flow to approximate permeability and hydraulic conductivity relationships. In turn, this information and appropriate boundary conditions are combined for input into a two-dimensional, unsaturated, finite element flow code called TWOD (Nieber et al, 1991). Results are used for the development and optimization of a site specific hydrologic design for in situ leaching in heterogeneous, fractured, and initially unsaturated copper oxide ore deposits.

Physical Property Assessment of Casa Grande Copper Oxide Ore

Sample and Petrographic Description

Representative samples of copper ore were obtained from drillholes at the 335 m level (mean sea level) of the Cyprus Casa Grande mine. These samples were used to assess the spatial variability in hydraulic properties between these boreholes. Six 2.54-cm diameter by 2.54-cm length samples were prepared from each drillcores and tested for saturated hydraulic permeability and porosity by the mercury porosimetry method.

Thin sections were prepared for determining the predominant mineralogy, texture and porosity of the copper ore. Examination of these sections were aided by using a standard axioplan microscope at 3x magnification with a fullwave gypsum filter. The typical mineral assemblage consisted of fine grained rounded quartz mass, with phenocrysts of altered plagioclase feldspar (now kaolinte), biotite, hematite and quartz.

By using an x-ray, electron microprobe, elemental distribution maps were prepared. These maps demonstrate that aluminum was present among the primary elements associated with plagioclase feldspars. This suggested the presence of kaolinitic clay. Copper was found to be associated with both the altered plagioclase feldspar and biotite minerals. The mineralization suggests that preexisting microfractures once served as preferential pathways for the primary deposition of copper and quartz. These ancient microfractures now appear as solid red stringers, or meanders, throughout the sample. The Quartz, however, showed no association with either the mica or clay minerals.

Discontinuities are evident in all of the copper ore samples, as a result of two distinct porosity systems. Examination of back scattered x-ray images at various magnifications, reveals a bimodal porosity distribution. A magnification of 40 x reveals microfractures, while a magnification of 3000 x reveals the existence of micropores at grain boundaries. The present microfractures are believed to represent a distinct episode of failure since they transect fractures previously filled with copper and quartz. It is important to note that these microfractures provide a network for the lixiviant to access copper hosted minerals, increasing the relative surface area for contact. The microfactures appear to have similar aperture range (5-15 micron) in both the feldspars and biotite minerals, while smaller apertures exist in those cracks transecting the quartz mass.

Moisture Retention Properties

Understanding the transient nature of fluid migration associated with the leaching of an unsaturated copper ore deposit, requires characterization of its moisture retentive properties (or moisture capacity). Insight into the copper ore moisture capacity can be gained through knowledge of the size and distribution of its interstices. In an unsaturated medium, hydraulic pore radii and/or hydraulic fracture aperture are reflected by variations in the

pressure head Ψ which, in turn, causes changes in the saturation S or moisture content. The graphical expression is called the moisture retention, capillary pressure, or characteristic curve. The slope at any given point on the moisture retention curve represents the specific moisture capacity of the medium.

The functional relationship between saturation and water pressure head for the Casa Grande copper ore was derived using the mercury porosimetry method. Mercury porosimetry provides an indirect method for obtaining the moisture retention curve. A total of six mercury intrusion drainage tests were performed (three from each hole), and then adjusted to account for the differences between the properties of mercury and water for use in the fluid flow model (Friedel, 1991).

Pressure Head and Saturation

Figure 1 depicts 2 of the 6 water retention drainage curves derived from mercury intrusion data for the copper oxide core obtained from holes A, and B. These curves typify moisture retention properties characteristic of those sampled. Conformity of these retention curves (similar shape over the same range of pressure head) implies structural homogeneity over the distance spanned by these boreholes. Hence, any one sample would suffice for the analysis.

The shape of a drainage curve often reflects the relative homogeneity of the pore size distribution. If the pressure head remains constant over a large water saturation interval, the related pore dimension is considered homogeneous. Conversely, a variation in pressure head as a function of saturation implies that pore dimensions are relatively heterogeneous.

Figure 2 depicts the equivalent moisture retention drainage curve for a typical copper oxide sample. Two prominent pore distributions are obvious; the first reflects microfractures at low, negative pressure head values associated with relative saturation of 0.8095 to 1, while the other reflects micropores at pressure head values associated with saturations from 0 to 0.8095. These results are consistent with interpretations based on the axioplan and scanning electron microscope analyses observed earlier.

To better assess the range of pressure head values over which the saturation varies, the saturation is plotted against the log of pressure head (fig. 3). Micropores in the saturation range between 0.8095 to 0 are associated with pressure head values ranging from -150 m to -10,000 m; while saturation of microfractures between 0.8095 and 1 correspond to pressure head values of -150 m to -0.1 m, respectively. Test results at water pressure head values less than about -3,500 m should be considered inaccurate, because of the inability of the mercury intrusion method to penetrate micropores less than about 0.002 micron. This limitation is further reinforced because residual saturation does not, as expected, reach an asymptotic value slightly above zero (field capacity).

Hydraulic radii, reflecting the pore size distributions "seen" while draining (or drying), are calculated (Friedel, 1991) and displayed in figure 4. The microfractures appear to have the broadest pore size distribution (greatest slope) with hydraulic half width apertures ranging from 0.15 to 33 microns. The most uniform hydraulic half width aperture distribution exists between 1 to 4 microns which is consistent with that observed using the microscope. The hydraulic radii associated with the micropore distribution ranges from about 0.0015 to 0.05 microns; however, it is uniform between 0.0025 to 0.0075 microns.

Estimating the Hydraulic Properties

To be able to study the behavior of injection and recovery of leach solutions in an unsaturated setting, knowledge of permeability, or the hydraulic conductivity (also known as the coefficient of permeability, or capillary conductivity), and its relationship to moisture content is needed. The most direct way to obtain this relationship is by experiment. Reliable estimates of unsaturated hydraulic permeability are difficult to obtain, mainly because of difficulty in obtaining representative samples, and the time and expense involved. An estimate of the permeability function was obtained, however, from the moisture retention properties already discussed, i.e. saturation as a function of pressure head (Friedel, 1991). Although, fluid flow phenomena in partially saturated media normally involves two-phase flow of a wetting and non-wetting fluid, usually air and water, the flow of air is seldom of major significance. Hence, the present investigation is restricted to the permeability of the water phase only.

Several unsaturated permeability models have been developed that are based on probability functions describing the relationship between the measured moisture content and water pressure head. Using the Brooks and Corey (1966), and Brutsaert (1968) power functions, it was found that their two dependent parameters did not yield reasonable results for fitting the moisture retention curves associated with Casa Grande ore. On the other hand, the closed form expression developed by Van Genuchten (1980) seemed to provide reasonable results, requiring three dependent coefficients to be estimated.

A plot of the nonlinear relative microfracture permeability distribution is presented in figure 5. This permeability function was calculated using the relationship outlined by Friedel (1991) and the Van Genuchten constants: $\alpha = 0.30$ 1/m, $m = 0.525$, and $n = 2.105$. It is noteworthy that permeability is nonlinear and observed to decrease one order of magnitude with a 20 percent reduction in saturation. Figure 6 depicts the saturation plotted as a log function of permeability. By inspection the permeability diminishes with decreasing saturation ultimately spanning 6 orders of magnitude. The maximum rate of permeability decrease for the Casa Grande ore occurs at saturations below 45 percent. Using the range of saturated permeability values, 10^{-2} to 10^{-1} md, corresponding permeability values in md can be obtained from the product of the relative permeability and saturated permeability. Assuming a best case, the range of permeability would be 10^{-1} md ($S_e = S_r = 1$) to about 10^{-6} md ($S_e = 0$, $S_r = .8095$). While the absolute permeability for the

micropores can not be firmly established, it appears to represent the end of the microfracture continuum at about 10^{-4} md. Therefore, fluid in micro-pores can be assumed to be immobile for the purposes of this study. Hence, the remaining portion of this study investigates only the fluid movement in the microfractures.

One obvious conclusion from the foregoing is that a decrease in saturation results in decreasing the permeability in the medium, and thereby inhibiting fluid flow. From an environmental viewpoint, leach mining in an unsaturated setting presents a tractable scheme under which luxiviants may better contained. From a production standpoint, however, this may require permeability enhancement by high pressure injection, hydrodilation, hydrofracing and/or in-situ rubblization. For either objective, site specific modeling is required to assess injection-recovery pressure requirements.

Hysteresis

Unsaturated porous media typically displays a hysteretic behavior. The two branches of the hysteretic loop (drainage and wetting) therefore "see" a different average effective pore size distribution, depending on whether the sample is being saturated or desaturated. Since the drainage branch exhibits higher moisture content than the wetting branch at any given pressure head, the porous media becomes more retentive during the drying cycle. Hence, the average effective pore size distribution during a drainage experiment shifts toward smaller values of pore radius than one for the wetting branch. This may, in part, explain why the half width apertures calculated from a drainage experiment are slightly less than those observed when using the microscope approach.

For modeling fluid flow from the injection well into unsaturated copper ore, knowledge of the wetting boundary curve is required. Since a mercury extraction curve was not obtained during porosimetry testing, an equivalent wetting boundary curve was not originally determined. The similarity hypothesis (Maulem, 1977) provided a means to derive the wetting boundary curve, based on knowledge of the drainage boundary curve.

The dimensionless curves for the hysteretic Maulem model II, or for the case when hysteresis is not present is depicted in figure 7. When there is no hysteresis effect, a linear relationship exists and flow either drainage, or wetting, follows the same path. The Maulem model II, however, produces an expected departure from the straight line flow path. Since hysteresis is normally present in rock, it is incorporated in the finite element, unsaturated flow model. Figure 8 compares corresponding hysteretic loops for microfractures. Using the Van Genuchten approach, both the drainage and wetting branch constants could be calculated. These are summarized in table 2.

Table 2. Summary Van Genuchten constants describing microfracture hysteresis.

Hysteretic	α	m	n
Drainage	0.152 1/m	0.070	1.075
Wetting	0.300 1/m	0.525	2.105

It is cautioned that the microfracture drainage curves, however, are suspect at pressures at or beyond about -3,500 m pressure head.

Computer Modeling of Underground In Place Leaching

Mathematical Model for Unsaturated Fluid Flow

Modeling the movement of water in a partially saturated porous medium has been discussed by many authors. A review of the state-of-the-art can be found in a recent text edited by Evans (1987). Basically, the movement of water must take into account the movement of liquid water, water vapor, air and the medium itself. The simplified approach taken here invokes the assumption of single phase flow. Hence, the water is considered mobile, while the air is assumed immobile.

An equation describing partially saturated and unsaturated flow of water in porous media, neglecting air-water interactions, can be derived by the principle of conservation of mass and the constitutive relationship given by Darcy's law. This governing nonlinear, second-order partial differential equation is known as the Richard's equation.

Finite Element Mesh and Flow Boundary Conditions

The nature of fluid flow is generally a 3-dimensional phenomenon, however, a 2-dimensional representation of the Casa Grande tool crib operation can be approximated by considering radial flow in the region perpendicular to a well. That is, we consider the surface that exists along the contact between the fanoglomerate (cemented gravels) and copper oxide ore (hanging wall). This surface undulates in cross section (fig. 9) but can be characterized in a 2-dimensional plan view by projecting each well onto this plane. This approach appears justified, since only the interval spanning the copper oxide ore is perforated. Figure 10 gives a cross-sectional representation of the total well field for the hanging wall. Wells related to a given fan pattern are depicted by connecting each group of wells by a solid line.

The corresponding finite element grid for the hanging wall cross section is given in figure 11. The FE solution domain is represented by a 100 m x 100 m mesh with 512 simplex triangular elements and 300 corresponding node points. The x-direction represents the horizontal distance along the tool crib drift, while the y-direction denotes the vertical distance along the hanging wall. The lower, left-hand corner represents the 0 m, 0 m mesh coordinate, and the upper, right-hand corner represents the 100 m,100 m coordinate. The distance between any horizontal or vertical pair of node points is 6.25 m. The complete modeling domain was chosen to be large enough so that there would be no interaction between boundary conditions associated with its surface and sides. If interactions exist, the calculations of both pressure and flux would be inaccurate.

The boundary conditions employed for the site specific simulations included no flow at the upper and side boundaries, a unit hydraulic gradient along the lower boundary, and a point source or sink at the interior of the mesh.

Injection and/or recovery is assumed to occur at node point 145, the center of the mesh. A schematic depicting these boundary conditions with respect to the finite element mesh is shown in figure 12.

Inverse Modeling

Since the Casa Grande tool crib site is known to have macroscale fractures linking various wells (Schmidt, 1990), it is necessary to identify a "tight" well. A "tight" well, defined as one that had minimum observed flow rates, is used to represent fluid flow through the rock matrix. Since the Casa Grande site has had extensive permutations in pressure conditions over a 1-year period, an additional requirement is to select an interval from the onset of leaching to the first permutation in well conditions.

Figure 13 depicts the flow rate and corresponding pressure history recorded for the first 100 day period in well 758. The mean flow rate and injection pressure are calculated to be 0.315 gpm and 528 psi, respectively. These values are used during subsequent inversion of the FE model to determine the appropriate saturated permeability and ambient degree of saturation.

The first inversion involved calibrating the model by adjusting the saturated permeability until the computed initial flux matched that observed in the field. Figure 14 gives flow rate (flux) for a range of saturated permeability values. The maximum permeability of 0.1 md resulted in a maximum flow rate (1.92 gpm), while the minimum value of 0.01 resulted in a minimum flow rate (0.19 gpm). A saturated permeability value of 0.016 md matched the flow rate (0.315 gpm) observed in well 758. This agrees with the value 0.0177 md from the using a geostatistical analysis used to estimate permeability. The in situ permeability estimate obtained from well 758 (0.016 md) also matches that obtained from core samples.

The second simulation involved estimating the ambient degree of saturation by direct inversion. The ambient degree of saturation is defined as that saturation which existed prior to in situ leaching. Estimating the ambient degree of saturation was accomplished by perturbing the initial pressure condition until the transient pressure response matched the results observed in well 758, i.e. where injection pressure was equal to 371 m at the 100th day. The initial pressure head condition (zero time) was decreased incrementally beginning with 0 m until transient pressure conditions were matched (fig. 15). The -1 m initial pressure condition corresponds to an ambient saturation of 95 percent.

Since laboratory moisture determinations were not available, it was not possible to verify this ambient degree of saturation. An alternative approach was used, however, to qualitatively check the calculated minimum saturation, based on draining the initially saturated domain over a large time period. From the 1,000 year simulation based on the Van Genuchten microfracture drainage constants, a permeability of 0.016 md correspond to a minimum effective saturation of about 88 percent. The gravity effect is clearly evident from the moisture tongue in the center of the figure 16, demonstrating that, at least qualitatively, the derived ambient degree of saturation appears realizable.

The effect that the tool crib, and other drifts at the 900 and 1100 levels, have on fluid distribution in the rockmass is shown in figure 17. These results portray a 25-year simulation approximating the time since these drifts were created. This analysis was necessary to assess whether the boundary conditions associated with these drifts would need to be integrated into the forward model. Van Genuchten constants again reflect the drainage curve, with a saturated permeability of 0.016 md and ambient degree of saturation of 95 percent. The effect of imposing drifts essentially increases the moisture gradient in a region of about 2 1/2 times the radius of each drift. The regional effect on ambient degree of saturation, however, is largely unaffected.

Forward Modeling

The primary purpose of transient unsaturated flow modeling is to provide insight into the hydrologic design of in situ leaching operations in deposits where copper mineralization is disseminated in segmented blocks of ore. Forward (predictive) modeling is performed using TWOD with reference to a single injection or recovery well drilled into a homogeneous block of ore, or equivalently with reference to a single linear fracture which acts as a source or sink for a single block of ore. Well 758 is seen as an example of a well in the tool crib pattern that is drilled entirely within a single ore block.

Values of ambient degree of saturation (95 percent), and saturated hydraulic permeability (0.016 md) derived during the inversion process, and those Van Genuchten constants previously described, were used to simulate fluid flow in forward modeling. The effect of injection pressure on the transient build-up of a saturated plume in an ore block is shown in figure 18. For early analysis of plume development, the solution domain was reduced to 25 m by 25 m, corresponding to a internodal distance of 1.56 m, while using the same mesh (fig. 11) and boundary conditions (fig. 12).

Flow simulations demonstrate that an injection pressure of 1500 psi (currently the practical limit at the tool crib site) sustained for about a 150 day period is required before a circular block of ore with a radius of 5 m becomes completely saturated. The hydraulic head (elevation head plus pressure head), pressure head, and fluid distribution for an injection source (such as well 758) after a 1 year period, while subjected to an injection pressure of 1500 psi, are given in figure 19. The symmetry of the pressure plume in these figures reflects the assumption of homogeneous and isotropic conditions within an ore block. The steepness of the cone is attributed to the large moisture gradient existing about the source. While lesser pressures could be employed, the waiting period for solution penetration would be correspondingly longer. Pressures at or below 500 psi would effectively contain solution within a 2.5 m radius around the injection source.

Converting the injection source after a 1 year period to a recovery sink, with a zero gage pressure or a negative (suction) pressure affects the head and fluid distribution, as shown in figures 20 and 21. In each case, the pressure plume around the sink is reduced. The square surface at an effective saturation (S_e = 1) in figure 20 is an artifact produced by the contouring package. This is in reality a cone with a diameter equal to slightly less than the length of its side.

Since the zero gage pressure would not be less than or equal to the microfracture air entry value (about -4 m), only 1 percent of the injected solution can be recovered by the sink. The bulk of the solution remains captive in the rock by capillary tension. Because of the capillary effect, a dramatic increase in solution recovery, i.e. about 95 percent, can be achieved by inducing a suction head of -10 m at the sink as shown in figure 22.

Hydrologic Design

Forward modeling shows that solution penetration into ore blocks can be achieved, despite the reduced permeability associated with unsaturated conditions, if well injection pressures are of sufficient magnitude. From an operational standpoint, if the target ore zone were a single homogeneous ore block, a flux rate of .05 m/day would be unacceptably low. At the closest spacing, wells in the tool crib pattern are 5 m apart.

The observed breakthrough times for flow of solution between injection and recovery wells at the tool crib site ranges from 1 to 150 hours, after the start of injection, indicating that the network of macrofractures which transects the target ore zone is, initially at least, the dominant flow path through the ore zone.

A hydrologic design suggested by the results of forward modeling is a variant of the push-pull test method. Injection in a core region of the tool crib wells at pressures of 1500 psi is maintained for 30 to 60 day period. The injection interval serves to completely saturate the ore blocks and build pressure in the saturated macrofracture network. Following the 30 to 60 day interval wells are selectively converted from injection to recovery mode. Suction pressure is applied, if practical. Otherwise, the lowest possible head condition should be imposed. To ensure that there is ample residence time to load the injected leach solution with copper, and that the sorption of copper, and/or precipitation of gangue minerals does not occur, flow rates during recovery can be regulated by shutting in the well to some degree. The advantage of applying back pressure in the well is to prevent the established pressure plume from dissipating too rapidly. The concentration of copper and gangue minerals in solution would need to be continuously monitored to adjust recovery flow rates.

A hydrologic design involving rubblization of a mineralized zone could be expected to improve fracture permeability in the ore zone by orders of magnitude. Rubblization conducted in a manner similar to that used for in situ oil shale retorting is just one possibility. A factor of central importance for determining the desired degree of rubblization (or the average block size) is the penetration rate of leach solution into unsaturated ore blocks.

Forward modeling suggests that maintenance of injection pressures of 500 psi, or below, would effectively confine solutions to a rubblized zone in which the average block radius of 2 m or less. Flow in blocks larger than this, on the periphery of the rubblized zone, would be effectively impossible in the absence of large-scale fractures or sinks, under the permeability constraints imposed by a partially saturated setting. The undisturbed (and unsaturated) rock would therefore serve to confine the solution plume within the rubblized zone, providing a safeguard against environmental contamination.

Conclusions

The Casa Grande copper oxide deposit is characterized as a variably-saturated tri-modal porosity system. A network of macrofractures segment the copper ore into blocks which have a bimodal porosity distribution including microfractures and micropores. Once the macrofractures are saturated they act as a source/sink to these ore blocks.

Moisture retention characteristics indicate that a microfracture-micropore permeability continuum exists in the rock blocks. The microfracture permeability diminishes nonlinearly with decreasing saturation, spanning 6 orders of magnitude; hence, fluid flow in the saturated micropores is essentially immobile. Since the microfractures provide internal access to copper-hosted minerals, the unsaturated condition (ambient saturation of 95 percent) will be the dominant control on flow capacity.

Forward modeling demonstrated that solution penetration into ore blocks can be achieved, despite the reduced permeability associated with unsaturated conditions, if well injection pressures are of sufficient magnitude and time permits. Post injection-recovery simulations demonstrated, however, that the bulk of solution injected at 1500 psi for 1 yr (roughly 98 percent) is held captive in the rock by capillary tension, when using the conventional air lifting technique. Conversely, inducing a suction head of -10 m (air entry value - 4 m) for a two-week period immediately following the injection period increases the capacity to recover leach solution (roughly 95 percent). By specifying proper time and pressure constraints, forward modeling can be used to optimize a mine design by determining the maximum block diameter to be derived through rubbilization. Upon rubbilizing a zone to an average block diameter of 4 m, and sustaining an injection pressure of 500 psi for a 100 day period, leach solution could be distributed effectively at the Casa Grande copper oxide tool crib site, while inhibiting flow outward into the surrounding rock mass.

References

Brooks, R. H., and Corey, A. T., 1966, Properties of Porous Media Affecting Fluid Flow. Journal of Irrigation and Drainage Division, Proceedings of the American Society of Civil Engineers, Vol. 92, IR2, pp. 61-89.

Bruce, W. A. and H. J. Welge, 1947, Restored State Method for Determination of Oil in Place and Connate Water. Oil and Gas Journal, Vol. 46, pp. 223-245.

Brutsaert, W., 1968, Probability Laws for Pore-Size Distributions. Soil Science, Vol. 101, pp. 85-92.

Evans, D. D. and T. J. Nicholson, 1987, Flow and Transport Through Unsaturated Fractured Rock. Geophysical Monograph 42, American Geophysical Union, Washington, D.C., pp. 187.

Friedel, M. J., 1991, Modeling In Situ Copper Leaching in an Unsaturated Setting. BuMines RI, In Press, 22 p.

Hassler, G. L. and E. Brunner, 1945, Measurement of Capillary Pressures in Small Core Samples. Trans. AIME, Vol. 160, pp. 114-123.

Klavetter, E. A., and R. R. Peters, 1987, An Evaluation of the Use of Mercury Porosimetry in Calculating Hydrologic Properties of Tuffs from Yucca Mountain, Nevada. SAND86-0286, Sandia National Laboratories, Albuquerque, NM, 1987.

Maulem, Y., 1977, Extension of the Similarity Hypothesis used for Modeling the Soil Water Characteristics. Water Resources Research, Vol. 132, No. 4, pp. 773-780.

McCullough, J. J., and F. W. Albaugh, 1944, Determination of Interstitial Water Content of Oil and Gas Sand by Laboratory Tests of Core Samples. Drilling and Production Practice (A.P.I.), Vol. 180, pp. 53-65.

Nieber, J. L., M. J. Friedel, and H. M. Munir, 1990, TWOD: Two Dimensional Finite Element Analysis of Variably Saturated Flow Using Simplex Elements: Theory, Program Documentation and Users Manual. Bureau of Mines IC (In Press), 35 pp.

Schmidt, R. D., K. C. Behnke, and M. J. Friedel, Hydrologic Considerations of Underground In Situ Copper Leaching. Society of Mining Engineers of AIME, pp. 12.

Thornton, O. F. and D. L. Marshall, 1947, Estimating Interstitial Water by the Capillary Pressure Method. Trans. AIME, Vol. 170, pp. 69-75.

Van Genuchten, T., 1980, A Closed Form Equation for Predicting the Hydraulic Conductivity of Unsaturated Soils. Soil Science Society American Journal, Vol. 44, pp. 892-898.

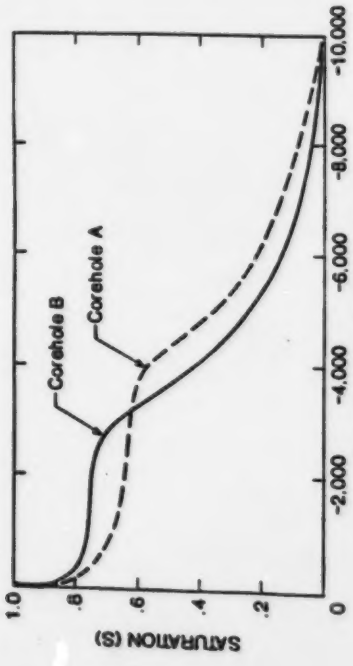

Figure 1. Equivalent moisture retention drainage curves derived from mercury intrusion data for the copper oxide ore obtained from holes A and B.

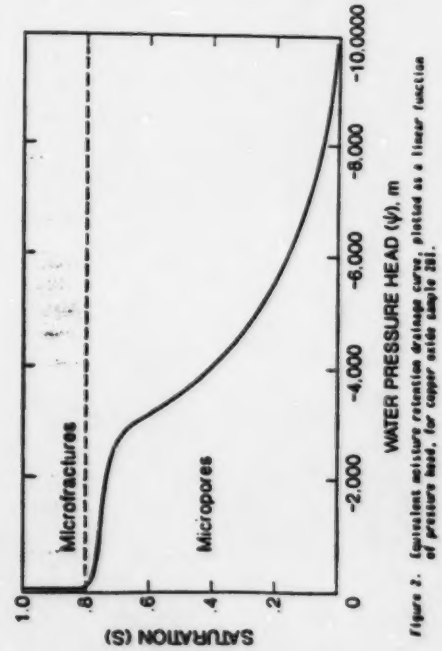

Figure 2. Equivalent moisture retention drainage curve, plotted as a linear function of pressure head, for copper oxide sample 381.

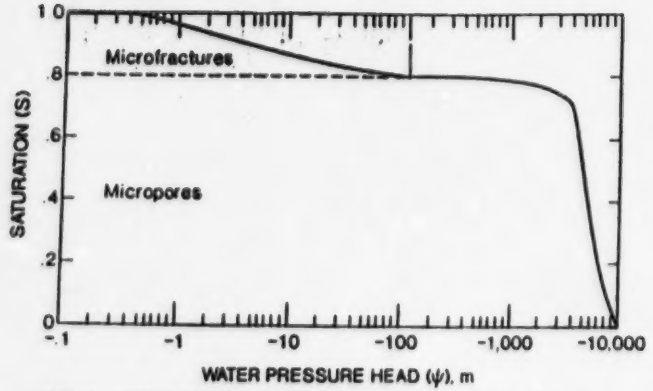

Figure 3. Moisture retention drainage curve plotted as a log function of pressure head, for copper oxide sample 281.

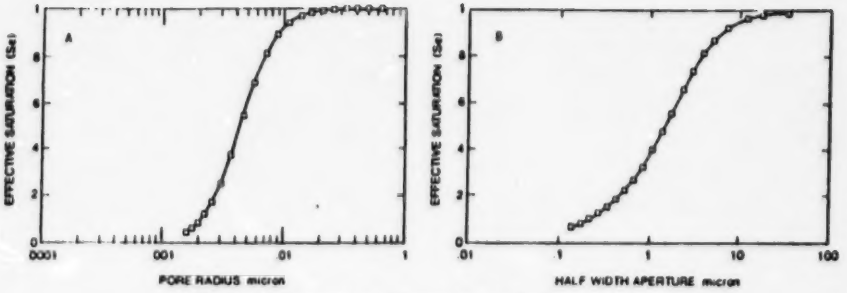

Figure 4. Hydraulic radii of micropores (A) and microfractures (B).

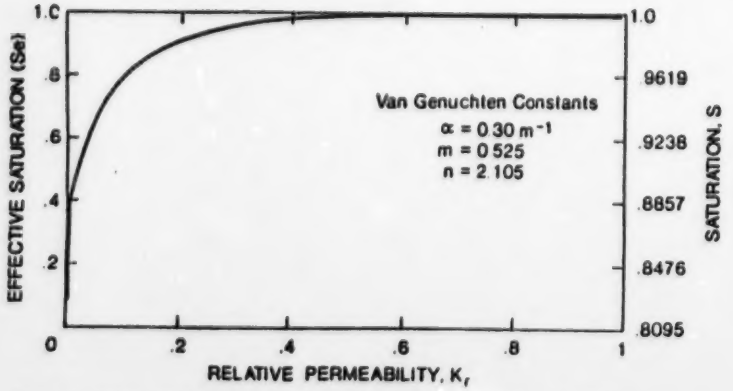

Figure 5. Microfracture saturation plotted as a linear function of relative permeability.

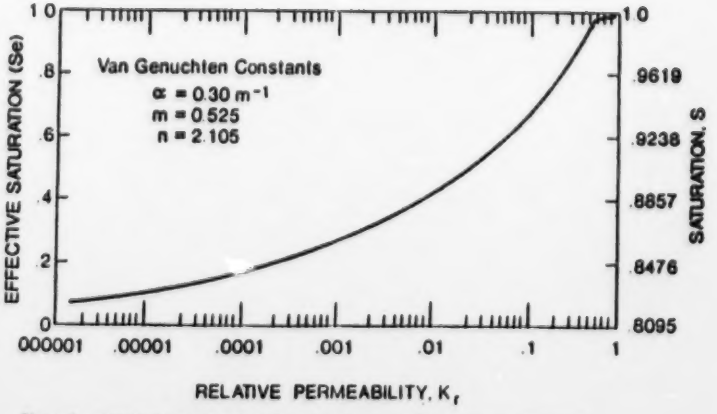

Figure 6. Microfracture saturation plotted as log function of relative permeability.

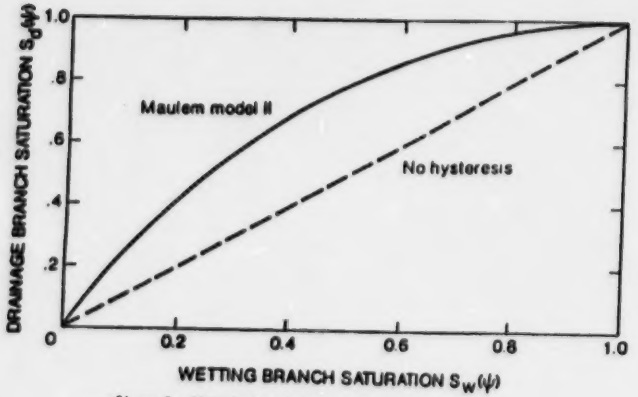

Figure 7. Dimensionless hysteresis curves.

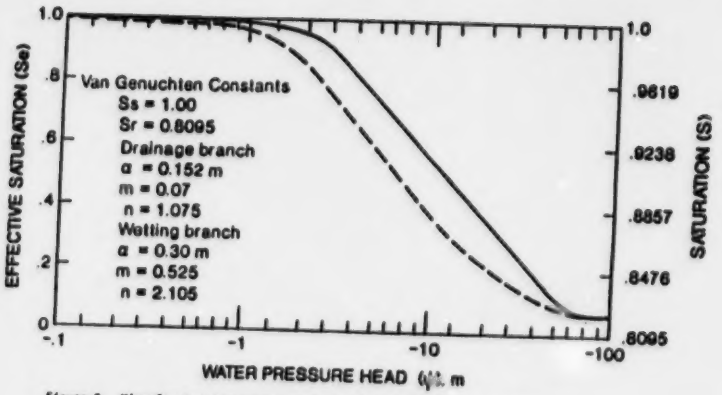

Figure 8. Microfracture hysteresis derived using similarity hypothesis.

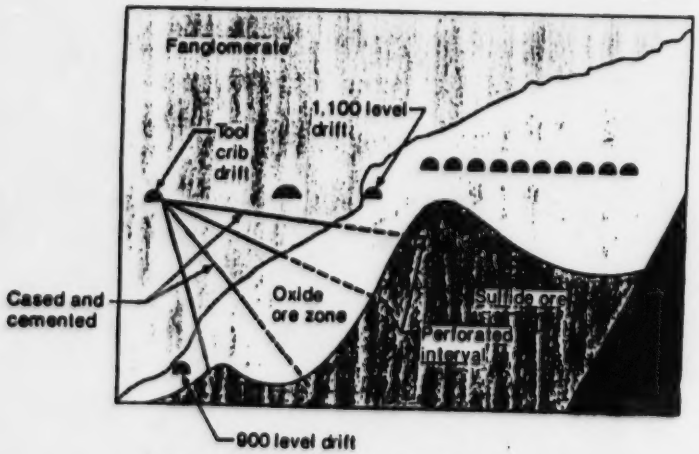

Figure 9. Cross sectional view of the Casa Grande tool crib site.

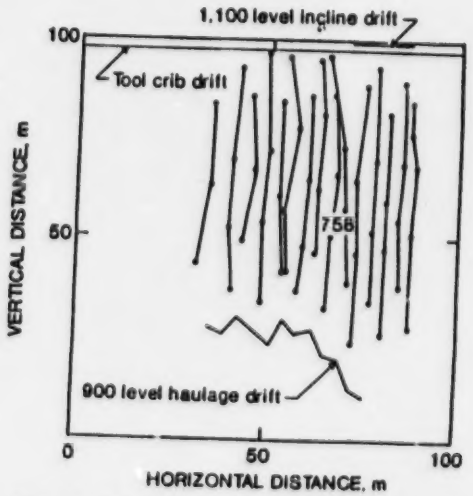

Figure 10. Cross sectional representation of the total well field for the hanging wall.

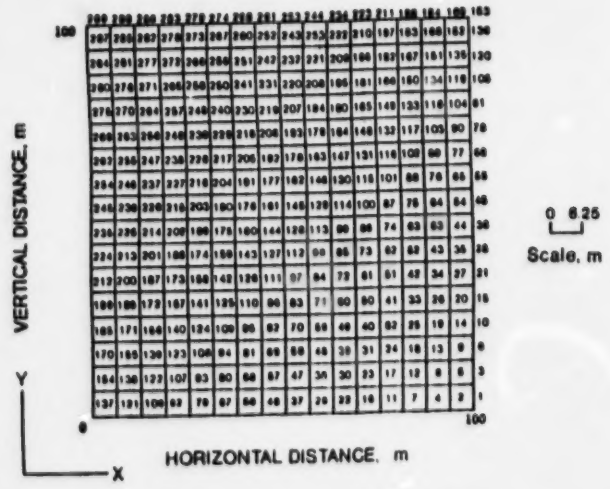

Figure 11. Finite element grid for the hanging wall cross section.

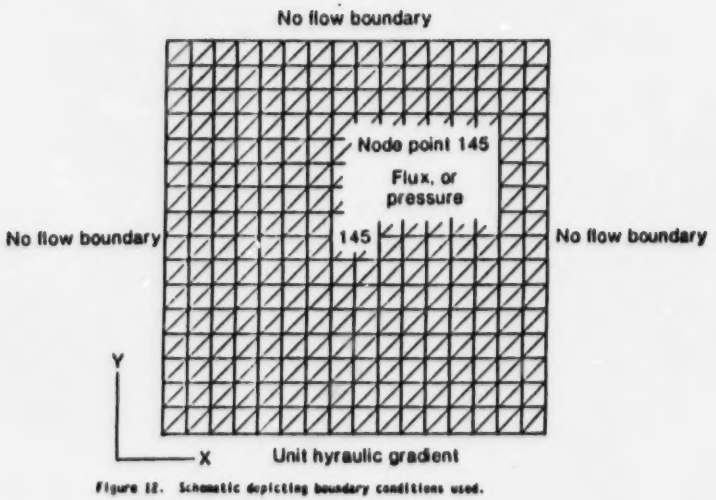

Figure 12. Schematic depicting boundary conditions used.

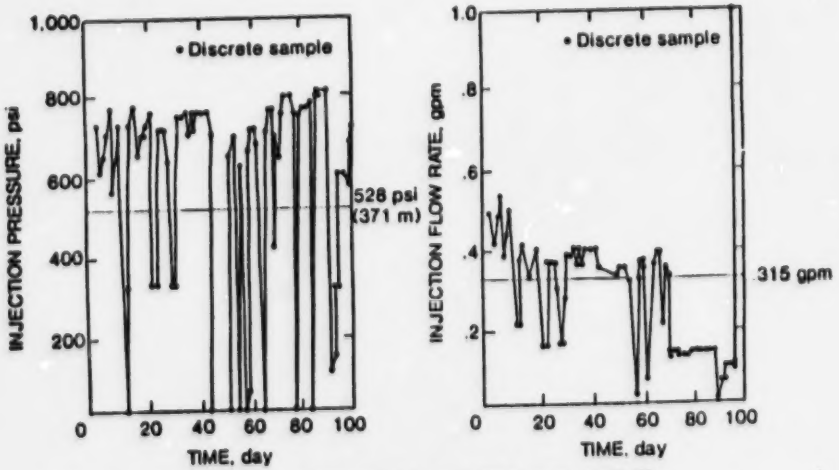

Figure 13. Flow rate and pressure history recorded for first 100 day period in well 75B.

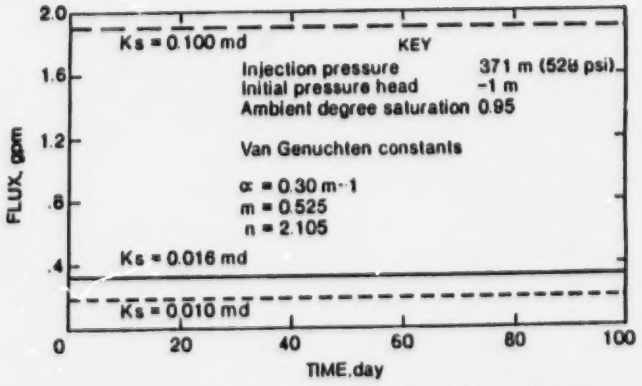

Figure 14. Calibration of model: effect of saturated conductivity on initial flux.

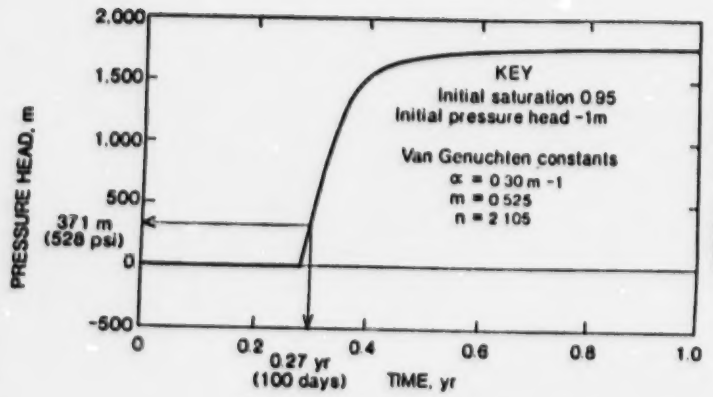

Figure 15. Estimating ambient degree of saturation.

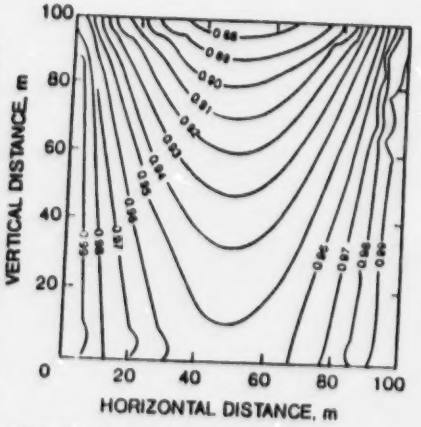

Figure 16. One thousand year drainage simulation.

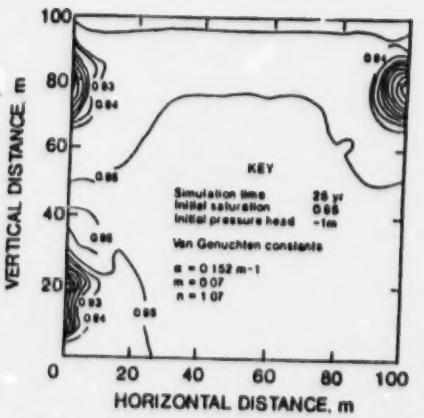

Figure 17. Twenty-five year simulation of impact of drifts on moisture distribution.

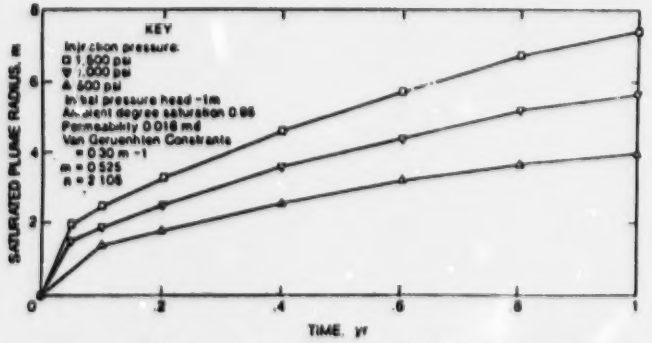

Figure 18. Injection pressure effect on transient build up of a saturated plume.

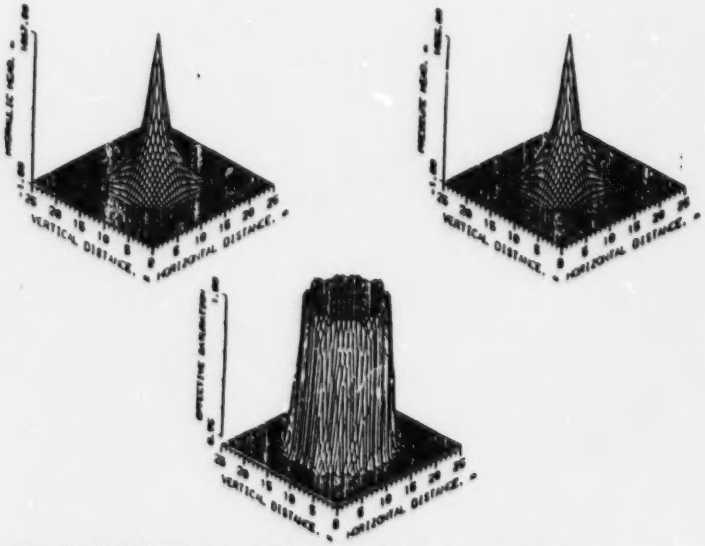

Figure 19. Hydraulic head, pressure head, and fluid distribution for well 258 after a one year period of injection.

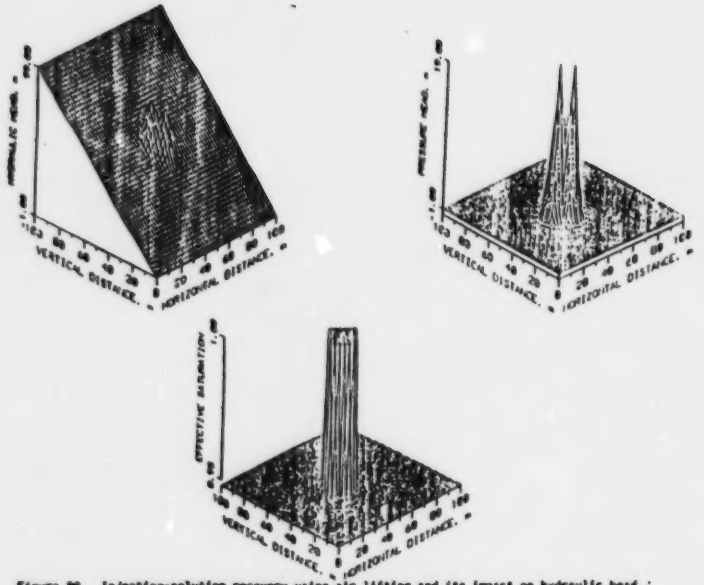

Figure 20. Injection-solution recovery using air lifting and its impact on hydraulic head, pressure head, and fluid distribution for well 758.

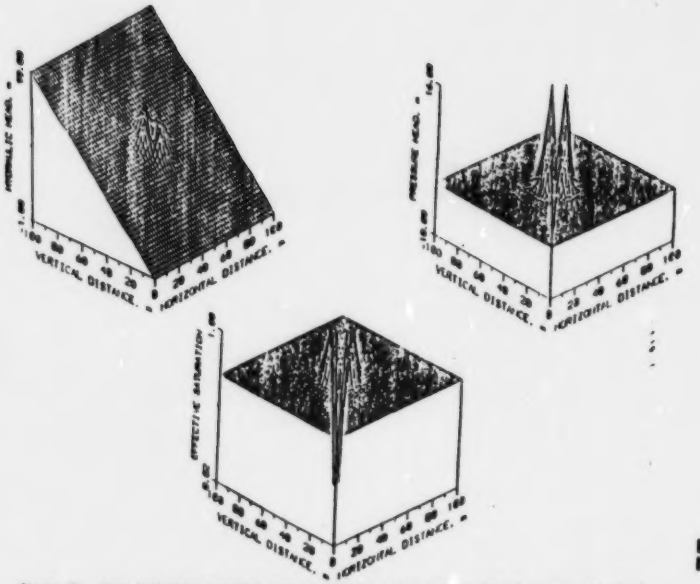

Figure 21. Post injection-solution recovery using suction and its impact on hydraulic head, pressure head, and fluid distribution for well 758.

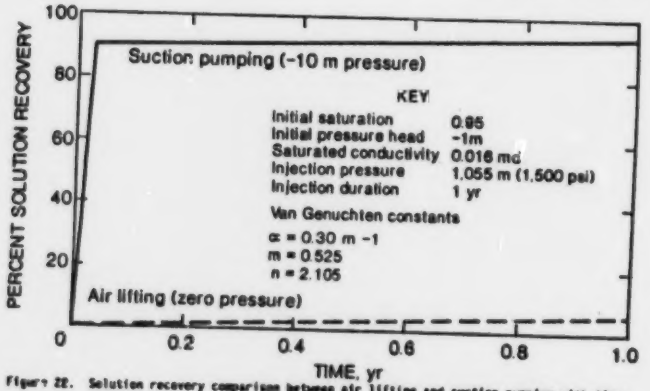

Figure 22. Solution recovery comparison between air lifting and suction pumping with time.

SOCIETY FOR
MINING, METALLURGY, AND
EXPLORATION, INC.

P.O. BOX 625002 • LITTLETON, COLORADO • 80162-5002

PREPRINT
NUMBER
91-177

AN EVALUATION OF THE POTENTIAL FOR SELECTIVE IN SITU LEACH MINING OF MANGANESE ORES

Dianne C. Marozas
Geologist

Steven E. Paulson
Geologist

Lloyd M. Petrie
Research Chemist

Twin Cities Research Center
Bureau of Mines
U.S. Department of the Interior
Minneapolis, Minnesota

For Presentation at the 1991 SME Annual Meeting
Denver, Colorado, February 25-28, 1991

Permission is hereby given to publish with appropriate acknowledgments, excerpts or summaries not to exceed one-fourth of the entire text of the paper. Permission to print in more extended form subsequent to publication by the Society must be obtained from the Executive Director of the Society for Mining, Metallurgy, and Exploration, Inc.

If and when this paper is published by the Society for Mining, Metallurgy, and Exploration, Inc., it may embody certain changes made by agreement between the Technical Publications Committee and the author, so that the form in which it appears is not necessarily that in which it may be published later.

These preprints are available for sale. Mail orders to PREPRINTS, Society for Mining, Metallurgy, and Exploration, Inc., P.O. Box 625002, Littleton, Colorado 80162-5002.

PREPRINT AVAILABILITY LIST IS PUBLISHED PERIODICALLY IN
MINING ENGINEERING

Abstract. The U.S. Bureau of Mines is conducting research to evaluate the potential for developing an in situ leach mining process that will selectively extract manganese from oxide ores, leaving gangue relatively undisturbed. To accomplish this, a geochemical approach, based on deposit-specific information such as mineralogy and geology, is used to constrain the operating parameters of the system. Among the studies being conducted are (1) leaching experiments to define reaction mechanisms and kinetics, (2) detailed petrologic characterization at the microscopic scale to assess Mn distribution and leaching efficiencies, (3) deposit characterization and evaluation, and (4) development of potential Mn recovery schemes. Data from these studies are being used to develop engineering design information for an in situ mining process. Specific details of the Bureau's research project are discussed, including results obtained to date.

Introduction

The Bureau of Mines is conducting research to develop cost effective, environmentally compatible advanced mining technologies for the selective extraction of critical and strategic metals. Critical and strategic metals (e.g. manganese, cobalt, and chromium) are essential to domestic steel, aerospace, electronic and defense-oriented industries. The United States no longer has high-grade deposits of these minerals and must import most of its supply from foreign sources (Dept. of Interior, 1990). Advanced mining technologies such as in situ leach mining (ISLM) could make domestic production of these metals feasible for ore deposits that are now unattractive to conventional mining because of their small size, low grade, or depth.

In situ leach mining requires lower capital investment, manpower requirements, and energy consumption than does conventional mining and milling. Therefore, in situ leach mining may be economically attractive for many critical and strategic metal deposits. In situ leach mining offers improved health and safety conditions for the miner and may be performed at substantially reduced environmental impact. Based upon criteria which include analysis of chemical and metallurgical characteristics, mineralogy, and deposit geology, the Bureau has determined that manganese is one critical and strategic commodity with potential for recovery using in situ leach mining techniques.

Manganese is a strategic commodity because of its importance in steel production. In 1989, 100 % of the manganese consumed in the United States was imported (Dept. of Interior, 1990). Industry has not been able to employ conventional mining techniques to recover manganese since the late 1940's, because of the prohibitive costs of mining and processing low grade, relatively small, and deep ore deposits. The United States has low grade deposits of manganese that could be utilized to reduce the reliance on foreign sources of supply, such as Artillery Peak in Arizona, the Cuyuna Range in Minnesota, and the Aroostook District in Maine. Previous research shows that manganese can be extracted from low grade domestic ores by leaching with aqueous sulfur dioxide (SO_2) solutions, but it is unknown whether this technique can be used to develop an overall in situ leach mining process. Therefore, the Bureau has initiated a new research program to study the application of in situ leach mining techniques to recover manganese from domestic deposits. This report presents the Bureau's experimental approach to this problem and preliminary findings from this research.

Previous In Situ Leach Mining Research by the Bureau of Mines

The Bureau of Mines has gained significant experience in the area of in situ leach mining (ISLM) research from its past and current projects on uranium and copper ores. The first successful application of ISLM in which the Bureau of Mines participated, was uranium leach mining of sandstones in Texas (Larson, 1978). More recently, the Bureau has concentrated on ISLM of a deep copper oxide deposit in Arizona. This project has demonstrated the importance of geologic characterization studies in predicting metal recoveries and in determining the physical and chemical constraints for in situ leach mining operations (Paulson et al., 1987; Paulson, 1989; Cook and Paulson, 1988; Cook, 1988; Paulson and Kuhlman, 1989).

ISLM has been found to be most effective when the commodity of interest can be selectively removed from the host ore. Selective leaching can be achieved in a variety of ways. The lixiviant can be a non-specific solvent such as acid which will react to dissolve both ore and gangue. In this type of system, selective leaching can be effective if the amount of acid contacting the ore minerals is much greater than that contacting gangue. An example of this situation is in fracture hosted porphyry copper deposits where flow channels are lined with copper bearing minerals. Selective leaching can also be achieved with a non-specific solvent if the ore dissolution reactions are much faster than the gangue dissolution reactions. An example of this is a copper oxide ore deposit where copper oxide minerals are much more soluble in dilute sulfuric acid than matrix gangue minerals such as quartz or feldspar.

Typically, manganese deposits do not have the required characteristics to be leached by a non-specific lixiviant. Oftentimes, manganese minerals are intimately associated with iron oxide minerals as part of the rock matrix and are not associated with fractures. Because of these characteristics effective leaching can only be achieved by lixiviant systems that are chemically selective for manganese in the presence of gangue minerals. Chemically selective techniques developed for manganese may also be applicable to other commodities in the future.

Previous Research on Manganese Ore Leaching

Much research has been reported on the leaching of manganese ores and on individual manganese minerals. Previous research that directly pertains to mining or mineral processing of manganese may also have application to in situ leach mining of manganese.

Domestic Mn Deposits and Their Leachability: A comprehensive discussion of worldwide manganese deposits, including U.S. deposits, is presented by Roy (1981). Potter et al. (1982) reported six U.S. locations with significant low grade manganese ore deposits. Pahlman and Khalafalla (1988) reported on SO_2 leaching of manganese ores, including a number of samples from the above six deposits (Table 1). In addition to manganese mineralogy, Table 2 lists the principal gangue mineralogy. Gangue consumption of lixiviant is an important consideration during in situ leach mining optimization as it depletes the lixiviant available for metal dissolution. Oxides are the most common and abundant manganese minerals found in U.S. deposits, followed by carbonates and silicates. Table 3 summarizes the composition and structure of the key manganese minerals found in U.S. manganese deposits, including the valence and coordination number of manganese metal centers.

Table 1. Location of Significant U.S. Manganese Ore Deposits

Artillery Peak, Arizona (oxides)
Batesville, Arkansas (manganiferous limestone)
San Juan Mountains, Colorado (silicates)
Chamberlain, South Dakota (manganese nodules)
Aroostook County, Main (silicates and carbonates)
Cuyuna Range, Minnesota (oxides and carbonates)

From a geochemical kinetics perspective, there are several observations to be made from the data in Table 3. First, these minerals have manganese centers with a range of oxidation states (4+, 3+, 2+). The charge on a manganese center significantly affects the chemical stability and dissolution reactivity of the mineral. Second, manganese centers usually have a bonding coordination number of six, indicating the octahedral bonding symmetry common to manganese ions in solution. Third, oxygen is the most common element bonded to manganese. Fourth, the structural differences of manganese minerals vary enough to possibly affect dissolution reactivity. For example, the basic unit for pyrolusite and manganite, form relatively tight chain structures, whereas romanechite consists of triple chains of units that form open tunnels (Burns and Burns 1979). This means that more romanechite Mn sites may be available for dissolution by the lixiviant than pyrolusite or manganite manganese sites.

Selective Oxide Dissolution with Dissolved SO_2: One lixiviant, sulfur dioxide (SO_2), has been extensively investigated since it is capable of rapidly dissolving acid resistant manganese oxides such as pyrolusite. The Bureau of Mines has a long involvement in the processing of low-grade manganese ores with SO_2 solutions. Early Bureau work was reviewed in a Bureau Information Circular by Dean, Leaver, and Joseph (1934), which detailed hydrometallurgical processes using SO_2. Wyman and Ravitz (1947) discussed the selective nature of SO_2 leaching for manganese over iron and other gangue in domestic ores. They determined the composition of the final leachates, but did not construct detailed composition versus time (or SO_2 amount) leaching curves.

Back, Ravitz, and Tame (1952) reported SO_2 processing of MnO_2 ores under aerobic conditions. They observed decreased $S_2O_6^=$ formation with lowered pH and increased agitation (i.e. increased solution oxygenation). For example, only 3 % $S_2O_6^=$ was formed at pH 0.75 versus 8 % at pH 1.90 for well agitated systems. This work was part of the research for the "dithionate process" that was developed by the Bureau for processing low-grade manganese dioxide ores.

Herring and Ravitz (1965) found that the rate of manganese dioxide reductive dissolution was faster at lower pH values, for example, 7.6 micromole min^{-1} $(cm^2)^{-1}$ at pH 1.82 versus 80.4 micromole min^{-1} $(cm^2)^{-1}$ at pH 1.09. These results indicated that manganese dissolution was approximately 10 times faster for SO_2 than for HSO_3^-. The reaction rates were also faster with increasing stirring rate, indicating a transport-controlled reaction. This was confirmed by a low apparent activation energy of 4.5 $\pm$ 0.2 kcal/mole.

Henn, Kirby, and Norman (1968) reviewed 10 major processes for manganese ore which employ SO_2. Nine of the processes use SO_2, H_2SO_4, or a combination of SO_2 and H_2SO_4. The tenth process uses a SO_2 roast at 600^0 to 850^0 C before a water leach.

Miller and Wan (1983) reported work devoted to the kinetics of reductive dissolution of electrolytic MnO_2 and pyrolusite. They concluded that the leaching process was rate-limited by a mineral surface reduction reaction obeying the following rate law:

$$\text{Rate} = d(MnO_2)/dt = k^* K_a^{0.5} A_c [SO_2]_{total}^{0.5} ([H^+]/([H^+]+K_a))^{0.5} \quad (1)$$

where k^* = heterogeneous rate constant
K_a = equilibrium constant for $SO_2 + H_2O = H^+ + HSO_3^-$
A_c = active surface area of MnO_2 mineral

TABLE 2. - Mn ore sample characteristics[7]

Sample	District	County and State	Mn[1] Form	Mn minerals	Principal gangue minerals	Origin
AZ-1..	Harshaw.....	Santa Cruz, AZ..	Ox.....	Psilomelane, pyrolusite, braunite.	Anglesite, quartzite, felsite, rhyolite, galena.	4
AZ-2..	..do.....	..do.....	..do...	Psilomelane, pyrolusite.	Quartzite, anglesite, felsite, rhyolite, galena.	4
AZ-3..	Tombstone.....	Cochise, AZ.....	..do...	..do.....	Quartz, calcite, dolomite.	4
AZ-4..	..do.....	..do.....	..do...	..do.....	..do.....	4
AZ-5..	Artillery Peak....	Mohave, AZ.....	..do...	Wad, pyrolusite, psilomelane	Quartz, albite, calcite, clay.	3
AR-1..	Batesville.....	Independence, AR	..do...	Hausmannite, braunite, wad, psilomelane, pyrolusite.	Calcite, clay, hematite, chert.	4
AR-2..	..do.....	..do.....	..do...	..do.....	..do.....	4
CA-1..	Paymaster.....	Imperial, CA....	..do...	Manganite, pyrolusite, psilomelane.	Calcite, barite, chalcedony.	4
CO-1..	Leadville.....	Lake, CO.....	..do...	Psilomelane, pyrolusite, manganosiderite.	Quartz, calcite, hematite, goethite.	4
CO-2..	Silvercliff.....	Custer, CO.....	Ox.....	Cryptomelane.	Quartz, hematite.	4
CO-3..	San Juan.....	San Juan, CO....	Sil....	Rhodonite[2].	Quartz, chalcedony, galena, sphalerite, pyrite.	4
ME-1..	Aroostook.....	Aroostook, ME...	Carb-sil	Braunite, bementite, rhodochrosite.	Hematite, quartz, pyrite, calcite.	5
ME-2..	..do.....	..do.....	..do...	Rhodonite, braunite, bementite, rhodochrosite.	..do.....	5
MN-1..	Cuyuna.....	Crow Wing, MN...	Ox-carb	Rhodochrosite, manganite, pyrolusite.	Goethite, siderite, quartz, groutite.	3
MN-2..	..do.....	..do.....	Ox.....	Stilpnomelane, pyrolusite.	Hematite, quartz.	3
MN-3..	..do.....	..do.....	..do...	Manganite, pyrolusite, stilpnomelane.	Hematite, quartz, talc.	3
MN-4..	..do.....	..do.....	..do...	..do.....	..do.....	3
MN-5..	..do.....	..do.....	..do...	Pyrolusite, stilpnomelane.	..do.....	3
NV-1..	Pioche.....	Lincoln, NV.....	..do...	Manganite, braunite.	Goethite, quartz, calcite.	4
NV-2..	Three Kids.....	Clark, NV.....	..do...	Wad, psilomelane, manganite.	Quartz, clay, mica, hematite, calcite	3
NV-3..	Virgin River.....	..do.....	..do...	Wad, psilomelane.	..do.....	3
NV-4..	Boulder City.....	..do.....	..do...	..do.....	Selenite, limonite, quartz, calcite.	3
NV-5..	Pioche.....	Lincoln, NV.....	..do...	Pyrolusite.	Calcite, quartz.	4
NV-6..	..do.....	..do.....	..do...	..do.....	Siderite, galena, dolomite, quartz.	4
SD-1..	Chamberlain.....	Lyman, SD.....	Carb...	Manganocalcite, pyrolusite, manganite.	Siderite, calcite, dolomite, quartz, clay.	6

[1] Ox oxide, Sil silicate, Carb carbonate.
[2] May be the pyroxmanganite variety.
[3] Sedimentary.
[4] Hydrothermal vein
[5] Submarine volcanic, sedimentary
[6] Fossil sea nodules, sedimentary.
[7] Source: Reference 8.

TABLE 3. - Composition and structure of key U.S. manganese minerals

Mineral	Composition	Structure	Oxidation of Mn	Coordination Number
pyrolusite	β-MnO_2	tetragonal	+4	6
romanechite (psilomelane)	$Ba(OH)_4Mn^{2+}Mn^{4+}{}_8O_{16}$	monoclinic	+4 +2	6 6
hausmannite	$Mn^{2+}Mn^{3+}{}_2O_4$	tetragonal	+3 +2	6 4
manganite	γ-MnOOH	monoclinic	+3	6
braunite	$(Mn^{3+}{}_2O_3)_3Mn^{2+}SiO_3$	tetragonal	+3 +2	6 6
rhodochrosite	$MnCO_3$	trigonal (rhombohedral)	+2	6
rhodonite	$MnSiO_3$	triclinic	+2	6

Dixit and Raisoni have reported their work in two recent reports. In the first report (1987), they demonstrated that sufficiently high concentrations of dissolved O_2 will suppress the reductive dissolution of MnO_2 with SO_2. Viewed from a geochemical perspective, this is a reminder that reductive dissolution of MnO_2 requires an overall reducing solution environment, i.e. a low Eh value. In their second report (Raisoni and Dixit, 1988), dissolution rates of MnO_2 fit the metallurgical equation for diffusion-controlled release of Mn^{2+} through an unreacted product layer:

$$\text{Dissolution Rate} = kt = 1 - 2/3\ a - (1 - a)^{2/3} \qquad (2)$$

where k = rate constant
t = time
a = fraction manganese leached

Khalafalla and Pahlman (1981) reported an important Bureau study that demonstrated the use of SO_2 for selective extraction of critical and strategic metals (i.e. Mn, Co, Ni) from Pacific ferromanganese nodules. For a series of batch leaching experiments, they observed that increasing molar ratios of SO_2 in the lixiviant to grams of nodules leached resulted in a reproducible sequence of different metals being preferentially leached:

$$\underset{\text{first}}{Mn} > Ni > Co >> Fe, Al, Cu \quad \underset{\text{last}}{} \qquad (3)$$

Figure 1, from Khalafalla and Pahlman (1981), shows their results and demonstrates the dramatic selective preference of SO_2 for Mn, then Ni and Co. Fe, Al, and Cu were leached only after most of the Mn, Ni, and Co had been leached.

Of the many research reports dealing with the rapid SO_2 dissolution of domestic manganese ores, the report by Pahlman and Khalafalla (1988) is the most relevant to in situ leach mining. They presented very encouraging new results from batch and column leaching of 25 U.S. manganese ores exposed to 5-6.4 wt % SO_2 solutions. Table 4 summarizes the batch leaching results. First, they achieved typically greater than 90% Mn recoveries for manganese oxides while solubilizing less than 10% of Fe from hematite (Fe_2O_3), a key gangue mineral. Less abundant Fe carbonate (siderite) and hydroxide (goethite) readily dissolved in SO_2 solution. Second, at low SO_2 application rates (1 mL/min) to the column, calcite ($CaCO_3$) solubilization was minimized by formation of an insoluble reaction layer, which suppressed further leaching of $CaCO_3$. The reaction layer was composed of a Ca-S compound, most likely gypsum. Lastly and very importantly, the SO_2 lixiviant was still effective in leaching Mn from ores with permeabilities as low as 10^{-2} to 10^{-4} darcies. This result strongly supports the argument that rapid dissolution of Mn minerals may increase permeability and thus, increase lixiviant penetration into the ore body.

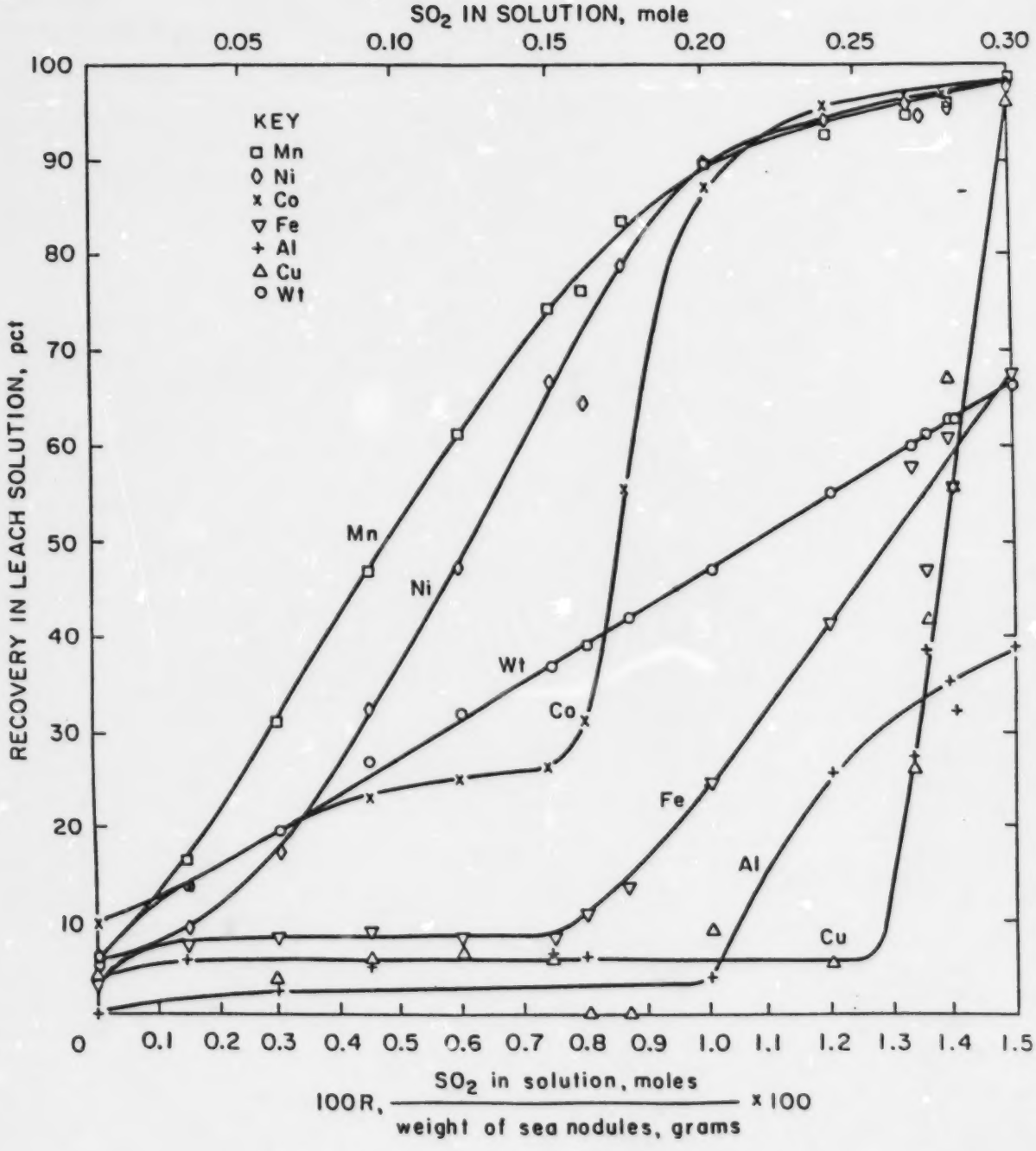

Figure 1. Leaching curves for several metals for 20 grams minus 200-mesh deep-sea nodule particles in water containing various quantitities of SO_2. Adapted from Khalafalla and Pahlman (1981), p. 10.

TABLE 4. - Batch leaching efficiencies for U.S. manganese ores[1]

Manganese Ore Mineralogy	No. of Samples[2]	Mn leached (%) Ave.	Range	Ca leached (%) Ave.	Range	Fe leached (%) Ave.	Range
pyrolusite, romanechite	6	95 ± 3	91-98	56 ± 25	25-81	14 ± 7[3]	1-25
hausmannite, braunite	2	79 ± 6	76-81	70 ± 20	56-84	4 ± 2	2-5
rhodochrosite	3	67 ± 11	55-76	64 ± 15	48-78	9 ± 1[3]	1-9
manganite	2	59 ± 7	54-64	34, 92[4]	34-92	5 ± 2	3-6
rhodonite	2	0	0	23, 75[4]	23-75	1, 23[4]	1-23

[1] Batch leach of -0.841 mm particles with 6.4 wt % SnO_2 at pH 1.1 for 30 minutes at ambient temperature and pressure. Source: Pahlman and Khalafalla (1988). The average leached amounts are stated as average ± standard deviation.

[2] Each sample represents a different ore body, generally from a different state, which contains the predominant manganese minerals listed.

[3] One sample had a 1% Fe leaching efficiency which was not used in the average.

[4] Due to the large difference between the two numbers, no average was calculated.

Other Lixiviants for Manganese Ore Dissolution: In addition to SO_2 leaching of manganese oxides, other chemical lixiviants have been used to leach manganese minerals. Some of these metallurgical reductants may be adaptable to an in situ leach mining process.

Warren and Devuysst (1972) reported hydrazine hydrate ($N_2H_4.H_2O$) extracted 90% of Mn from minus 65, plus 150 mesh pyrolusite in one hour. Hydrazine hydrate is a strong reductant but its high cost at the time prevented its consideration for commercial use.

Malati, Rophael, and Bhayat (1981) used $N_2H_4.H_2O$, followed by pyrophosphate ($H_2P_2O_7$), to reduce electrolytic γ-MnO_2 and β-MnO_2. They also reported that the reduction product of the Mn oxides with $N_2H_4 \cdot H_2O$ was $Mn^{3+}OOH$.

After investigating a number of strong reducing agents, Usatenko and Ryl'kova (1983) reported that potassium iodide (KI) was the most effective reductant for pyrolusite and romanechite in manganese ores. Using 20 wt. % KI in 0.3-0.4 M acetic acid, they dissolved 96 to 99 % of the pyrolusite and romanechite present. They also suppressed reduction of manganite by adding EDTA to prevent the further reduction of Mn^{3+} metal centers in manganite to water-soluble Mn^{2+}.

Dresler (1984) reported very rapid leaching of γ-MnO_2 with nitrous acid (HNO_2) solutions. Since his stirred reaction cell was similar to Herring and Ravitz's SO_2 leaching cell for γ-MnO_2 (28), Dresler compared overall leaching rates between his HNO_2 work and their SO_2 research. The overall leaching rates for HNO_2 were reported to be "slightly higher than those in sulfurous acid". It should be noted that NO_2^- has the same electron configuration as SO_2. Therefore, HNO_2 could be a promising potential lixiviant for in situ leach mining if the costs to produce nitrous acid were reasonable.

Recently, Dobos (1988) reported the effective use of a strong-acid cation exchange resin to accelerate acid leaching of metal carbonates such as rhodochrosite ($MnCO_3$) and recover the resulting cation. The resin was added to a sulfuric acid suspension containing 19 wt. % manganese ores. Optimization of the process was performed for such variables as temperature, pH, and supporting electrolyte (i.e. NaCl). Kinetic data was presented.

Selective Leaching of Manganese by SO_2 in the Presence of Gangue: An important aspect of advanced mining research is to develop leaching reagents that will selectively leach the target element (i.e. manganese) with a minimum of gangue dissolution. This ability is significant because selective mobilization will reduce processing of in situ mining leachant and will minimize the potential environmental impact of mining. In order to optimize the selectivity of a leach mining lixiviant system, it is necessary to have a detailed knowledge of the geochemistry of target and gangue minerals.

The Bureau of Mines is developing an approach to selective lixiviant development that centers on the geology and geochemistry of target ore bodies. It is called geochemical characterization to emphasize its close relationship to the geologic characterization (i.e. petrology) of a target ore body. Figure 2 summarizes this interactive lab experimentation and geochemical modeling process that begins with ore petrology, proceeds through basic

GEOCHEMICAL CHARACTERIZATION

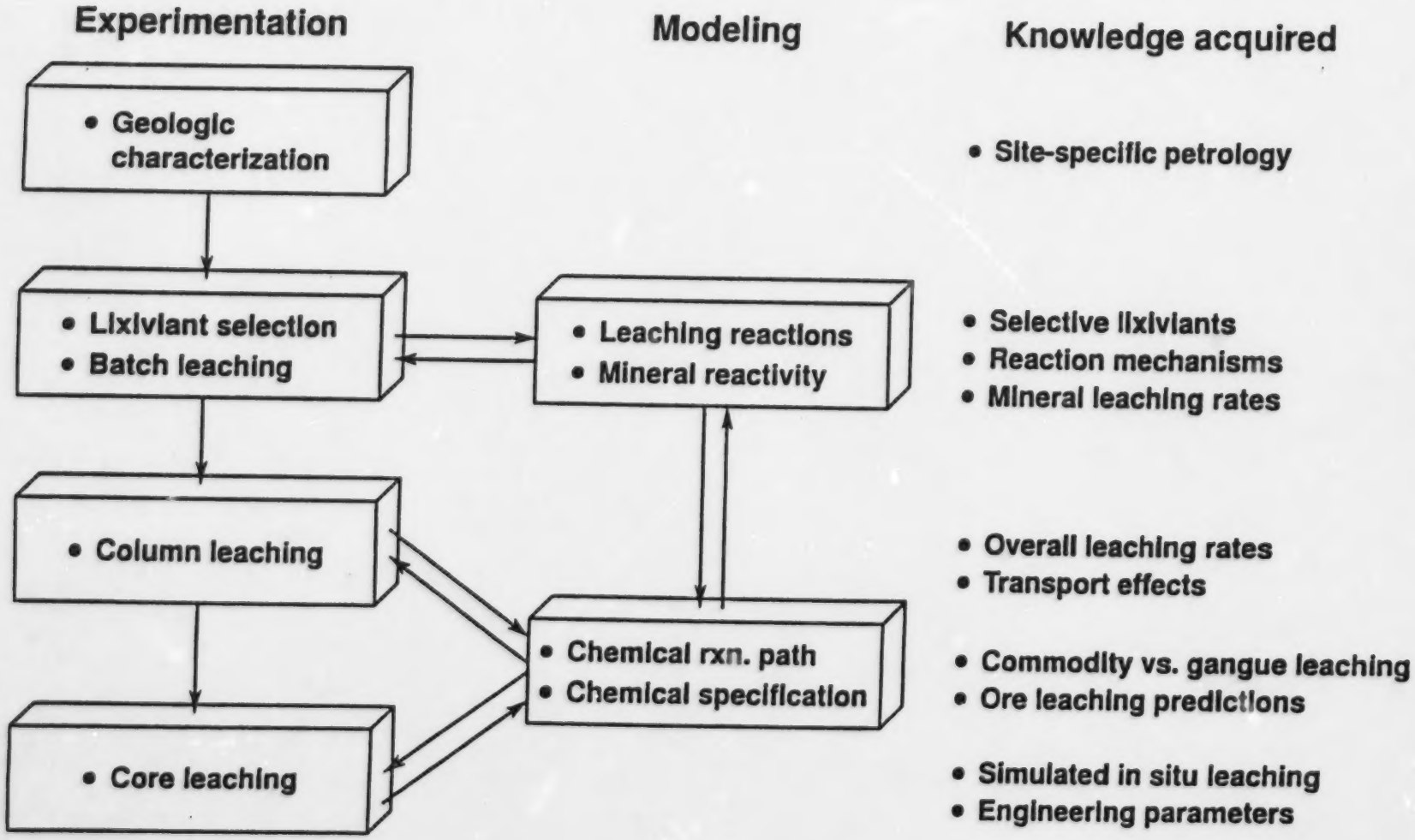

Figure 2. Description of geochemical characterization, which includes interrelated

single mineral leaching chemistry, and concludes with generation of design parameters for in situ leach mining.

It is important to emphasize that both a thermodynamic and kinetic study of mineral leaching is necessary because a number of geochemical processes, including mineral leaching, are frequently not at equilibrium or steady-state (Hoffman 1981, Morgan 1989). When ore leaching is not at equilibrium, the relative rates of mobilization of target metals versus gangue will depend on the relative dissolution rates of the minerals. Then the objective is to find a lixiviant system that rapidly dissolves target minerals and slowly dissolves gangue.

In the case of manganese, SO_2 has been shown to dissolve the abundant manganese oxides more rapidly than iron oxides, such as hematite (Fe_2O_3) (Pahlman and Khalafalla 1988). In fact, manganese oxides with Mn^{4+} (e.g. pyrolusite, romanechite) dissolve more rapidly than Mn^{3+} oxides (e.g. hausmannite, manganite).

A recent report by Petrie (1991) has provided a theoretical chemical explanation why Mn^{4+} minerals would react more rapidly with SO_2 than Mn^{3+} minerals. Manganese is most stable in water as Mn^{2+} ions. This means that dissolution of Mn^{4+} and Mn^{3+} minerals must involve reduction of the manganese to Mn^{2+}. Based on a molecular orbital treatment of manganese mineral reduction by SO_2, reduction of Mn^{4+} minerals (e.g. pyrolusite) should occur more rapidly than Mn^{3+} minerals (e.g. manganite). Further geochemical characterization is currently underway to further identify the leaching kinetics of manganese and gangue minerals present in key domestic manganese ore bodies.

Experimental Approach

The Bureau of Mines has been conducting in situ leach mining research since the 1970's. While this research has covered a number of different areas, perhaps the most important facet of this research has been to combine laboratory leaching (i.e. geochemical characterization) with geologic characterization studies. Information generated from these studies is essential to developing an understanding of the reaction mechanisms operating during leaching and in assessing a number of variables which impact on the overall process. The ultimate goal of such laboratory studies is to formulate predictions and estimates of what can be expected during actual in situ leach mining of candidate deposits.

Previous Bureau of Mines in situ mining research (BuMines 1981, BuMines 1989, and references therein) has led to the development of a systematic experimental approach which combines a variety of laboratory leaching experiments with detailed pre- and post-leach petrologic studies. This approach allows the study of ore leaching characteristics with respect to of variables such as ore and gangue mineralogy, textural features, and lixiviant composition. This information is then combined with deposit-specific data obtained from field studies to evaluate the potential for in situ leach mining of that particular deposit. In addition to laboratory research to study the leaching process, another very important part of the laboratory research is an evaluation of the various metal recovery options which are both technically and economically feasible. A viable metal recovery scheme is critical, because without it in situ leach mining will be unsuccessful, regardless of favorable leaching and field conditions. As part of the Bureau's critical and strategic minerals in situ mining program, a number of different domestic manganese deposits are being evaluated for their amenability to in situ leach mining. The following sections describe the types of laboratory and field studies that are being conducted to facilitate these evaluations.

Geochemical Characterization - Leaching Experiments

A variety of leaching experiments are conducted in order to determine the leaching characteristics of each ore type being evaluated. These experiments include batch, cube, column, and core leaching tests. It is important to closely control and monitor the experiments, since SO_2 is volatile and will be lost from an open system, thus complicating the interpretation of leaching results. Batch leaching tests are usually conducted on crushed or finely ground ore which are continuously agitated and are intended to determine the bulk reactivity of the ore and also yield information on kinetics of leaching. The batch tests are used to investigate the response of particular lithologies or mineral assemblages to the lixiviant. The batch experiments allow precise control and measurement of system variables such as pH, Eh, temperature, and SO_2 concentration in a closed system. The effects of modified lixiviants on leaching behavior can be quickly determined in batch tests. They are also useful for estimating maximum metal recoveries, recovery rates, and SO_2 consumption by gangue minerals. Cube leaching experiments are conducted by suspending a cube of ore in a continuously-agitated SO_2 solution, and are intended to determine how the leaching front advances and at what rate. These tests often illustrate the textural influences of the ore on leaching.

Once a basic understanding of the leaching characteristics is obtained through the batch and cube leaching studies, column and core leaching experiments are conducted to develop estimates of parameters such as Mn recovery, recovery rates, gangue reagent consumption, and permeability changes expected during true in situ mining. Column leaching tests using crushed ore are conducted at different scales depending on ore availability and leachant requirements. It is ideal to use a closed system for the column tests in order to avoid SO_2 volatilization prior to application to the columns or after collection of the Mn-bearing leachant if any unreacted SO_2 remains in solution (Figure 3). Compressed SO_2 gas is used to prepare the lixiviant

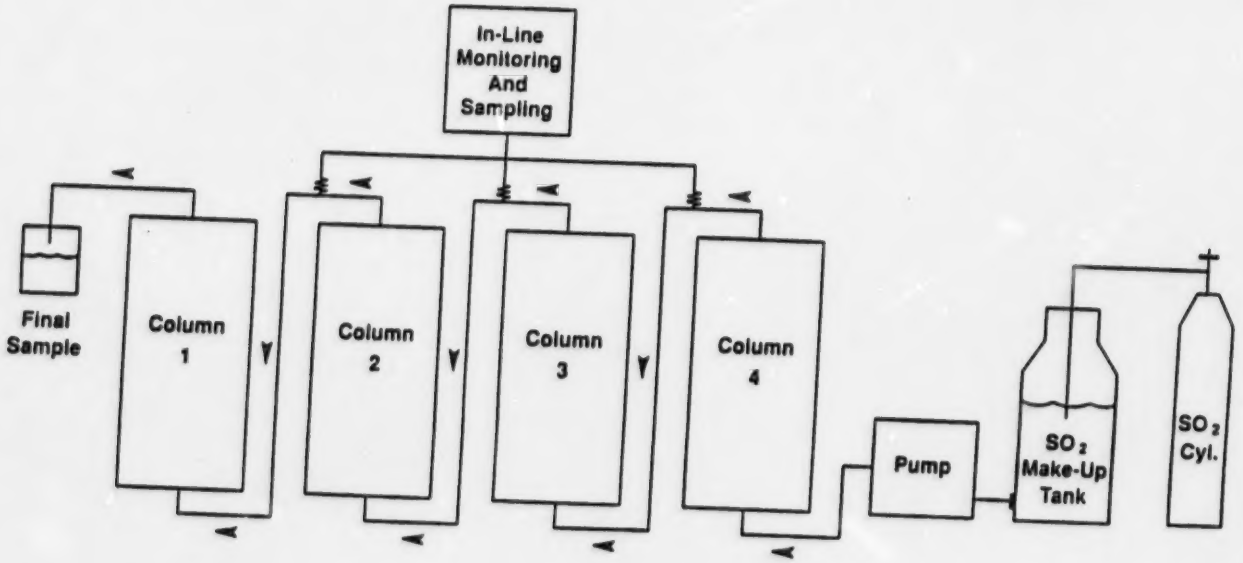

Figure 3. - Closed Column Leaching System

in a continuous batch fashion (Figure 3). This eliminates materials handling problems and allows for a completely closed leaching system to be maintained. A closed collection vessel pressurized with an inert gas (nitrogen, argon) ensures that unreacted SO_2 stays in solution. Such a leaching system allows for an assessment of the leaching chemistry as a function of time, including the total amount of SO_2 consumed. In line monitoring and computerized data acquisition are also utilized to obtain real-time data on pH, Eh, temperature, and pressure.

Leaching experiments conducted on samples of drill core are also an effective means to evaluate leaching chemistry and yield data not obtained from column leaching tests. In addition to providing chemical data, core leaching experiments will also provide information on permeability changes resulting from mineral dissolution, precipitation, or clay hydration. This is important since the maintenance of adequate permeability is critical to the success of any in situ leach mining operation. In a situation where the ore mineralization is fracture-hosted, core leaching experiments may yield significantly different data than column tests due to increased ore mineral accessibility (Paulson, 1989). A variety of configurations and materials can be used to conduct core leaching tests (Paulson and Kuhlman, 1989), but the basic design is similar in all: a section of core is placed within a piece of pipe, encased in epoxy and sealed with end caps. Lixiviant is pumped through the core in an axial direction and collected in a closed vessel prior to sampling and analysis (Paulson and Kuhlman, 1989). The differential pressure across the sample is monitored using a pressure transducer in order to evaluate real-time permeability changes. Upon completion of the experiment, the remaining core material is impregnated with epoxy and prepared for petrologic studies.

In summary, the combination pre- and post-leach petrologic studies with a variety of leaching experiments are intended to yield information which will ultimately allow for predictions as to what can be expected when applying in situ leach mining to an actual Mn deposit. Site-specific information is also a vital part of this assessment. And while it is not possible to attempt to scale a deposit down to a laboratory test, such tests certainly provide valuable and necessary data to evaluate a deposit's suitability for in situ leach mining.

Geologic Characterization

Prior to conducting any type of leaching experiments, it is important to have a thorough understanding of the nature of the material to be leached, as this will be essential for the interpretation of the leaching data and the correlation of the leaching characteristics exhibited by each ore type. It is particularly important to characterize the relationships between the various Mn and gangue minerals in the rock and the main fluid flow channels, as this is where most of the reactions will occur. This includes a detailed study of the chemistry and reactivity of the minerals located along these channels.

A number of different techniques are utilized for the characterization including, transmitted and reflected light microscopy, X-ray diffractometry, scanning electron microscopy, and electron probe microanalysis. The porosity and permeability of the samples is also measured to document changes in these properties as a result of mineral dissolution and precipitation reactions. A very important aspect of the characterization is the necessity for the pre-leach samples to be representative of the actual samples being leached. The failure to meet this requirement can make the correlation of pre- and post-leach characterization quite difficult. The acquisition of representative samples is often complicated by the significant variability in ore mineralogy and grade over a relatively short distance. Selection of representative samples is extremely difficult without the use of characterization techniques. These techniques provide the basis upon which a comparison can be made and "representativeness" can be judged.

Sample preparation is an important part of the characterization work, particularly when the samples are friable and susceptible to alteration during cutting, grinding, and polishing operations. Post-leach samples are often difficult to work with due to dissolution of the Mn minerals which comprise a significant fraction of the total rock volume. Thus, special preparation techniques are utilized which maintain the textural and mineralogical features to be studied. These techniques include the use of a variety of epoxies and impregnation procedures (Brink et al., 1990).

Transmitted and reflected light microscopy are used to conduct the initial characterization of the samples and to identify areas for more detailed study using scanning electron microscopy and electron probe microanalyses. Among the readily-observable features examined are (1) the associations of ore and gangue minerals to microfractures; (2) the frequency, length, width, and interconnectivity of fractures; and (3) the grain sizes, boundary relationships, and effective surface areas of both ore and gangue minerals (Brink et al., 1990). In addition to visual observations, systematic point counting techniques are also employed to quantify the modal mineralogy of the sample. This information is combined with the chemical compositions of the reactive minerals to predict Mn recovery during in situ leach mining.

After thorough examination by optical microscopy, the scanning electron microscope (SEM) and electron microprobe are used to examine and analyze particular areas of the samples at high magnification. The SEM can be used to obtain information on surface morphology and qualitative chemical data. A particularly useful feature of the SEM is the capability to map specific elements within the samples and also to overlay these maps as a way to

illustrate the distribution of particular minerals in the sample. The SEM is also useful for determining the width and frequency of microfractures which may act as primary or secondary flow channels during in situ mining.

The electron microprobe is used to determine the qualitative or quantitative chemical composition of an area as small as 1 micron. This instrument is particularly useful to assess the effects of the lixiviant on particular minerals in the system. For example, pre- and post-leach samples are compared to determine the extent of metals removal as a result of leaching with SO_2. This not only yields information on Mn removal efficiency, but it also helps to determine which gangue minerals consume SO_2 and to what extent. Traverses across mineral grains can identify zoning and can also yield information useful for evaluating leaching kinetics.

X-ray diffractometry (XRD) is another method used to obtain mineralogical data. The bulk mineralogy of an unidentified material can be determined relatively quickly using XRD, as each mineral has a distinctive X-ray pattern. X-ray diffractometry is particularly useful for analyzing very fine grained minerals, such as clay minerals, which are often difficult to identify using optical microscopy. The clay mineralogy of a sample can be very important, as ion exchange and hydration reactions can have significant effects on solution chemistry and rock permeability, respectively.

Deposit Characterization

In addition to geologic characterization studies performed in the laboratory, geologic field data is also crucial to evaluating a deposit for its amenability to in situ mining. Included in the field evaluation are (1) determinations of parameters such as the orebody geometry; (2) structural geology, including fracture and fault orientations; (3) porosity and permeability of both the ore and host rock; and 4) regional and local hydrologic conditions. These parameters are evaluated using a variety of methods including core and cuttings from drilling activity; downhole geophysical logging techniques such as gamma, neutron, sonic, resistivity, and temperature logs; surface electromagnetic and seismic techniques; borehole cameras; and downhole hydrologic techniques such as spinner surveys, packer tests, pumping tests, and injection tests. In addition, information generated from previous exploration or geological surveys is utilized for the deposit evaluation. This includes geologic maps, cross-sections, and drill core and cuttings.

Mn Recovery

In addition to favorable leaching characteristics, a viable metal recovery process is also needed to develop a complete in situ leach mining system. One without the other is an incomplete system. A preliminary assessment of potential Mn recovery options first required the identification of saleable end products. Due to current market conditions, Mn specialty products such as battery grade manganese dioxide and Mn chemicals appear to be the most likely target end products at this point (Redden, 1990). Since no viable Mn recovery process currently exists, research is being conducted to identify feasible recovery schemes that fit into the overall in situ leach mining design. A Mn recovery process may require initial steps such as solvent extraction or ion exchange to purify and concentrate the Mn prior to recovery. Recovery methods being investigated include precipitation (Hepworth, 1989), crystallization, and electrolytic techniques (Redden, 1990). After technically-feasible schemes are identified and refined, evaluations will be performed to determine the economic feasibility.

Prior to any field test projects, an in situ leach mining cost model will be developed to evaluate the economics of the whole mining process. This cost model will include parameters such as reagent costs, well field development and well completion costs, ore grade, expected recovery, surface processing costs, environmental monitoring costs, ore zone permeability, and a break-even selling price for the end product.

Results/Status of Bureau of Mines Research

The Bureau of Mines is using the systematic geologic and geochemical characterization approach described in section II to evaluate the potential for recovering manganese from domestic reserves by in situ leach mining. To show how this approach has yielded new information on the feasibility of in situ leaching of manganese, preliminary data from the Bureau's research program will be presented. Experimental work includes column, core, and batch leaching tests. Geologic characterization of ore samples before and after leaching has been completed to determine primary reaction mechanisms and leaching efficiency. Optimum solution chemistry conditions for selective leaching (i.e. pH and lixiviant strength) have been investigated experimentally by determining leaching reaction kinetics for various conditions. Field evaluation of manganese deposits has been initiated by core drilling and preparing field sites to conduct downhole geophysical and hydrologic tests. Recent advances in each of these areas will be discussed in detail in the following sections.

Leaching Experiments

Column Tests: Twelve column leaching tests were conducted on manganese ores from three domestic deposits that had previously shown good leaching characteristics in SO_2 solution (Pahlman and Khalafalla, 1988). These included ores from Artillery Peak in Arizona, the Pioche District in Nevada, and the Cuyuna Range in Minnesota. The leach

TABLE 5. - Column leaching test results

Domestic Deposit	Mn-wt%	Mn-% rec	Fe-wt%	Fe-% rec
Cuyuna Range, MN				
Mangan Mine	6	85	25	28
Hopkins Mine	4	88	37	10
Sagamore Mine	1	32	50	3
Hopkins Crude Ore	19	71	22	2
Gloria-Zeno Crude Ore	13	90	30	3
Gloria-Zeno Lean Ore	11	98	26	3
Pioche District, NV				
Prince Mine	11	96	10	45
Artillery Peak, AZ				
Level 1 - Basal Unit	3	97	11	3
High Grade	27	100	21	1

wt% - original grade; % rec - percentage extracted

tests followed the experimental design described by Pahlman and Khalafalla (1988). Tests were conducted in 10-cm. diameter columns that contained 3500 gm of -1 +1/2 inch pieces of crushed ore. Solutions of 5-volume-%-SO_2 were dripped on top of the column at a rate of 1 mL/min. The column was not tightly sealed and remained unsaturated throughout the experiment. Tests were run until the manganese in the leachant from the column dropped below 1 g/l. The duration of the tests ranged between 17-85 days.

Results from the column leach tests are displayed in Table 5. The data indicate that manganese can be recovered from all the ores tested by leaching with SO_2 solutions. Results also show that manganese is selectively leached with respect to iron in all the ores tested. Extraction of manganese ranged from 30 to 98 percent. Extraction of iron ranged from 2 to 40 percent. The slope of calculated extraction curves as shown in Figure 4 may reflect differences in the fundamental leaching properties of the ores being tested. For example, the extraction curves for the Gloria-Zeno Mine and the Hopkins Mine both show high overall recovery of manganese, but there is a change in slope of the curve for the Gloria-Zeno ore which is not observed in the Hopkins ore. Although the manganese mineralogy is similar for both ores there is a bimodal textural occurrence of manganese in the Gloria-Zeno ore which contributes to the two stage leaching pattern observed in the column tests.

After completion of preliminary column leach tests, ores from the Gloria-Zeno mine were selected for detailed study in a closed system column leach test. The column leach experimental design was modified to answer several questions that were raised after the first series of column leach tests. In the closed column design, information on the ratio of consumption of lixiviant to production of manganese could be answered because sulfur dioxide can not leave the system. The closed column tests are conducted under saturated conditions which will more closely represent conditions during in situ mining. On-line measurements of pH, conductivity, and temperature have been incorporated into the design of the new column leaching tests. Variation in pH had previously been documented during batch leach tests of manganese oxide, but this change was not observed in the first series of unsaturated column leach tests. In the closed column tests, on-line measurements have verified that there is a significant change in pH with leaching, which may have important implications on the overall leaching efficiency and for development of compatible metallurgical recovery techniques. Finally, fluids

Figure 4. - Column leaching extraction curves for Cuyuna Range Mn ores

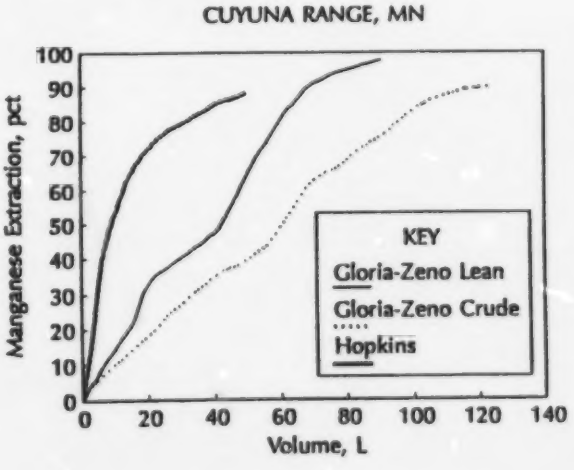

recovered from the closed columns tests on Gloria-Zeno ores had much higher maximum manganese concentrations (26 g/L) than the open system tests (5 to 11 g/L). This difference is most likely due to longer solution residence times and minimal SO_2 loss in the closed system experiment.

Batch Tests: Batch leaching tests of manganese ore were designed to complement the information from the column tests. One type of batch leach test consisted of placing a cube-shaped sample in an inert plastic sample basket suspended in a stirred, stoppered Erlenmeyer flask containing an aqueous SO_2 solution. Small samples of the solution were removed periodically with a filtered syringe for chemical analysis. An equivalent amount of fresh lixiviant was added to maintain a constant fluid/rock ratio. Solution pH, Eh, and temperature were measured by probes inserted through the stopper.

The cubic samples of ore were approximately one cm on a side, cut with faces parallel and perpendicular to bedding. The cubes were photographed, weighed and measured before leaching. Petrographic thin sections and briquettes for optical and electron microscopy were prepared from the rock sample immediately adjacent to the cube faces, and examined as 'pre-leach' sample. After a sample was leached; it was removed, dried, weighed, photographed, and again examined by light and electron microscopy. In examining the sample, special attention was paid to textural changes resulting from lixiviant/mineral interactions. The batch tests of ores from the Cuyuna Range and Emily District in northern Minnesota, confirmed the results from column tests of high manganese recovery (75-100%) and high selectivity for manganese relative to iron [i.e. Mn/(Mn+Fe) in solution >0.975]. However, observed leaching rates of ores with different manganese mineralogies (manganite versus pyrolusite) did not agree with predictions based on earlier batch leaching tests of single minerals (Pahlman and Khalafalla, 1988). These earlier tests and a theoretical evaluation of reaction equilibria (see the section on selective oxide dissolution) indicate that pyrolusite should leach more readily than manganite in SO_2 solution. Recent batch leaching tests show the reverse: the manganite ore samples leach more readily than the pyrolusite samples.

This behavior can be explained by consideration of the ore mineral textures identified in each sample. The Emily manganite sample was composed of massive manganite with inclusions of hematite and some quartz. As leaching progressed, non-reactive hematite and quartz spalled off the reacting surface, exposing fresh manganite to the lixiviant. As the experiment proceeded to completion, all the manganite dissolved, leaving a slurry of insoluble gangue residue on the bottom of the beaker. The Gloria-Zeno pyrolusite ore sample, however, occurs in bedding planes and fracture fillings surrounded by and intimately associated with quartz and hematite. In order to remove the manganese from that sample, the lixiviant must penetrate the rock sample, the manganese dissolution reactions must occur, and the dissolved manganese must exit the sample. Thus, the ore texture of the Gloria-Zeno sample provided a kinetic barrier to leaching not present in the Emily ores. This illustrates the significant control of texture on leaching characteristics and the need for detailed geologic characterization studies to interpret such leaching characteristics.

Core Leach Tests: One core leaching test was completed on a high grade sample from the Gloria-Zeno mine in Minnesota. The concentration of manganese in the leachant reached a maximum of approximately 40 g/L while iron concentration was near 0.5 g/L. Data also showed there is a change in pH from an input level of about 0.7 to an output of about 3.5.

The core leach test results demonstrate the complexity of the variables controlling the leaching process. Permeability changes in the sample were observed during leaching. Initially, distilled deionized water was pumped through the sample. However, when aqueous SO_2 injection was started, the permeability rapidly decreased causing the system pressure to reach the maximum allowable level. At that point, the core was inverted and pumping was initiated from the opposite end of the core. In a field setting, this procedure might be analogous to switching a recovery well to an injection well. Injecting in the opposite direction resulted in a significant increase in permeability. Permeability changes were continuous and variable during the operation of this experiment. One possible explanation for the observed permeability variation is that the dissolution of manganese, and consequent erosion of solid iron minerals would plug up flow channels as reactions proceeded. This would act to force lixiviant into new flow channels and open up new areas of fresh manganese mineralization. With time, there should be an increase in overall permeability by the selective removal of manganese minerals. Preliminary geologic characterization analyses support these hypotheses.

Geologic Characterization

Post-leach ores from the batch, column, and core leaching tests were investigated by techniques described above in the experimental approach section. Examination of mineralogic and lithologic differences between ore samples can answer several questions about the differences in extraction ratios achieved in leaching tests . For example the lowest recovery of manganese achieved (30 wt %) was from an ore sample with a very low initial manganese content similar to country rock surrounding a deposit. Since the total volume of manganese minerals was low, the manganese in this ore was not easily accessible to leaching solutions, new flow paths to manganese never developed, and good recovery was not achieved. One of the highest manganese recoveries (97 wt %) was

recovered within 15 days from a very porous sandstone which facilitates rapid and complete contact of lixiviant with ore minerals. The highest amount of manganese recovered (98 wt %) was extracted in 80 days time from the Gloria-Zeno ore which has a bimodal occurrence of manganese mineralization. Pyrolusite occurs in fracture fillings and disseminated in the matrix of this ore. With sufficient time, both types of manganese were removed from the ore.

Another major influence on the leachability of ores is the physical relationship between the ore and gangue minerals. For example, theory indicates that the mineral pyrolusite should be more leachable than the mineral manganite in sulfur dioxide solution. However, Bureau experiments on ore samples containing these minerals, showed that the opposite occurred: manganite was more leachable than pyrolusite. Comparison of pre- and post- leach samples using optical and electron microscopy show that the pyrolusite occurs in the rock surrounded by gangue minerals, while the occurrence of manganite in fractures allows the lixiviant more access for leaching. This example highlights the importance of geologic characterization in applying leaching to individual deposits.

Microscopic examination of ores leached by sulfurous acid also offer insight into the chemical reactions occurring during dissolution. In post-leach examination of massive manganite ores which contain hematite inclusions, sulfurous acid dissolves the host manganite while leaving the hematite unaffected. In pyrolusite-hematite-quartz ore a similar process is observed in which a residue of hematite and quartz was left unleached. In the case of a batch leach test of cryptomelane ore from the Emily District, the suspension of hematite and quartz was left in the flask after all the cryptomelane had been dissolved. These observations of the physical results of leaching supports the selectivity of sulfurous acid for manganese oxides over certain iron oxides, a result that is also indicated in the leach chemistry, and changing permeability conditions.

Deposit Characterization

In addition to mineral texture and leaching tests, the specific geology of a deposit on a regional scale is an important step in assessing an area's potential for in situ leach mining. Because of the significance of the size of the Cuyuna Range in Minnesota to total domestic manganese reserves, field studies of this area were initiated to begin the Bureau's field characterization program.

Iron formation in the Cuyuna Range of Minnesota contains low grade, high tonnage deposits of manganese oxides and manganese carbonate. Core drilling was completed at the Gloria-Zeno mine site to a total depth of 1200 feet and at the Emily District to a total depth of 800 feet. Core was successfully recovered from the ore horizon and from the hanging and footwall formations. Preliminary assessment of the geology indicates that the zone of oxidized manganese mineralization at the Gloria-Zeno Mine extends much deeper than was previously thought and that previous structural interpretations of the site will require some modification. Because the footwall formations of the Cuyuna Range have not been well characterized, data gained from this drill hole will for the first time allow accurate determination of the permeability of the leach zone footwall. The holes were not subjected to final abandonment procedures so that future down hole geophysical and hydrologic testing of the deposits can be conducted after thorough characterization of the ore zone.

Conclusions

The Bureau has developed a research protocol for investigating how advanced leach mining techniques could be applied to critical and strategic mineral commodities. This research protocol has been used to investigate the mining of manganese oxide ores by in situ leaching. Many of the techniques found to be significant research tools when developing in situ mining for base metals were used to define leaching parameters for manganese. These techniques include geologic characterization by optical microscopy, electron microprobe analysis, and x-ray diffraction analysis; geochemical characterization by batch, column, and core leaching tests; and field characterization by core drilling, geophysical, and hydrologic tests.

Results showed that efficient leaching of manganese oxide mineral deposits requires a lixiviant that is chemically selective for manganese because of the intimate relationship between iron and manganese oxide minerals in the deposits studied. New metallurgical recovery processes are needed to recover saleable products of manganese from manganese sulfate solutions in a way that allows solution recycling. Stratified, steeply dipping ore zones typical of some manganese deposits will require development of well patterns designed to utilize stratigraphy to control solution flow. The Bureau has used proven techniques and incorporated commodity specific research to develop a process oriented approach to the in situ leaching of manganese.

Acknowledgment

The authors wish to thank Lorin Redden from the Bureau of Mines Salt Lake Research Center for his input pertaining to Mn recovery research.

REFERENCES

Back, A.E., S.F. Ravitz, and K.E. Tame, 1952, "Formation of Dithionate and Sulfate in the Oxidation of Sulfur Dioxide by Manganese Dioxide and Air," RI 4931, U.S. Bureau of Mines, 14 pp.

Brink, S., Eidukat, B., Earley, D., and Blake, R., 1990 "The Application of Petrographic Techniques to Assess In Situ Leach Mining Potential: Tools Used and Types of Information Generated", Bureau of Mines Information Circular (in press), Washington, D.C.

Bureau of Mines, 1981 "In Situ Mining Research", IC 8852, U.S. Bureau of Mines, Washington, D.C., 107 pp.

Bureau of Mines, 1989 "In Situ Leach Mining", IC 9216, U.S. Bureau of Mines, Washington, D.C., 107 pp.

Burns, R.G., and V.M. Burns, 1979, "Manganese Oxides," Marine Minerals,ed. by R.G. Burns. Mineralogy Society of America, Washington, D.C., pp1-46.

Cook, S.S. and S.E. Paulson, 1988, "Leaching characteristics of selected supergene copper ores," Mining Engineering, v. 41, no. 1, pp. 33-39.

Cook, S.S., 1988, "Geocharacterization of Copper Oxide Ores for In Situ Mining," Proceedings - Engineering Foundation Conference: In Situ Recovery of Minerals, Oct. 25-30, 1987, Santa Barbara, CA, pp. 81-98.

Raisoni, P.R., and S.G. Dixit, 1988, "Leaching of Manganese Ore with Aqueous Sulfur Dioxide Solutions," Bull. Mater. Sci., Vol. 10, pp. 479-483.

Dean, R.S., Leaver, E.S., and Joseph, T.L., 1934, "Manganese; Its Occurrence, Milling, and Metallurgy, Part III," IC 6770, U.S. Bureau of Mines, pp. 167-189.

Dept. Of Interior, Bureau of Mines, 1990 Mineral Commodity Summaries, 199 pp.

Dixit, S.G. and P.R. Raisoni, 1987, "Effect of Oxygen on the Leaching of Manganese Dioxide by Aqueous Sulfur Dioxide Solution," Indian J. Tech., Vol. 25, pp. 517-5199.

Dobos, G., 1988, "Studies on the Kinetics of Ion-exchange Leaching of the Hungarian Rhodocrosite Ore of Urkut Origin," Reactive Polymers, Vol. 7, pp. 277-288.

Dresler, W., 1984, "Leaching of Manganese Dioxide in Nitrous Acid," Can. Metall. Quart., Vol. 23, pp. 271-279.

Henn, J.J., R.C. Kirby, and L.D. Norman, 1968, "Review of Major Proposed Processes for Recovering Manganese from United States Resources. Part 3. Sulfur Dioxide Processes, "IC 8368, U.S. Bureau of Mines, 36 pp.

Hepworth, M.T., 1989, "Preliminary Manganese Studies: Separation of Manganese from Leach Liquors", unpublished report to U.S. Bureau of Mines.

Herring, A.P., and S.F. Ravitz, 1965, "Rate of Dissolution of Manganese Dioxide in Sulfurous Acid," SME Transactions, Vol. 232, pp. 191-196.

Hoffman, M.R., 1981, "Thermodynamic, Kinetic, and Extrathermodynamic Considerations in the Development of Equilibrium Models for Aquatic Systems," Environ. Sci. Tech., Vol. 15, pp. 345-53.

Khalafalla, S. E., and J. E. Pahlman, 1981, "Selective Extraction of Metals from Pacific Sea Nodules with Dissolved Sulfur Dioxide," RI 8518, U.S. Bureau of Mines, 26 pp.

Larson, W.C., 1978, "Uranium In Situ Leach Mining in the United States," Information Circular 8777, 1978, U.S. Bureau of Mines, Washington, D.C.

Malti, M.A., M.W. Rophael, and I.I. Bhayat, 1981, "The Kinetics of Pyrophosphate Leaching of Partially Reduced Manganese Dioxides," Electrochim. Acta, Vol. 26, pp. 239-243.

Miller, J.D., and R. Wan, 1983, "Reaction Kinetics for the Leaching of MnO_2 by Sulfur Dioxide," Hydromet., Vol. 10, pp. 219-242.

Morgan, J.J., 1989, "Principles of Metal Speciation and Transport," Workshop Metal Speciation and Transport in Groundwaters, May 24-26, Jekyll Island, GA.

Pahlman, J. E., and S. E. Khalafalla, 1988 "Leaching of Domestic Manganese Ores with Dissolved SO2," RI 9150, U.S. Bureau of Mines, 15 pp.

Paulson, S.E., L.J. Dahl, and H.L. Kuhlman, 1987, "In situ mining geologic characterization studies: Experimental design, apparatus, and preliminary results," Minerals and Metallurgical Processing, Vol. 4, No. 4, pp. 181-189.

Paulson, S.E., 1989, "Core leaching experiments to assess leaching characteristics during in situ mining of oxide copper ores," Proceedings-Engineering Foundation Conference: In Situ Recovery of Minerals, Oct. 25-30, 1987, Santa Barbara, CA, pp. 113-134.

Paulson, S.E. and H.L. Kuhlman, 1989, "Laboratory Core Leaching and Petrologic Studies to Evaluate Oxide Copper Ores of In Situ Mining," Information Circular 9216, 1989, U.S. Bureau of Mines, Washington, D.C.

Petrie, L.M., 1991, "Lixiviant Selection for Manganese In Situ Leach Mining: A Geochemical Approach," Open File Report (in press), U.S. Bureau of Mines.

Potter, G.M., E.A. Nordhausen, J.B. Fletcher, J.L. Lake, J.V. Rouse, and F. Wojtasiak., 1982, "Technological Investigation to Determine the Feasibility of In Situ Leaching Metallic Ores Other Than Copper and Uranium. (contract J0295032, Mountain States Res. and Dev., Inc.)," Vol. 1, U.S. Bureau of Mines, 140 pp.

Raisoni, P.R., and S.G. Dixit, 1988, "Leaching of Manganese Ore with Aqueous Sulfur Dioxide Solutions," Bull. Mater. Sci., Vol. 10, pp. 479-483.

Redden, L.D., 1990 "Assessment of Metal Recovery Options From Manganese Bearing Leach Liquors", Bureau of Mines internal report.

Roy, S., 1981, Manganese Deposits, Academic Press, New York, 458 pp. U.S. Department of the Interior, 1990, "The Mineral Position of the United States -- 1990," Annual Report of the Secretary of the Interior, Under the Mining and Minerals Policy Act of 1970, U.S. Dept. Int., 1990, 120 pp.

Usatenko, Y.I., and A.S. Ryl'kova, 1983, "Dissolution Kinetics of Manganese Oxide Ores in an Acetic Acid Solution of Potassium Iodide," J. Anal. Chem. U.S.S.R. (English version), Vol. 38, pp. 66-70.

Warren, I.H., and E.A. Devuyst, 1972, "Leaching of Iron and Manganese with Ammonium Carbamate," Transactions of SME, AIME, Vol. 252, pp. 388-391.

Wyman, W.F., and S.F. Ravitz, 1947, "Sulfur Dioxide Leaching Tests on Various Western Manganese Ores," RI 4077, U.S. Bureau of Mines, 12 pp.

SOCIETY FOR MINING, METALLURGY, AND EXPLORATION, INC.

P.O. BOX 625002 • LITTLETON, COLORADO • 80162-5002

PREPRINT NUMBER

91-70

LABORATORY BLASTING TESTS IN GRANITE BLOCKS TO ASSESS PERMEABILITY ENHANCEMENT FOR MODIFIED IN SITU MINING

S. A. Rholl

R. E. Otterness

M. S. Stagg

Twin Cities Research Center
Bureau of Mines
Minneapolis, Minnesota

For presentation at the 1991 SME Annual Meeting
Denver, Colorado - February 25-28, 1991

Permission is hereby given to publish with appropriate acknowledgments, excerpts or summaries not to exceed one-fourth of the entire text of the paper. Permission to print in more extended form subsequent to publication by the Society must be obtained from the Executive Director of the Society for Mining, Metallurgy, and Exploration, Inc.

If and when this paper is published by the Society for Mining, Metallurgy, and Exploration, Inc., it may embody certain changes made by agreement between the Technical Publications Committee and the author, so that the form in which it appears is not necessarily that in which it may be published later.

These preprints are available for sale. Mail orders to PREPRINTS, Society for Mining, Metallurgy, and Exploration, Inc., P.O. Box 625002, Littleton, Colorado 80162-5002.

PREPRINT AVAILABILITY LIST IS PUBLISHED PERIODICALLY IN MINING ENGINEERING

Abstract. This paper describes the Bureau of Mines experimental test program which evaluated the effectiveness of using high explosives to enhance orebody permeability. To determine the effect of stress on the fracture network generated by blasting, fifteen single-hole laboratory tests in granite blocks up to .067 m^3 (2.4 ft^3) in size were blasted using .12 to .20 m (4.8 to 8.0 in) of $1.6x10^{-3}$-, $3.2x10^{-3}$-, or $6.5x10^{-3}$-kg (25-, 50-, or 100-grain) detonating cord. In situ stresses were simulated using polyaxial load cells to apply uniform stresses of $1.72x10^6$ to $1.76x10^7$ Pa (250 to 2550 psi). All of the blocks were sawed to expose the blast-induced fracture patterns for analysis.

Introduction

In situ recovery of minerals has great potential as a mining technology to mine deposits that might otherwise be overlooked by conventional techniques. Some hard-rock deposits, however, will not have adequate permeability to permit successful in situ mining and will require permeability enhancement of the rock deposit prior to leaching. The leaching process in this instance becomes modified in situ mining rather than true in situ mining.

This paper examines the use of high explosives to create fractures and make ore deposits more permeable which will allow better rates of mineral recovery. Blasting can be used to fragment both orebodies located near the surface and those at depth. If the ore deposit to be leached is well below the surface it may also possess inadequate permeability due to increased in situ stresses, as reported by McKee et al. (1983), and blasting in this case could play an important role in permeability enhancement prior to successful in situ mining.

Although other fracture techniques exist, such as hydraulic fracturing, blasting with high explosives can potentially create a distribution of fractures not achievable by the other techniques. Warpinski et al. (1979) examined multiple fracturing in a volcanic ash-fall tuff formation using three different propellants, and mineback facilities provided the opportunity to directly observe the resulting fracture network. They concluded using high explosives could cause considerable crushing and compaction around the borehole, possibly sealing off any cracks that were formed.

Laboratory studies conducted by Science Applications International Corporation (SAIC) for the Gas Research Institute, and reported by Schatz et al. (1987), involved the numerical prediction and interpretation of multiple radial fractures using black powder and high explosives. Their work, however, was conducted in hydrostone, an easily cast gypsum-based cement, whose physical properties and fracture characteristics are significantly different from deep hard-rock deposits.

Steckley et al. (1975) and D'Andrea et al. (1976,1977,1978) conducted blasting experiments to recover copper from deposits by in situ mining, but their research did not involve the application of leach solutions. Ahlness (1983) summarized the Bureau work and concluded that all of the test patterns investigated produced adequate fragmentation for in situ mining.

Very little data exist on the effects of high explosives to enhance the permeability of hard-rock deposits at depth. This paper describes fifteen single-hole laboratory shots which used high explosives detonated in granite blocks to create fractures. Three different polyaxial load cells were used to simulate in situ stresses from $1.72x10^6$ to $1.76x10^7$ Pa (250 to 2550 psi). All of the blocks were sawed open to expose the fracture network generated by the blasting. The nature and the extent of the fracture patterns are reported.

Confinement Cells

The laboratory test blasts were carried out in polyaxial load frames which simulated in situ stresses and were located in the blasting shelter at Twin Cities Research Center, and in facilities operated by TerraTek Geoscience Services, Salt Lake City, Utah, and SAIC, Las Vegas, Nevada, respectively. The latter two laboratories utilized special equipment to achieve greater stress levels and this equipment was not available at Twin Cities.

The Bureau tests utilized a .51- by .51- by .56-m (20- by 20- by 22-in) confinement cell constructed out of six .019 m (3/4 in) thick steel plates. Threaded rods held the cell together. The fully assembled test cell is shown in figure 1. To compensate for blocks of differing size, grout was used to fill the gaps between the block and the assembly walls. After the grout had hardened, the nuts were torqued to give the desired stress level. All of the tests conducted at the Bureau utilized a maximum stress level of $1.72x10^6$ Pa (250 psi).

The confinement cells at both TerraTek and SAIC utilized a steel box surrounded by six flat jacks and a hydraulic control system to provide independent pressures on 3 axes of the granite blocks. These cells were capable of simulating three dimensional stresses up to $2.1x10^7$ Pa (3000 psi). In the tests conducted for the Bureau the stress levels were varied from $1.72x10^6$ to $1.76x10^7$ Pa (250 to 2550 psi). All of the confining pressures applied in the tests represented uniform stresses, i.e., there were no variations in differential stress.

Charge Configuration

The general charge configuration consisted of an exploding bridgewire detonator (EBW) taped to the end of a piece of detonating cord, centrally located in the granite blocks, as shown in figure 2. For these tests, $1.6x10^{-3}$-, $3.2x10^{-3}$-, or $6.5x10^{-3}$-kg (25-, 50-, or 100-grain) detonating cord was inserted in $9.5x10^{-3}$ m (3/8-in) holes. The main component of the central core of the detonating cord is pentaerythritol tetranitrate (PETN), a molecular-type military explosive.

Charcoal Granite

Careful consideration was exercised to select a rock sample for use in these tests. Except for one sample, all of the blocks used were cut from a single large block of St. Cloud gray granodiorite obtained from a quarry located near St. Cloud, MN. St. Cloud gray granodiorite is

often referred to by its trade name, charcoal granite. Besides being relatively homogeneous, charcoal granite was also readily availability and massive in character. All of the test samples were fine grained and dark in color. Physical properties of charcoal granite were reported by Crum et al.(1990) and are listed in table 1. The other test sample was a block of oracle granite, obtained from a Bureau cooperative field site located near Casa Grande, AZ, where an in situ copper mining experiment is being conducted.

Test Summary

The various test parameters are summarized in table 2. Tests 8-12 were conducted at TerraTek and tests 14-15 were conducted at SAIC. To calculate the amount of explosive used in each test, the explosive contained in the detonating cord was added to the explosive in the EBW initiator. The explosive contained in the detonating cord represents the actual amount of PETN, rather than the nominal values designated by the manufacturer. All of the shots, with the exception of shot 7, were fully coupled. A quick-drying grout was used to completely fill each borehole.

Two of the tests at TerraTek, numbers 11 and 12, were vented to the atmosphere. Although they were fully coupled, they were not stemmed. Once the grout, upon addition, reached the top of the explosive column, no further grout was added. At the time these tests were conducted, it was believed that such venting would lower the long-term gas-pressure strain.

Results

After the blocks were blasted, they were cut perpendicular to the borehole in the middle of where the explosive column once existed. Figure 3 shows a typical fracture pattern. The blocks were carefully inspected to determine if severe crushing or compaction existed around the borehole. Although numerous fractures were observed close to the borehole, there was no evidence that the borehole radius changed in any of the fifteen tests, including test 7, the uncoupled shot. Although the degree of damage near the borehole wall was not quantified, the grout surrounding the explosive column remained intact.

To assess the fracture network, the number of cracks intersecting concentric circles at .013 m (1/2-inch) intervals was counted. Dye penetrants were used but did not facilitate the crack counting. The results are shown in table 3, where the number of cracks is tabulated against the radial distance from the center of the borehole. Two characteristic trends were observed when examining the fracture patterns. First, in all cases, a dense zone of tight radial fractures existed around the borehole. These fractures extended out to 20 to 30 charge diameters, in agreement with the results of Spathis et al. (1987). By comparison with previous Bureau researchers, Olson et al. (1973) reported 9-10 charge diameters for tests in granite using C-4 (a military explosive), Siskind et al. (1973) reported 21-27.5 charge diameters for tests in shale using 60 pct dynamite, and Siskind and Fumanti (1974) reported 7 charge diameters for tests in granite using ANFO. The second characteristic trend observed was that in some of the cases, approximately 2 to 6 gas-driven fractures propagated out to the edge of the block.

These trends can be identified in figure 4, where the number of cracks is plotted versus radial distance for tests 8 and 15. In test 15 the number of cracks falls off quickly. In test 8, however, several cracks propagated out to the edge, past the largest radial distance for which cracks were counted. When the size of the block was increased sufficiently, the second trend was not observed and the dense zone of tight radial fractures around the borehole remained essentially unaffected.

In the case of block 3 (the granite block obtained from the Sacaton mine in Arizona) numerous blast-induced fractures could not be accurately counted due to preexisting cracks and the intergranular boundaries. The preexisting cracks or open joints, about .15 m (6 in) long, acted as free surfaces, and at least one radial crack opened upon intersecting a joint.

To verify that the number of cracks increases with increased explosive mass, the number of cracks at a radial distance of .051 m (2 in) was plotted against the amount of explosives used for all of the cases where the simulated in situ stress level was 1.72×10^6 Pa (250 psi). These results are shown in figure 5. The least squares fit through the points is also displayed. Although there is some scatter, the data supports the above hypothesis.

To determine the effect of in situ stress on the fracture pattern generated, the number and total length of cracks were plotted against stress for those tests using 1.6×10^{-3}-kg detonating cord, and are shown in figures 6 and 7, respectively. In figure 6, the number of fractures at a radial distance of .051 m (25 hole diameters) was chosen to be representative of the results. The total crack length was determined by summing up the lengths of individual cracks at the same .013-m (1/2-in) intervals at which the number of cracks was determined and adjusted for any cracks which exceeded the .076-m (3-in) radial distance. Although there is considerable scatter in the data, especially at lower stress levels, the results are similar to the results for tests conducted in hydrostone and reported by Schatz (1987), where crack length of fractures showed some scatter at lower stress levels. Using an envelop of the data, increasing the stress level from 6.89×10^6 to 1.72×10^7 Pa (1000 to 2500 psi) reduces the number and length of cracks by about 33 pct.

Although blasting-induced permeability enhancement is of interest to this paper, no permeability measurements were made. The existing laboratory test procedures to measure the permeability of rock samples, as reported by Lewis and Jandanand (1974), is limited to about 9.9×10^{-11} m^2 (0.1 md). For rocks considerably less permeable than that, for example, granites with permeabilities of 9.9×10^{-22} m^2 (1 nd) and below, Brace et al. (1968) devised a transient flow test.

The Bureau was unable to perform transient tests, because the equipment needed to do them

was not available. Because there has been no observed crushing near the borehole wall in any of the tests conducted by the Bureau (which might seal off cracks which are formed), it is assumed that the crack data obtained in the laboratory will be adequate to assess the feasibility of using high explosives to enhance permeability. The Bureau is investigating using computerized tomography techniques to determine lixiviant flow in the damaged zone closed to the borehole wall. Permeability tests will be performed in the field, where blasting and leaching tests will eventually be done.

To corroborate the crack data, P-wave velocities were measured in some of the blocks (edge to edge, perpendicular to the borehole axis). The results are listed in table 4. The greatest attenuation in velocity, 50 pct, occurred in blocks 1 and 3 (6.5×10^{-3}-kg and 3.2×10^{-3}-kg detonating cord, respectively). The P-wave tests were not conclusive in defining the extent of rock damage. Further testing is needed to relate these results to the visually obtained data.

Conclusions

The Bureau of Mines conducted 15 single-hole tests to determine if high explosives could be effectively used to enhance permeability in hard-rock deposits for in situ mining. Two distinct trends were observed. High explosives generated a zone of numerous (e.g., 20) tight radial fractures that extended at least 20 to 30 explosive diameters. In situ stresses up to 1.76×10^7 Pa (2550 psi) were applied. The data appear to suggest that in situ stress influences the fracture density and the total overall length of cracks, but more data are needed to substantiate this conclusion. Increasing the in situ stress from 6.89×10^6 to 1.72×10^7 Pa (1000 to 2500 psi) reduced the fracture density and total overall length of cracks by approximately 33 pct. If the blocks were not large enough, gas-driven fractures were able to propagate to the edges of the blocks, but a zone of dense radial fractures was, nevertheless, still observed. To prevent fractures from propagating to the edges of blocks in single-hole tests under the conditions described in this paper, it is recommended that .41 m (16-in) cubes or larger blocks be used. The observed fracture patterns imply that a blast design including .25 m holes placed 12 m apart would be adequate to sufficiently fracture ore deposits for modified in situ mining down to 305 m.

Acknowledgments

The authors express their appreciation to TerraTek and SAIC and their employees Phil Halleck and Mike Sanderson, and Robert Bellman and Nancy Patti, respectively, for their cooperation and assistance in completing the tests conducted at those facilities.

References

1. Ahlness, J. K., and M. G. Pojar, 1983. In Situ Copper Leaching in the United States: Case Histories of Operations. BuMines IC 8961, 37 pp.

2. Brace, W. F., J. B. Walsh, and W. T. Frangos, 1968. Permeability of Granite Under High Pressure. J. Geoph. Res., Vol. 73, No.6, pp. 2225-2236.

3. Crum, S. V., S. A. Rholl, and M. S. Stagg, 1990. The Fragmentation of Granite Cylinders Using High Explosives. Paper in Proceedings of the 6th Research Symposium on Explosives and Blasting Technique. (Orlando, FL, Feb. 4-9, 1990). Soc. Explos. Eng., Solon OH, pp. 179-191.

4. D'Andrea, D. V., W. C. Larson, P. G. Chamberlain, and J. J. Olson, 1976. Some Considerations in the Design of Blasts for In Situ Copper Leaching. Paper in Proceedings of the 17th U. S. Symposium on Rock Mechanics, University of Utah, Snowbird, Utah, Aug. 25-27, 1976, pp. 5B1-1 - 5B1-4.

5. D'Andrea, D. V., W. C. Larson, L. R. Fletcher, P. G. Chamberlain, and W. H. Engelmann, 1977. In Situ Leaching Research in a Copper Deposit at the Emerald Isle Mine. BuMines RI 8236, 43 pp.

6. D'Andrea, D. V., P. G. Chamberlain, and J. K. Ahlness, 1978. A Test Blast for In Situ Copper Leaching. Pres. at 1978 AIME Ann. Meeting, Denver, CO, Feb. 26-Mar. 2, 1978, Preprint 78-AS-112, 15 pp.

7. Lewis, W. E., and S. Tandanand (eds.), 1974. Bureau of Mines Test Procedures for Rocks. BuMines IC 8628, 223 pp.

8. McKee, C. R., R. H. Jacobson, and S. C. Way, 1983. Design Criteria for In-Situ Mining of Hard Rock Deposits. Paper in Proceedings of the 9th Conference on Explosives and Blasting Technique, ed. by C. J. Konya. (Dallas, TX, Jan. 31-Feb. 4, 1983). Soc. Explos. Eng., Solon OH, pp. 412-450.

9. Olson, J. J., R. J. Willard, D. E. Fogelson, and K. E. Hjelmstad, 1973. Rock Damage From Small Charge Blasting in Granite. BuMines RI 7751, 44 pp.

10. Schatz, J. F., B. J. Zeigler, R. A. Bellman, J. M. Hanson, M. Christianson, and R. D. Hart, 1987. Prediction and Interpretation of Multiple Radial Fracture Simulations. Final Report for the Gas Research Institute. Contract No. 5084-213-1149. Prepared by Science Applications International Corporation, July 1987.

11. Siskind, D. E., R. C. Steckley, and J. J. Olson, 1973. Fracturing in the Zone Around a Blasthole, White Pine, Mich. BuMines RI 7753, 20 pp.

12. Siskind, D. E. and R. R. Fumanti, 1974. Blast-Produced Fractures in Lithonia Granite. BuMines RI 7901, 38 pp.

13. Spathis, A. T., D. P. Blair, and J. R. Grant, 1987. Blast Damage Assessment of Rock by Using the High Frequency Cross Hole Seismic Method. Paper in Second International Symposium on Rock Fragmentation by Blasting, ed. by W. L. Fourney and R. D. Dick (Keystone, CO, Aug. 23-26, 1987). Soc. for Exp. Mech., Bethel, CT, pp. 488-491.

14. Steckley, R. C., W. C. Larson, and D. V. D'Andrea, 1975. Blasting Tests in a Porphyry Copper Deposit in Preparation for In Situ Extraction. BuMines RI 8070, 47 pp.

15. Warpinski, N. R., R. A. Schmidt, P. W. Cooper, H. C. Walling, and D. A. Northrop, 1979. High-Energy Gas Frac: Multiple Fracturing in a Wellbore. Paper in Proceedings of the 20th U. S. Symposium on Rock Mechanics, Austin, TX, June 4-6, 1979, pp. 143-152.

Table 1. - Physical Properties of Charcoal Granite, Crum (1990)

Density:	2720 kg/m^3
Compressive Strength:	282 MPa
Tensile Strength:	6.97 MPa
P-wave (pulse) Velocity:	4600 m/sec
Dynamic Young's Modulus:	48.4 GPa
Dynamic Shear Modulus:	23.9 GPa
Poisson's Ratio:	0.25
Porosity:	0.08 pct.
Permeability:	< 1 x 10^{-10} m/sec
Fracture toughness:	2.5 MPa $m^{1/2}$

Table 2. - Design Parameters for Blasting Tests

Test No.	Rock Type	Block Size, m	Length of Detonating cord, m	Explosive mass, kg	In Situ Stress, Pa
1	Charcoal granite	.30 x .30 x .38	.16[3]	3.0x10^{-3}	1.72x10^6
2	Charcoal granite	.30 x .30 x .38	.17[2]	1.6x10^{-3}	1.72x10^6
3	Oracle granite	.30 x .30 x .38	.17[2]	1.6x10^{-3}	1.72x10^6
4	Charcoal granite	.30 x .30 x .38	.17[2]	1.6x10^{-3}	1.72x10^6
5	Charcoal granite	.30 x .30 x .38	.17[1]	8.4x10^{-4}	1.72x10^6
6	Charcoal granite	.30 x .30 x .38	.17[1]	8.4x10^{-4}	1.72x10^6
7	Charcoal granite	.30 x .30 x .38	.17[2]	1.6x10^{-3}	1.72x10^6
8	Charcoal granite	.25 x .25 x .37	.20[2]	1.8x10^{-3}	6.89x10^6
9	Charcoal granite	.25 x .25 x .37	.20[1]	9.7x10^{-4}	6.89x10^6
10	Charcoal granite	.25 x .25 x .37	.20[1]	9.7x10^{-4}	1.76x10^7
11	Charcoal granite	.25 x .25 x .37	.20[1]	9.7x10^{-4}	6.89x10^6
12	Charcoal granite	.25 x .25 x .37	.20[1]	9.7x10^{-4}	1.72x10^6
13	Charcoal granite	.41 x .41 x .41	.15[1]	7.8x10^{-4}	1.72x10^6
14	Charcoal granite	.41 x .41 x .41	.12[1]	5.8x10^{-4}	6.89x10^6
15	Charcoal granite	.41 x .41 x .41	.12[2]	1.1x10^{-3}	6.89x10^4

[1]1.6x10^{-3}-kg (25-grain) detonating cord
[2]3.2x10^{-3}-kg (50-grain) detonating cord
[3]6.5x10^{-3}-kg (100-grain) detonating cord

Table 3. - Number of cracks as a function of radial distance

Test No.	NUMBER OF CRACKS				
	Radial Distance, m				
	.025	.038	.051	.064	.076
1	75	61	57	44	43
2	48	39	26	21	20
3	ND[1]	ND	ND	ND	ND
4	33	23	21	14	11
5	25	13	6	3	2
6	42	31	23	11	4
7	50	32	5	1	1
8	37	33	24	20	14
9	35	26	14	3	1
10	21	17	9	3	2
11	20	10	4	1	0
12	30	22	20	13	5
13	25	19	13	7	4
14	28	16	4	0	0
15	30	15	10	7	2

[1]ND. No data available (see text).

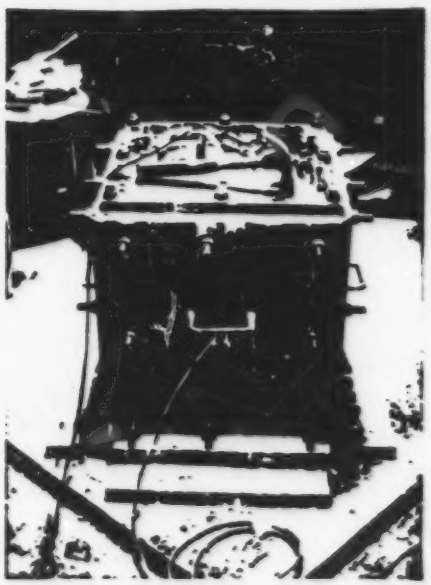

Figure 1. Bureau of Mines polyaxial confinement cell to simulate in situ stresses

Table 4. - P-Wave velocities measured in fractured blocks

Test No.	P-Wave Velocity (m/sec)	Attenuation, (pct)
1	2300	50
2	3800	17
3	2300	50
5	4500	2.2
6	3800	17
8	4200	8.7

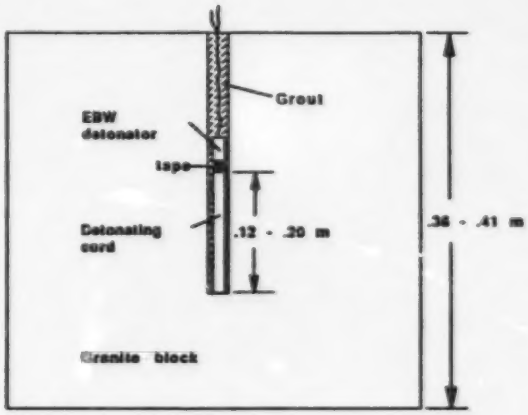

Figure 2. General charge configuration for blasting tests

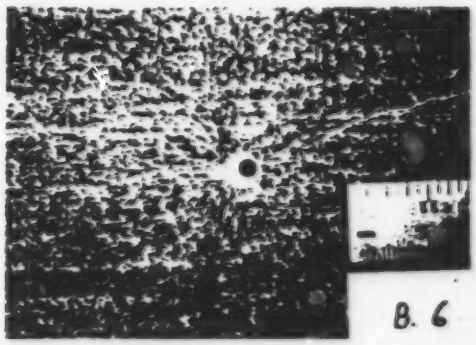

Figure 3. Typical fracture pattern generated by blasting with high explosives

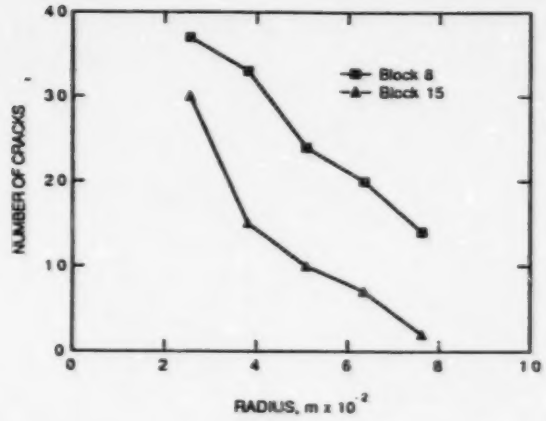

Figure 4. Number of cracks as a function of radial distance for blocks 8 and 15

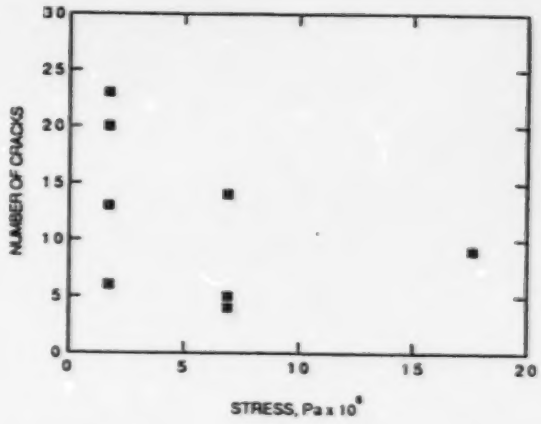

Figure 6. Scatter diagram for number of cracks and confining stress at a radial distance of .051 m for those tests using 1.6×10^{-3} -kg detonating cord

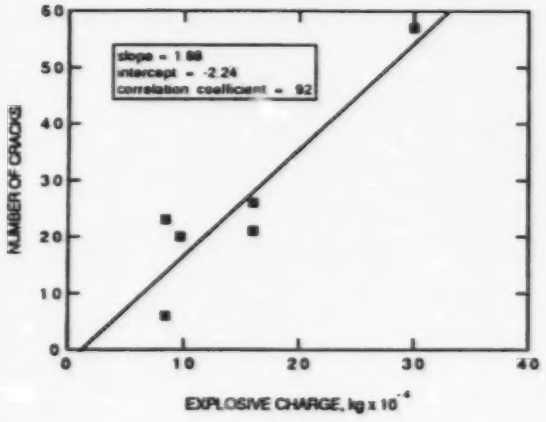

Figure 5. Number of cracks as a function of explosive charge at a triaxial confining pressure of 1.72×10^{6} Pa and a radial distance of .051 m

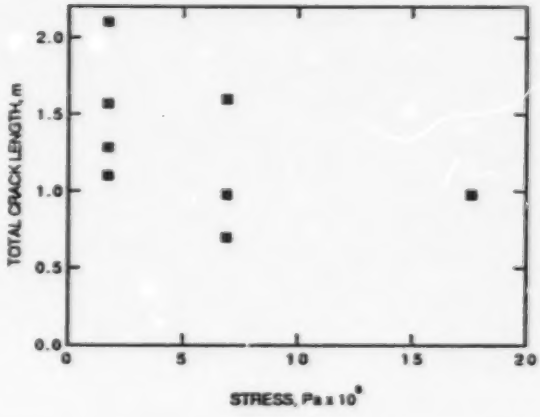

Figure 7. Scatter diagram for total crack length and confining stress for those tests using 1.6×10^{-3} -kg detonating cord

SOCIETY FOR MINING, METALLURGY, AND EXPLORATION, INC.

P.O. BOX 625002 • LITTLETON, COLORADO • 80162-5002

PREPRINT NUMBER

91-75

DEVELOPMENTS AND INNOVATIONS IN BACTERIAL OXIDATION OF REFRACTORY ORES

P.C. van Aswegen

M. W. Godfrey

D. M. Miller

General Mining Metals and Minerals Limited
Johannesburg, South Africa

A. K. Haines

General Mining Metals and Minerals Limited
Marshalltown, South Africa

For presentation at the 1991 SME Annual Meeting
Denver, Colorado - February 25-28, 1991

Permission is hereby given to publish with appropriate acknowledgments, excerpts or summaries not to exceed one-fourth of the entire text of the paper. Permission to print in more extended form subsequent to publication by the Society must be obtained from the Executive Director of the Society for Mining, Metallurgy, and Exploration, Inc.

If and when this paper is published by the Society for Mining, Metallurgy, and Exploration, Inc., it may embody certain changes made by agreement between the Technical Publications Committee and the author, so that the form in which it appears is not necessarily that in which it may be published later.

These preprints are available for sale. Mail orders to PREPRINTS, Society for Mining, Metallurgy, and Exploration, Inc., P.O. Box 625002, Littleton, Colorado 80162-5002.

PREPRINT AVAILABILITY LIST IS PUBLISHED PERIODICALLY IN MINING ENGINEERING

Abstract. The Bacterial Oxidation (BIOX®) process for the pre-treatment of refractory ores for gold recovery developed by Genmin, the mining division of Gencor, has been operating successfully at the Fairview mine since October 1986. The continuous operation of a pilot plant at Genmin Process Research has resulted in further process developments to improve plant operating efficiencies. These new developments which include a higher solids content of the pulp feed to BIOX®, lower retention times, higher operating temperatures, lower power utilisation for oxygen dispersion and reduced nutrient addition have all been successfully implemented on the Fairview plant.It has furthermore been confirmed that the arsenic precipitate formed in the neutralisation of effluent solutions complies to the United States of America EPA standards. Continuous cyanidation pilot plant work conducted on BIOX® product has indicated that cyanide consumption can be drastically decreased if a continuous flowsheet is implemented in preference to a batch leaching system.

Introduction

The bacterial oxidation (BIOX®) process for the pre-treatment of refractory ores for gold recovery was developed by the Genmin Process Research laboratory. Early work started in the late 1950's when the bacteria strain, *"Thiobacillus ferrooxidans"* was isolated from effluents pumped from the West Rand Consolidated underground mine but at this stage the focus was on the recovery of uranium.

It was only in the late 1970's that research into the use of bacterial oxidation of refractory gold ores prior to cyanidation was initiated. This work was carried out at a fairly low key until a need for an alternative to the Fairview mine roaster arose.

The arsenopyrite/pyrite concentrate from Fairview is highly refractory and only 35% of the gold is dissolved by direct cyanidation.

A continuous pilot plant to treat 750 kg per day of Fairview concentrate was commissioned at Process Research during 1984 and was operated for two years.

The pilot plant testwork led to the following conclusions:

- Gold recoveries of 97% can be achieved with pulp residence times of four days and W:S ratio of 8:1 of feed pulp.
- The key process control variables were temperature, pH, dissolved oxygen and pulp feedrate.
- Bacteria strains developed were sufficiently hardy to withstand mishaps normally experienced in industrial plant operations.
- Process engineering appeared to be unsophisticated.

With the confidence gained from the pilot plant operation, a 10 ton per day concentrate treatment BIOX® plant was commissioned at the Fairview mine in October 1986.

The plant has been operating very successfully with feedrates of 17 tons per day being achieved. The higher throughput was reached as a result of decreasing the W:S ratio of the feed to 4:1.

A mini-plant, treating 100 kg per day concentrate has operated in parallel with the Fairview plant at Process Research since 1987.

This plant has been used for ongoing process development work and new operating parameters to improve plant operating efficiencies, capital and working costs, have been developed. These improvements include:

- Reduction of the W:S of pulp feed to 4:1
- Decrease in pulp residence time to three days
- Operating temperatures of 45 °C
- Decrease in mixer power utilisation of 50%
- Reduction in nutrient addition.

Fairview BIOX® Plant Operation

The Fairview Mine, situated near the town of Barberton in the Eastern Transvaal region of South Africa, has been in operation since 1912 and the present metallurgical plant was commissioned in 1955.

The bulk of the proven ore reserves are sulphidic and refractory. The main minerals are pyrite and arsenopyrite with trace amounts of chalcopyrite, sphalerite, stibnite, galena, pyrrhotite and pentlandite.

The metallurgical operations at Fairview comprises a typical refractory gold processing plant treating the sulphidic ore body, a second plant treating the quartzitic ore, a flotation tailings treatment plant and an arsenic refining plant.

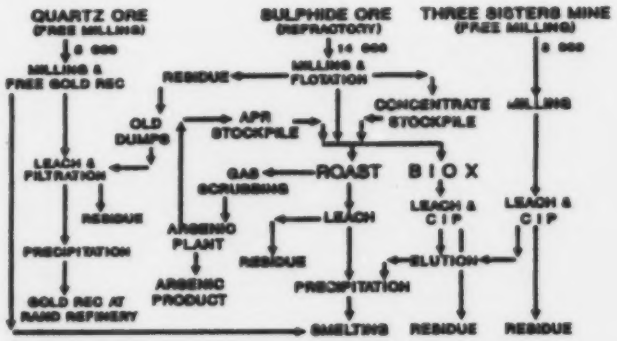

Figure 1. Fairview Flowsheet

Typical ore and concentrate analyses for Fairview ore are depicted in Table I.

Table I. - Ore and concentrate analyses

	Gold g/t	Sulphur %	Arsenic %
Run-of-Mine Ore	7,0	0,6	0,3
Concentrate	109	23,0	4,5

The BIOX® plant currently treats 40-60 percent of the mine flotation concentrate production. The remainder of the concentrate is treated by an Edwards Roaster.

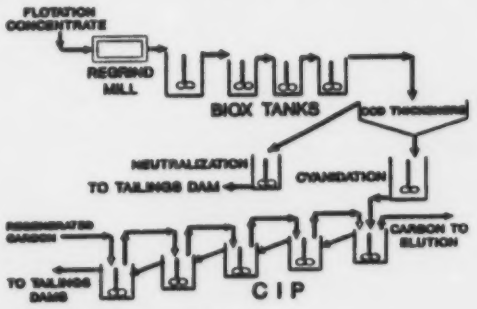

Figure 2. BIOX ® Plant Flowsheet

The performance of the BIOX® plant over the past four years is summarised in Table 2.

Table 2. - Summary of BIOX® plant performance

	Yearly average			
	1987	1988	1989	1990
Concentrate feed t/month	228	263	330	350
Concentrate gold content g/t	105	99	108	109
Concentrate sulphur content % S.	29,36	27,38	24,50	23,09
Gold recovery %	92,1	93,0	93,2	95,2
Pulp feed W:S	6,0	6,5	4,8	4,0
Residence time days	4,5	4,0	4,0	4,0
Operating temperature °C	41,2	41,5	40,9	40,3
Plant availability %	95,44	99,0	98,4	98,3

Temperature has been one of the most important control variables and as can be observed has been held at 40 °C by cooling. The temperature has often peaked at values as high as 53 °C for short periods. Although oxidation rates were still acceptable, a definite loss in bacteria activity was noticed. The time period at the high temperature was nevertheless too small to assess the effect on the oxidation rates.

Monthly plant treated tonnages of 390 tons have been achieved. Peak daily feed rates of 17 tons could not be maintained due to an insufficient concentrate production from the flotation plant.

As from 1988 residue filter cake from the arsenic recovery plant and fly-ash from the roaster stack were blended with flotation concentrate feed to the BIOX® with little effect on the overall recovery.

Typical analyses and feed rate of the arsenic plant residue and fly-ash are summarised in Table 3.

Table 3. - Analyses of Arsenic Plant Residue, Fly-ash and Feed Rates

	Feed tons per month	Gold g/t	Sulphur %	Arsenic %	Gold dissolution by direct cyanidation %
Arsenic plant residue	45	45	4,0	4,85	65
Fly-ash	30	60	2,8	2,0	30

During 1989/1990 flotation concentrate from a neighbouring mine was also blended with BIOX® feed at an average rate of 80 tons per month.

The plant efficiency was not affected by these changes in feed material, which confirms the versatility of the process and the adaptability of the bacteria strain.

BIOX® Process Improvements

Three mini plants, each with a capacity of up to 100 kg per day are operated at Genmin Process Research. The plants are employed to confirm design parameters for treatment of concentrates for new projects internal and external and also to evaluate new process developments.

Possible new process routes are defined and evaluated on the pilot plant. Feasible developments are then implemented and confirmed on the Fairview plant.

Pulp Retention Time and W:S ratio

Since 1984 pulp residence time and W:S ratio have been slowly decreased to improve the capacity of the plant. Table 4 sets out the changes that have been made to both the mini plant and the Fairview plant.

Table 4. - BIOX® Retention Times

	Pilot Plant				Fairview Plant	
Retention days	10	4	4	3	4	4
W:S ratio	8:1	8:1	4:1	4:1	8:1	4:1
kg ore/m³ plant per 24 hours.	10	30	60	75	30	50
Gold dissolution %	97,0	96,8	96,8	93		
Sulphide oxidation %	97,4	84,4	84,8	72		

Optimum mini plant conditions could not be duplicated on the Fairview plant due to a lack of blower capacity. At the lower W;S ratio blower delivered pressure was insufficient to overcome the increased head.

Power Consumption

High rates of sulphide oxidation in BIOX reactors result in high rates of oxygen consumption. Efficient air dispersion and oxygen mass transfer are thus required.

Traditionally this required gas dispersion was provided by the use of a Rushton or flat blade turbine, having a high power draw.

Recently high solidity axial flow impellers have been developed for gas dispersion applications. Various impellers of this design were evaluated and encouraging results achieved.

Results confirmed that these axial flow impellers consume less power, whilst maintaining good gas dispersion and oxygen mass transfer, and have the potential for significant operating and capital cost savings.

Similar Kla values are reported for the two types of agitators. Oxygen utilisation of the axial flow impeller at 17%, is however lower than the 27% achieved by a flat blade.

A trial agitator has been in operation at Fairview since January 1990. Indications to date are that a saving in power drawn of up to 50% will be possible. Gas dispersion and oxygen utilisation is however slightly lower than that for the flat blade.

Plant Operating Temperature

A second characteristic to a highly active BIOX® plant is the high energy release.

All BIOX® studies have, in the past, been conducted at a controlled maximum temperature of 40 °C.

At Fairview mine plant operating temperatures often exceed 40 °C during summer months, sometimes peaking at 53 °C.

A pilot plant run was completed over a period of ten months to adapt the BIOX culture and to confirm that operating temperatures can be continually maintained at 45 °C.

During this period the plant retention time was gradually decreased from eight to four days and it was shown that equivalent gold recoveries were maintained at this temperature.

Gold dissolutions and sulphur oxidation rates achieved during the pilot run at 45 °C are depicted in Figure 4 and Figure 5.

Continuous operation at 45 °C is expected to reduce cooling coil requirements by 20 to 30%.

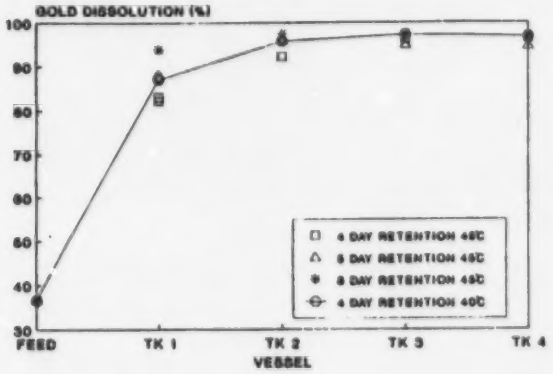

Figure 4. Gold Dissolution Profiles

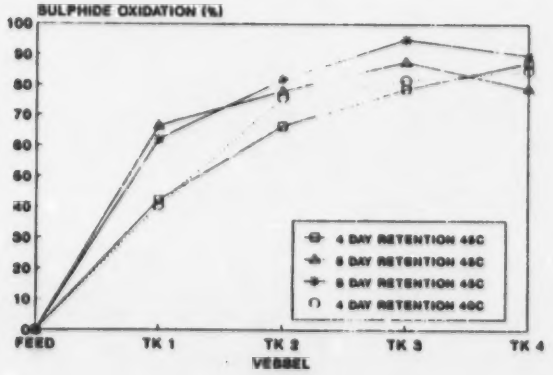

Figure 5. Sulphide Oxidation Profiles

Nutrient Addition

On going studies on nutrient addition has led to considerable reagent savings on the Fairview BIOX® plant. The optimum conditions are still to be determined.
Table 5 gives changes that have been brought about.

Table 5. - Nutrient Addition

	ADDITION RATE kg/t CONCENTRATE		
	1987	1988	1989
NH_4^+	9,62	8,73	8,40
K^+	13,05	4,27	1,43
PO^{3-}_4	1,50	1,52	1,56

These nutrients are conveniently provided as $(NH_4)_2SO_4$, KOH and H_3PO_4. Alternative sources include K_2SO_4 and $(NH_4)_3PO_4$.

Stability of Precipitates

During the bio-oxidation process arsenic and sulphur are solubilised and the resultant effluents are neutralised by limestone and/or milk of lime.

The neutralisation is normally completed in two stages viz neutralisation to pH 5 in the first stage and then to above pH 8 in the final stage. This has the advantage of better control at a pH of 5 and hence formation of a more stable product. Use of limestone has an added economic advantage.

The arsenic and sulphur contained in the effluent are then precipitated as basic ferric arsenate $(FeAsO_4)(FeOH_3)$ and calcium sulphate. Dissolved arsenic values of less than 0,5 ppm, are achieved.

Testwork has also indicated that the ferric arsenate precipitate is stable and does not redissolve if the pH is maintained between the levels of 2 and 9, and if the initial Fe^{3+} : As^{5+} ratio in the solution to neutralisation exceeds 3,5:1.

The long term stability of the precipitate can be evaluated according to a specific method developed by the United States Environmental Protection Agency. (EPA).

According to the EPA standards a solid waste exhibits the characteristics of toxicity if the toxicity characteristic leaching procedure (TCLP) produces a liquid containing specified contaminants at specified concentrations.

Application of the TCLP procedure to precipitates from neutralised effluent solutions yielded acceptable concentrations for the specified contaminants.

Results are depicted in Table 7.

Table 7. - TCLP Specifications

Contaminant	Concentration - ppm ≤	Typical Test results ppm
Arsenic	5,0	0,02
Barium	100,0	0,15
Cadmium	1,0	0,02
Chromium	5,0	0,20
Lead	5,0	0,48
Mercury	0,2	0,02
Selenium	1,0	0,04
Silver	5,0	0,05

Continuous Cyanidation

Cyanide consumptions are normally higher for the treatment of BIOX products compared to those produced through either roasting or pressure oxidation. This is especially so for the bio-oxidation of pyrite/arsenopyrite concentrates where the higher cyanide consumptions incurred result in increased reagent costs.

Continuous cyanidation was tested on a pilot scale with controlled cyanide concentrations in each stage. Results confirmed that a cyanide saving of approximately 30% can be expected compared to operation in batch mode where the average cyanide concentration is much higher. Cyanide consumptions for Fairview concentrate has been reduced from 15 kg/t to 10 kg/t during the pilot plant campaign.

Future Developments

The continued successful operation of the BIOX® plant at Fairview mine, as well as new improved process developments, has confirmed that bio-oxidation is a viable process for the pre-treatment of refractory gold ores before cyanidation.

With this confidence, Genmin has made the following decisions:

- Plant treatment capacity at Sao Bento is to be increased by the installation of a BIOX system in series with the autoclaves. The first step is the installing of a single 550 m³ tank which will effectively increase the overall capacity by 12,5 percent. This tank is due for commissioning in November 1990.
- The Fairview plant is being expanded to treat the total concentrate production. This plant will be commissioned during March 1991. The Edwards roasters will then be decommissioned.
- Work is to commence on the treatment of ores not amenable to flotation.
- To date all Genmin BIOX® development work has been done on flotation concentrate.
- It is envisaged that oxidation rates will be rapid and lower pulp W:S ratios could be possible. This will result in treatment of high tonnages of run-of-mine ore being feasible. The BIOX®/Pressox combination has good potential in this area.

Conclusion

With four years of operation, the BIOX® plant at the Genmin Fairview Mine can be considered a commercial success. The key variables in the process are air dispersion, W:S ratio, heat removal, and stability of the arsenic contaminated residues.

High solidity axial flow impellers for solids suspension and air dispersion exhibit considerable savings in power but at a lower air absorption efficiency.

The W:S ratio can be reduced to 4:1 without effect on the activity of the bacteria. The bacteria strain as used at Fairview can be adapted to operate continuously at 45 °C and can tolerate peaks of up to 53 °C.

The stability of the precipitated arsenic meets EPA standards.

Finally it has been shown that where an autoclave plant is in existance the installation of a BIOX system as a preoxidation step to the autoclaves is a viable alternative in expanding capacity.

Acknowledgement

The authors would like to acknowledge Genmin for permission to publish the paper. Special acknowledgement is also made to the personnel of Genmin Process Research and the Fairview mine for their contribution to the development of the process and their continued interest and support.

References

1. Haines A.K., van Aswegen P.C.,
1990, "Process and Engineering Challenges in the Treatment of Refractory Gold Ores". International Deep Mining Conference, Johannesburg. Vol 1, Innovations in Metallurgical Plant.

2. Van Aswegen P.C., Marais H.J., Haines A.K.,
1988, "Design and Operation Of A Commercial Bacterial Oxidation plant at Fairview", Perth International Gold Conference.

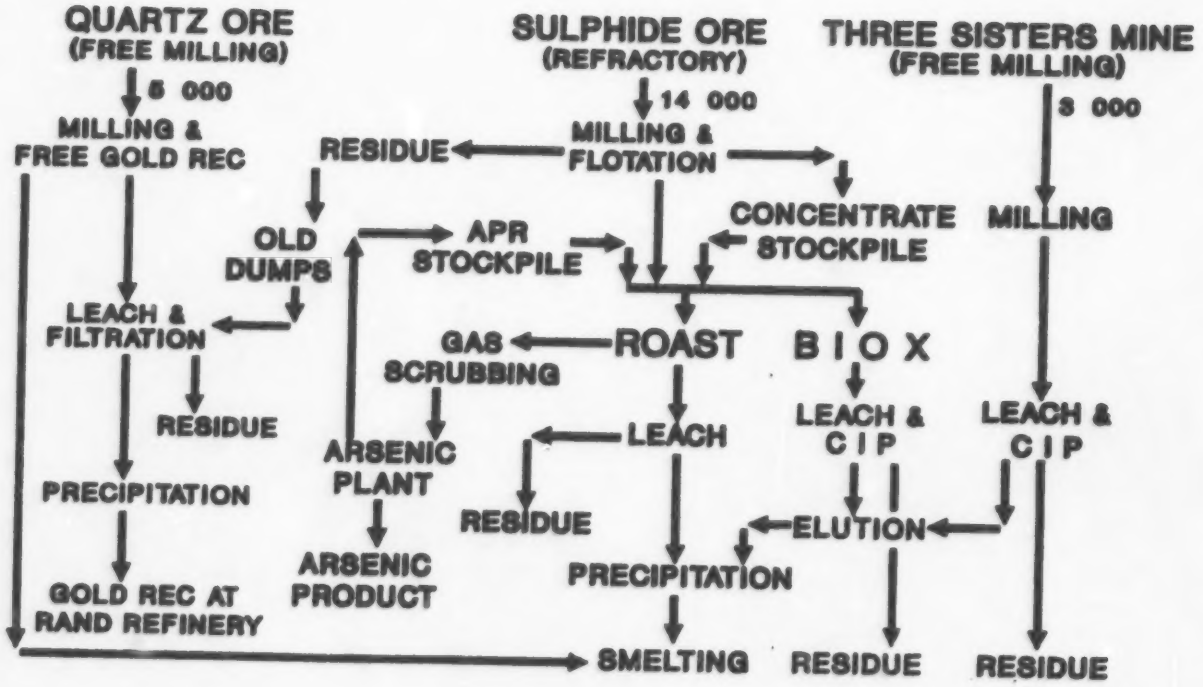
QUARTZ ORE
(FREE MILLING)
5 000
MILLING &
FREE GOLD REC
LEACH &
FILTRATION
RESIDUE
PRECIPITATION
GOLD REC AT
RAND REFINERY
SULPHIDE ORE
(REFRACTORY)
14 000
MILLING &
FLOTATION
RESIDUE
OLD
DUMPS
APR
STOCKPILE
CONCENTRATE
STOCKPILE
GAS
SCRUBBING
ROAST
ARSENIC
PLANT
ARSENIC
PRODUCT
LEACH
RESIDUE
PRECIPITATION
SMELTING
THREE SISTERS MINE
(FREE MILLING)
3 000
MILLING
B I O X
LEACH &
C I P
ELUTION
RESIDUE
LEACH &
C I P
RESIDUE

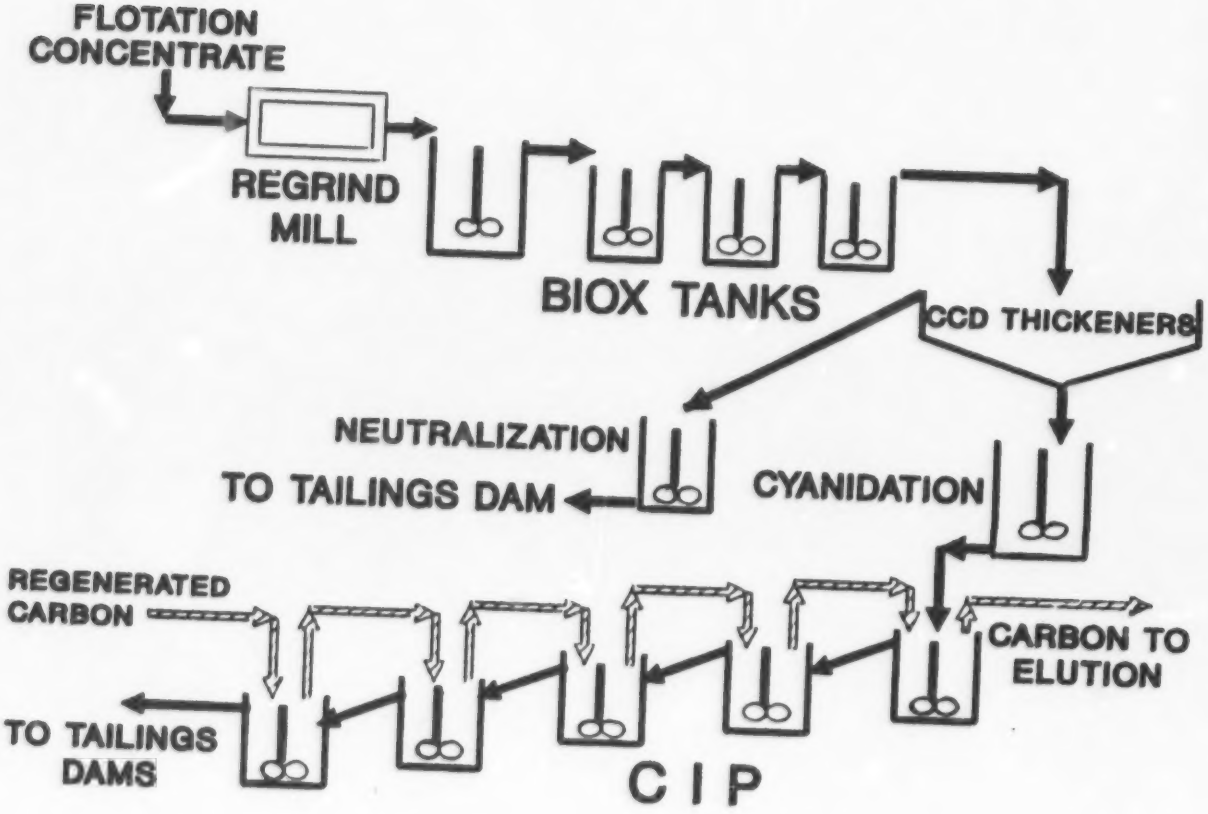
FLOTATION CONCENTRATE
REGRIND MILL
BIOX TANKS
CCD THICKENERS
NEUTRALIZATION
TO TAILINGS DAM
CYANIDATION
REGENERATED CARBON
CARBON TO ELUTION
TO TAILINGS DAMS
CIP

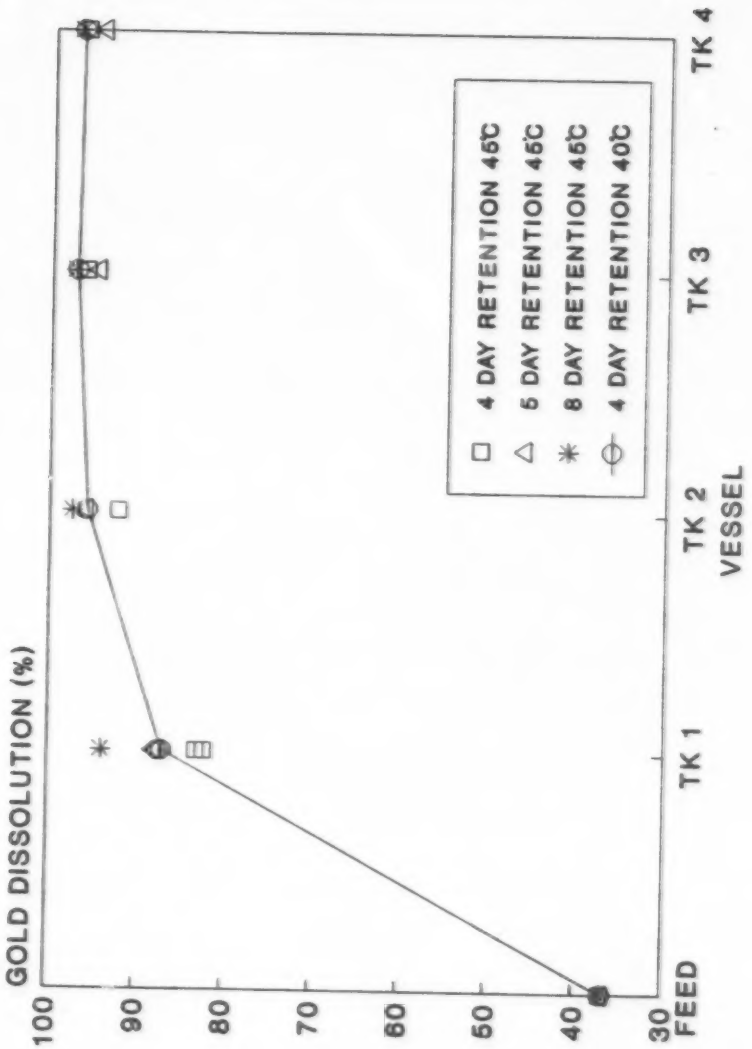
GOLD DISSOLUTION (%)
100
90
80
70
60
50
40
30
FEED
TK 1
TK 2
TK 3
TK 4
VESSEL
4 DAY RETENTION 45C
5 DAY RETENTION 45C
8 DAY RETENTION 45C
4 DAY RETENTION 40C

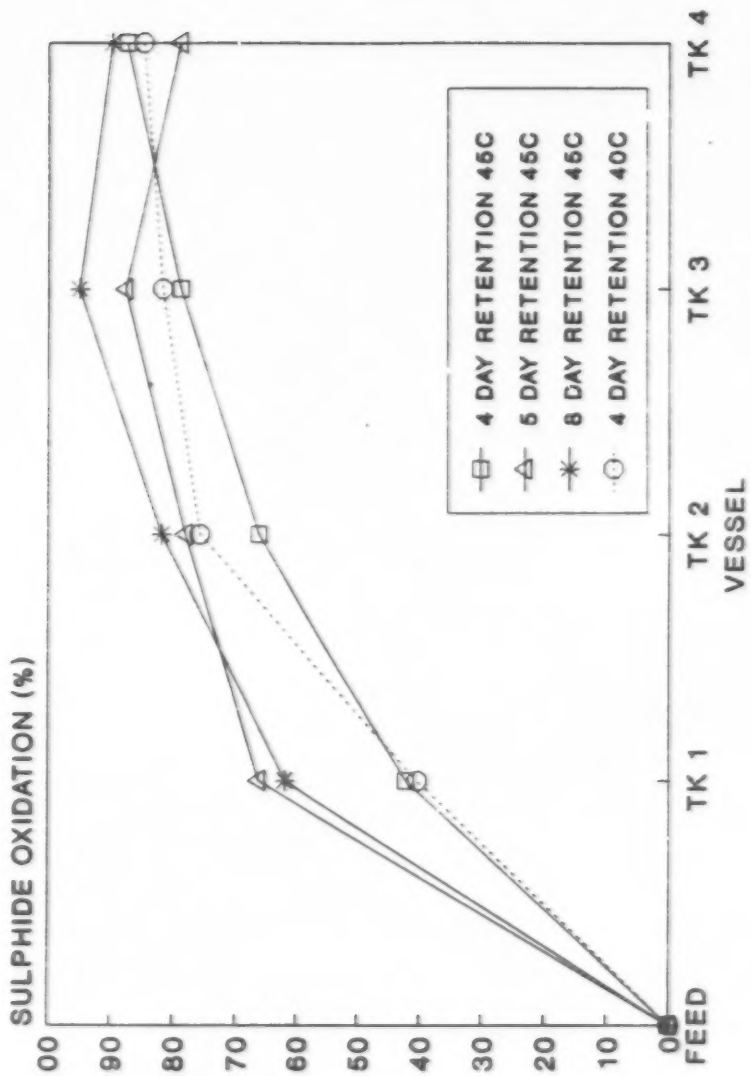
SULPHIDE OXIDATION (%)
100
90
80
70
60
50
40
30
20
10
0
FEED
TK 1
TK 2
TK 3
TK 4
VESSEL
4 DAY RETENTION 45C
5 DAY RETENTION 45C
8 DAY RETENTION 45C
4 DAY RETENTION 40C

SOCIETY FOR MINING, METALLURGY, AND EXPLORATION, INC.

P O BOX 625002 • LITTLETON COLORADO • 80162-5002

PREPRINT NUMBER

91-38

MECHANISM OF ELECTROOXIDATION OF REFRACTORY GOLD ORES

F. Arslan

P. Duby

Columbia University
New York, New York

For presentation at the 1991 SME Annual Meeting
Denver, Colorado - February 25-28, 1991

Permission is hereby given to publish with appropriate acknowledgments, excerpts or summaries not to exceed one-fourth of the entire text of the paper. Permission to print in more extended form subsequent to publication by the Society must be obtained from the Executive Director of the Society for Mining, Metallurgy, and Exploration, Inc.

If and when this paper is published by the Society for Mining, Metallurgy, and Exploration, Inc., it may embody certain changes made by agreement between the Technical Publications Committee and the author, so that the form in which it appears is not necessarily that in which it may be published later.

These preprints are available for sale. Mail orders to PREPRINTS, Society for Mining, Metallurgy, and Exploration, Inc., P.O. Box 625002, Littleton, Colorado 80162-5002.

PREPRINT AVAILABILITY LIST IS PUBLISHED PERIODICALLY IN MINING ENGINEERING

ABSTRACT

Gold extraction from refractory ores is still a problem. Gold losses in the cyanidation process are mainly due to the presence of sulfides and carbonaceous materials. Oxidation of carbon and sulfide minerals by sodium hypochlorite is a possible method to render the ore amenable to cyanidation, and earlier work by the USBM indicates that electrochemical generation of hypochlorite is promising. Laboratory work was carried out on the oxidation of pyrite and carbon in an electrochemical cell with a sodium chloride electrolyte. The results of preliminary tests are discussed in relation to the mechanism of electrooxidation of refractory gold ores and the estimation of current efficiency.

INTRODUCTION

Gold ores are considered to be refractory if a significant portion of the gold can not be extracted by conventional cyanidation process. Refractory gold ores can be classified into two groups – sulfidic and carbonaceous ores. Ores containing chalcocite, covellite, chalcopyrite, pyrrhotite, realgar, orpiment and stibnite are accessible to cyanidation but create two kinds of impurities, such as metal cations and sulfur compounds ($S^{2-}, S_2O_3^{2-}, SO_3^{2-}$).[1] Metal cations form complexes with cyanide and consume reagent while the sulfide ions form thiocyanide ions according to the following reaction:[1,2]

$$S^{2-} + 1/2O_2 + CN^- + H_2O \longrightarrow CNS^- + 2OH^-$$

Sulfide ions also adsorb on a gold surface and inhibit the dissolution reaction by passivation. The existence of iron oxide coatings around gold particles also results in the retardation of gold dissolution.[1]

In some ores cyanidation is incomplete because a large portion of the fine gold remains locked within the host mineral and never comes in contact with the cyanide solution. Finely disseminated gold can be found in sulfides (pyrite and arsenopyrite) or siliceous minerals. In several deposits, a significant portion of the gold occurs in submicroscopic form, and even fine grinding fails to liberate the gold. Therefore, it is necessary to break down the crystal lattice of the host mineral in order to liberate the gold. The Carlin type Nevada ores, for instance, contain up to 3% pyrite.[3]

Carbonaceous gold ores are refractory to cyanidation because of poor release of gold from carbonaceous material and readsorption of dissolved gold to the carbonaceous leach residue.[1,4,5] These ores contain a) an activated carbon component (capable of adsorbing gold complexes from the solution), b) a mixture of hydrocarbons usually associated with activated carbon components which form a gold complex during the deposition that is not attacked by cyanide, and c) an organic acid similar to humic acid (contains functional groups capable of interacting with gold complexes to form organic gold compounds). The mineralogy of carbonaceous materials may vary, but all of them have the carbon–containing compounds which often interact adversely with dissolved gold. The carbonaceous material is intimately associated with quartz, sericite, carbonate and some sulfide. Most of the Carlin carbonaceous ores contain from 0.4 to ~ 1% organic carbon with occasional samples as high as 4%.[5]

Various techniques have been investigated to treat these ores prior to cyanidation such as flotation, roasting, biological oxidation, pressure oxidation and chemical oxidation.[6]

Researchers at the USBM have shown that, when the carbonaceous ore was added to the oxide ore, gold extraction by direct cyanidation decreased linearly from 95% to 32%.[7] The analysis of tails showed that $Au(CN)_2^-$ was adsorbed on carbonaceous components. Various oxidation systems were chosen for initial experiments in pretreating the carbonaceous samples to destroy the deleterious carbon. These systems include ozone, chlorine, sodium hypochlorite, calcium hypochlorite, permanganates, perchlorates, chlorates, oxygen and sulfuric acid.[8,9] Gold extraction by cyanidation after

oxidation was increased in nearly every case over that obtained without pretreatment. It was concluded that a comparatively mild chemical oxidation treatment would be sufficient to disrupt that association of gold with carbon and organic compounds.

The Newmont Gold Company (Nevada) has been processing carbonaceous and sulfidic refractory ores by chlorination prior to cyanidation.[9] NaOCl is another oxidant which is inexpensive, readily available, and easy to handle. Electrooxidation was investigated by the USBM as a means of generating oxidizing conditions in-situ in the ore pulp prepared from finely ground ore and NaCl brine.[10,11] Initial tests were conducted on the Carlin type carbonaceous ores. Molybdenum and rhenium recovery from molybdenite concentrates and silver and mercury recovery from tailings and cinnabar ores were also studied.[12,13]

These authors investigated several parameters such as salt concentration, electrolysis time, temperature, current density, types of electrodes, electrode spacing, particle size of the ore and pulp density.[14] Optimum salt concentration was found to be 10%, pulp density 40%, temperature 40°C, current density 775–1163 A/m^2 of anode surface.

Similar to the refractory gold ores, coal also contains organic and inorganic sulfur (pyritic). Although soluble sulfates and coarse pyrite can be removed physically, most of the finely disseminated pyrite and the organic sulfur remain untouched. Chlorination is one of the chemical desulfurization processes. Recently, the kinetics of the chlorination of the pyrite in aqueous media was studied.[15] Optimum temperature found to be 36°C and pyrite oxidation increased with decreasing particle size.

The purpose of our experimental study is to achieve a better understanding of the mechanism of electrooxidation. Therefore, it will be concentrated on the electrooxidation of pyrite and carbon, in order to explain the electrooxidation process. At the same time, the hypochlorite production process will also be investigated.

EXPERIMENTAL PROCEDURE

The experimental setup is shown in Figure 1. The cell had separate anolyte and catholyte compartments connected through a porous glass frit. A circulation of nitrogen gas removed the reaction products of the anodic process. The out-going gas stream was sparged through a 0.5 M sodium hydroxide solution to adsorb the chlorine and the carbon dioxide. A saturated CaO solution was placed after the NaOH solution cells in order to assure that no CO_2 gas escaped. A current of 1.0 A was applied to the cell using a D.C. power supply. A copper coulometer was in series with the cell. A Pt/Ir (70/30) coated (5 g/m^2) titanium plate was the anode and a spiral-shaped platinum wire served as cathode.

In all experiments 10 wt% NaCl solutions were used. In the case of carbon oxidation, 5 wt% petroleum coke (supplied by Amax), and in the case of pyrite oxidation, 5 wt% pyrite in the range of -275+325 mesh (from Huanzala, Peru), were added to the anolyte.

The temperature was measured during the experimental runs. It was found that in one hour, the anolyte temperature went up to 35–40°C and remained constant. Since the optimum temperature was found to be 40°C by the USBM, there was no need for controlling the temperature during the preliminary tests.

Cell potentials, anodic potentials (versus saturated calomel electrode, SCE), and anolyte pH were also recorded during the runs. Anolyte pH was adjusted with 5.0 M NaOH whenever required. Anolyte and catholyte solutions were stirred in order to provide a good mixing. The cell was designed in such a way that 5 ml of sample solution could be withdrawn at known time intervals for analysis.

At the end of each run, in the case of oxidation of carbon and pyrite, anolyte and catholyte solutions were filtered. Anolyte, catholyte and NaOH solutions were analyzed for Cl^- by potentiometric titration with silver nitrate, and for OCl^- by iodimetry, in all cases. In addition to those analyses, solutions were also ana-

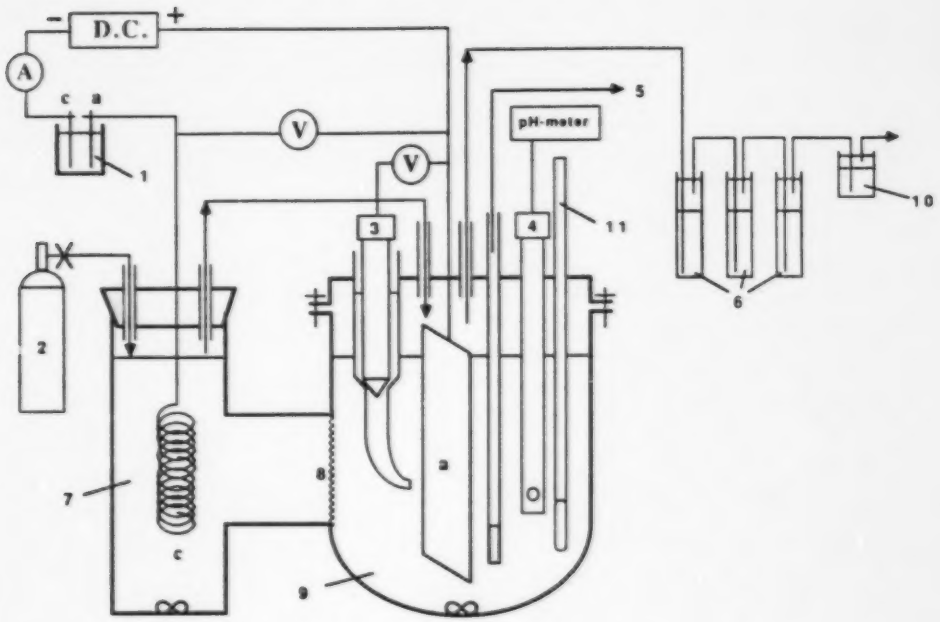

Figure 1. Experimental setup for the electrooxidation process.

A :	Ammeter	4 :	pH electrode
V :	Voltmeter	5 :	Sampling
c :	cathode	6 :	0.5 M NaOH solution
a :	anode	7 :	Catholyte
D.C.:	Power supply	8 :	Glass frit
1 :	Copper coulometer	9 :	Anolyte
2 :	Nitrogen gas tank	10 :	Saturated CaO solution
3 :	Saturated Calomel Electrode	11 :	Thermometer

lyzed for CO_2 by acid-base titration in the case of carbon oxidation experiments, and for total iron by spectrophotometry (Hach, DR/2000) in the case of pyrite oxidation.

EXPERIMENTAL RESULTS

In preliminary experiments a one-compartment cell was used. Three different sets of anode–cathode were tested: graphite–copper, graphite–graphite, and Pt/Ir coated titanium–copper. Hypochlorite production was almost the same in all cases. During the experiments a precipitate was observed at the copper cathode. When a graphite anode was used, it was oxidized resulting in mechanical degradation with time which was evidenced by the existence of dissolved CO_2 in the electrolyte in the hypochlorite production experiments. The Pt/Ir coated Ti anode was found chemically and dimensionally stable in this system and was used in subsequent tests.

Experimental results are summarized in three parts: hypochlorite production, pyrite oxidation, and carbon oxidation. Total concentrations of hypochlorite, iron, and carbon were calculated based on the initial volume of 500 ml. No corrections for evaporation were made.

Hypochlorite Production

Figure 2 illustrates hypochlorite production versus time. When the anolyte pH was controlled between 5 and 8, hypochlorite production increased sharply with time at the beginning but levelled off after 6 hours. Initial current efficiency was about 85%. In the case of no pH control, hypochlorite production increased gradually with time and started to level off after 12 hours, reaching higher values than in the pH controlled case. Initial current efficiency was approximately 60%. The second curve represents three runs at the same experimental conditions showing good reproducibility. At the end of the runs the hypochlorite production was twice that in the case of pH control.

Anolyte pH change with time is shown in Figure 3. As soon as current was started, the anolyte pH decreased from about 6 to 2.5 in one hour; it increased gradually to the initial pH at the end of 10 hours and stayed there for the remaining of the run. Catholyte pH was about 13 at the end of the runs in both cases.

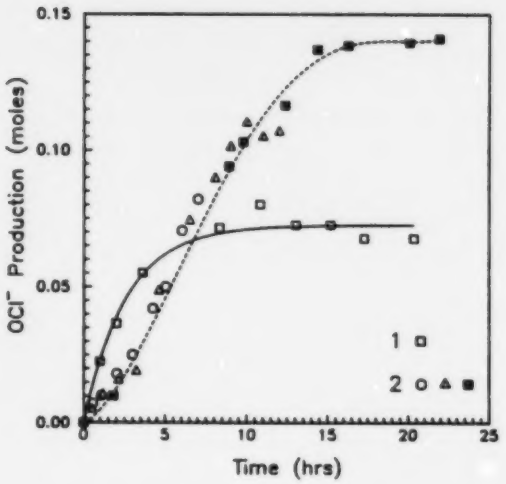

Figure 2 : Hypochlorite production versus time (Current = 1.0 A). Anolyte pH is (1) controlled, and (2) not controlled.

Oxidation of Pyrite

Results are shown in Figure 4. The amount of total iron oxidized increased gradually with time. Current efficiency was about 100% and initial oxidation rate of pyrite was about 0.4 g pyrite/hr. During the experiment, each sample was also analyzed for hypochlorite. Results showed that hypochlorite was not consumed totally by pyrite.

Anolyte pH change with time is shown in Figure 3. Anolyte pH decreased very sharply to 1 in one hour and continued to decrease slowly until the end.

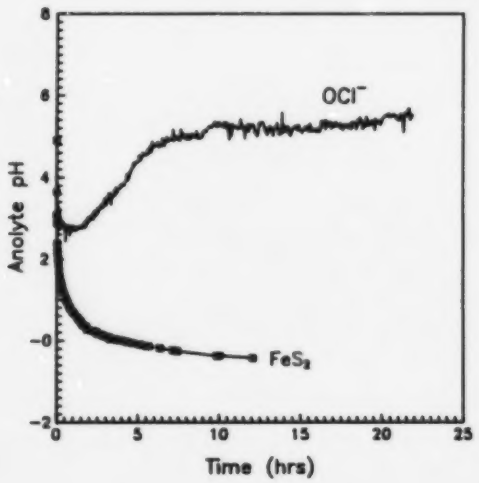

Figure 3 : Change of anolyte pH with time during the production of OCl^-, and the oxidation of pyrite.

Oxidation of Carbon

Figure 5 shows carbon oxidation versus time. Carbon oxidation increased gradually with time and levelled off after 10 hours. Current efficiency for initial oxidation was about 100%. Analysis of solutions showed that hypochlorite was not consumed totally by carbon during the oxidation. Oxidation rate was about 0.4 g carbon/hr. Anolyte pH dropped to 1 in one hour and stayed there until the end.

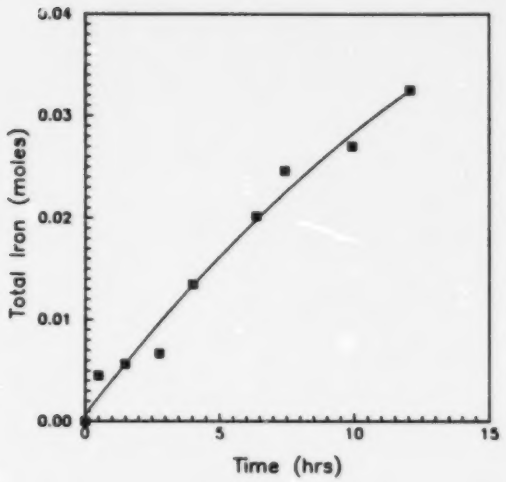

Figure 4 : Oxidation of pyrite versus time in 500 ml solution containing 10 wt% NaCl, and 5 wt% FeS_2 (Current = 1.0 A).

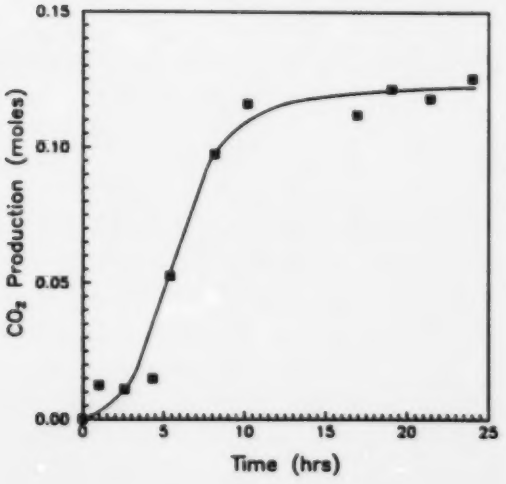

Figure 5 : Oxidation of carbon versus time in 500 ml solution containing 10 wt% NaCl, and 5 wt% petroleum coke (Current = 1.0 A).

DISCUSSION

Chemical reactions which occur during the electrooxidation process can be expressed as follows. The chloride ion is converted to chlorine at the anode:

$$2Cl^- \longrightarrow Cl_2 + 2e^- \qquad (1)$$

At the cathode, water is hydrolyzed to produce hydroxyl ion and hydrogen:

$$2H_2O + 2e^- \longrightarrow H_2 + 2OH^- \qquad (2)$$

At the anodic side hypochlorite is produced according to the following reactions. Chlorine reacts with water to produce hypochlorous acid:

$$Cl_2 + H_2O \longrightarrow HClO + H^+ + Cl^- \qquad (3)$$

then, hydroxyl ions produced at the cathode react with hypochlorous acid to form hypochlorite:

$$HClO + OH^- \longrightarrow ClO^- + H_2O \qquad (4)$$

and with hydrogen ions to form water:

$$H^+ + OH^- \longrightarrow H_2O \qquad (5)$$

Hypochlorite then, reacts with carbonaceous material in the ore:

$$C + 2ClO^- \longrightarrow CO_2 + 2Cl^- \qquad (6)$$

and with pyrite:

$$2FeS_2 + 15ClO^- + H_2O + 2H^+ \longrightarrow 2Fe^{3+} + 4HSO_4^- + 15Cl^- \qquad (7)$$

According to equation (3), Cl_2 produced at the anode reacts with water resulting in the production of HClO along with H^+ and Cl^-. This explains the pH decrease when the current was switched on, as seen in Figure 3. As soon as OH^- ions (produced at the cathode) start to diffuse toward the anolyte they react with H^+ ions as in equation (5) and the anolyte pH starts to rise until it reaches the initial pH value and stays there until the end.

After a certain time, hypochlorite production levels off as shown in Figure 2. This is attributed to the production of chlorates, either chemically:

$$2HClO + ClO^- \longrightarrow ClO_3^- + 2H^+ + 2Cl^- \quad (8)$$

or electrochemically:

$$6ClO^- \longrightarrow 6ClO + 6e^- \quad (9)$$

$$6ClO + 3H_2O \longrightarrow 2ClO_3^- + 6H^+ + 4Cl^- + 3/2O_2 \quad (10)$$

Electrochemical reduction of hypochlorites at the cathode is also possible according to the following reaction:

$$ClO^- + 2H^+ + 2e^- \longrightarrow H_2O + Cl^- \quad (11)$$

Analysis of catholyte at the end of each run shows some hypochlorite which diffused from anolyte, supporting the hypochlorite reduction at the cathode. The reactions above, (8) to (11), explain the levelling off of hypochlorite concentration.

In the case of pyrite oxidation, the anolyte pH decreases continously as illustrated in Figure 3, due to the production of HSO_4^- according to the reaction (7). The measured anode potentials, as seen in Figure 6, support the oxidation of pyrite to Fe^{3+} according to equation (7). Oxidation of pyrite is dependent on the production of hypochlorites. During the pyrite oxidation, no elemental sulfur formation is observed. The analysis of pyrite concentrate and the filter cake shows similar Fe/S ratio which is about 0.75. SEM micrographs of pyrite concentrate used in the preliminary experiments and pyrite residue (after 7 hours of oxidation) are very similar as seen in Figure 7. They also agree with the chemical analysis showing no elemental sulfur formation during the oxidation.

In the case of carbon oxidation, CO_2 production with time also levels off with the hypochlorite concentration. This shows that the oxidation of carbon depends on the hypochlorite production. According to Figure 6, the value of anode potential, in the case of carbon oxidation, supports equation (6) for carbon oxidation.

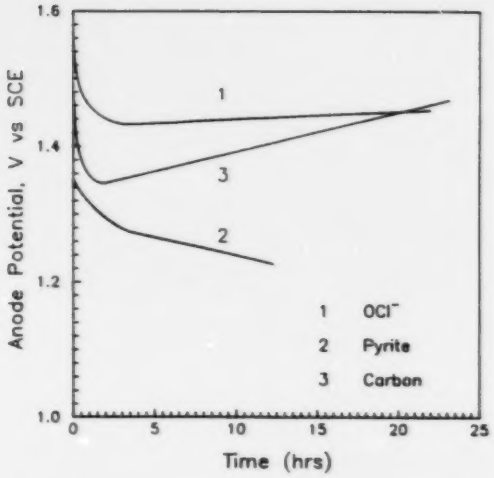

Figure 6 : Anode potential change with time during the production of hypochlorite (1), electrooxidation of pyrite (2), and electrooxidation of carbon (3).

CONCLUSION

Electrochemical generation of hypochlorite in 10 wt% NaCl solutions at 40°C is possible. Although the initial current efficiency was found to be higher when the solution pH was controlled, total hypochlorite production levelled off earlier than that of pH was not controlled.

According to the preliminary test results, pyrite and carbon can be oxidized by the hypochlorite generated electrochemically in the cell with about 100% initial current efficiency. This shows that pyrite and carbon in the refractory gold ores can be efficiently oxidized by electrooxidation. Future experiments will be concentrated on the oxidation of refractory ores and the modelling of the process. It appears that electrooxidation can be an efficient and economical treatment for the refractory gold ores.

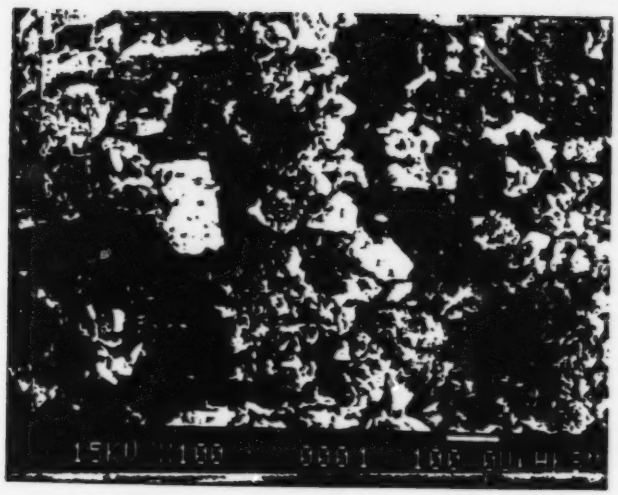

Figure 7.a : SEM micrograph of pyrite concentrate.

Figure 7.b : SEM micrograph of pyrite residue, at the end of 7 hour-run.

ACKNOWLEDGEMENT

One of the authors (F. Arslan) wishes to thank to the Turkish Government for its financial support. This research has been partially supported by the Department of the Interior's Mineral Institutes Program administered by the Bureau of Mines under allotment grant number G1184136.

REFERENCES

1. Demopoulos, G.P., "Mineralogical and Technological Aspects of Gold Extraction from Refractory Ores", presented at the Professional Development Seminar in Mineral Processing of Gold Ores held at the Department of Mining and Metallurgical Engineering, McGill University, April 2–May 2, 1987.

2. Chemistry of Cyanidation, Mineral Dressing Notes, American Cyanide Company, AIME Annual Meeting, N.Y., Feb. 13–16, 1950.

3. Hauser, D.M., "Process Mineralogy of Auriferrous Pyritic Ores at Carlin, Nevada", Process Mineralogy, Eds. D.M. Hauser and W.C. Park, TMS Publication, 1981, pp. 271–289.

4. Osseo–Asare, K., Afenya, P.M., and Abotski, G.M., "Carbonaceous Matter in Gold Ores: Isolation, characterization, and adsorption behaviour in aurocyanide solutions", Precious Metals: Mining, Extraction, and Processing, Eds. V. Kudryk, D.A. Corrigan, and W.W. Liang, TMS Publication, 1984, pp.125–144.

5. Guay, W.J. and Gross, M.A., "The Treatment of Refractory Gold Ores Containing Carbonaceous Material and Sulfides", AIME Annual Meeting, Chicago, Illinois, Feb. 22–26, 1981.

6. Scheiner, B.J., "Relation of Mineralogy to Treatment Methods for Carbonaceous Gold Ores", SME Annual Meeting, Denver, Colorado, Feb. 24–27, 1987.

7. Scheiner, B.J., Lindstrom, R.E., and Henrie, T.A., "Oxidation Process for Improving Gold Recovery from Carbon–Bearing Gold Ores", Bureau of Mines Report of Investigations, 1971, RI 7573.

8. Scheiner, B.J., Lindstrom, R.E., and Henrie, T.A., "Investigation of Oxidation Systems For Improving Gold Recovery from Carbonaceous Materials", Bureau of Mines Heavy Metals Program Technical Progress Report, July 1968, U.S. Department of Interior.

9. Seymour, D., Ramadorai, G., Traczyak, F., and Hill, D., "Rapid Oxidation of Refractory Gold–Bearing Ores by Intense Flash Chlorination at Newmont Gold Company", Precious Metals '89, Eds. M.C. Jha and S.D. Hill, The Minerals, Metals, and Materials Society, 1988, pp. 165–178

10. Scheiner, B.J., Lindstrom, R.E., and Henrie, T.A., "Process for Recovering Gold from Carbonaceous Ores", U.S. Patent No. 3,574,600, April 13, 1971, and U.S. Patent No. 3,639,925, Feb. 8, 1972.

11. Scheiner, B.J., Lindstrom, R.E., Guay, W.J., and Peterson, D.G., "Extraction of Gold from Carbonaceous Ores: Pilot Plant Studies", Bureau of Mines Report of Investigations, 1972, RI 7597.

12. Lindstrom, R.E. and Scheiner, B.J., "Extraction of Molybdenum and Rhenium from Concentrates by Electrooxidation", Bureau of Mines Report of Investigations, 1973, RI 7802.

13. Scheiner, B.J., Pool D.L., and Lindstrom, R.E., "Recovery of Silver and Mercury from Mill Tailings by Electrooxidation", Bureau of Mines Report of Investigations, 1972, RI 7660.

14. Scheiner, B.J., Lindstrom, R.E., and Henrie, T.A., "Processing Refractory Carbonaceous Ores for Gold Recovery", Journal of Metals, March 1971, pp. 37–40.

15. Bayrakçeken, S., Yaşar, S., and Çolak, S., "Kinetics of the Chlorination of Pyrite in Aqueous Suspension", Hydrometallurgy, Vol. 25(1990), pp. 27–36.

Chapter 30

CARBON SAMPLING IN GOLD CIRCUITS

by

Tom Bruington
Mine Development Associates
Reno, Nevada

ABSTRACT

This paper discusses the accuracy of determining the quantities of gold and silver on activated carbon in various stages of process for typical precious metals flowsheets. Accurate plant performance evaluation depends upon reliable estimates of carbon and precious metals inventories. The sources of sampling error are identified and methods of reducing them discussed. Several case studies illustrating the sensitivity of flowsheet performance to sampling error are presented.

INTRODUCTION

Metallurgical performance of gold and silver mineral processing flowsheets is typically evaluated using assay balance and production balance techniques. With assay balance the millfeed, tailings, and some intermediate streams are sampled and assayed. Plant performance can then be evaluated using mass balance techniques. Unsteady plant conditions and difficulties in sampling and measuring moving streams are some problems with this method. Production balance measures two rather tangible quantities, tons milled and ounces poured, combines this with the tailings assay to calculate head grade and recovery. Changes to in-process inventory must be monitored as the production balance is highly sensitive to this factor.

The primary inventory location for flowsheets utilizing activated carbon is gold (and silver) on the carbon. Thus a production balance must include a sampling program to determine the amount of carbon in the various stages of process and the gold adsorped on that carbon. To get an accurate estimate of the inventory the sampling program must satisfy 5 conditions:

1) The concentration of carbon in the sample must be representative of the concentration of carbon in the vessel sampled.

2) The gold grade of the ample must be representative of the gold grade of the carbon in the vessel.

3) The sample preparation procedure must not introduce a bias of the assay sample from the original sample.

4) The assay methodology must reflect the true grade of the assay sample.

5) The samples must be taken at a time that coincides with the termination of the production period.

Accurate estimation of gold inventory will assist in scheduling and control of the carbon and strip circuits, improve production forecasting, and provide increased security controls.

ESTIMATION OF CARBON INVENTORIES

The first task is to measure the quantity of carbon in the various process stages. In carbon columns (CC) or strip vessels where only carbon is present, a direct volumetric measurement is possible. In carbon-in-pulp (CIP) or carbon-in-leach (CIL) systems it is necessary to obtain a sample from the agitated mix of carbon and pulp. Wetted carbon will settle (sp gr 1.35) in water. Thus a complex situation involving pulp rheology (sp gr, viscosity, and % solids), carbon particle parameters (size, density, and shape), and agitation dynamics determines the suspension of the mix.

The accuracy of the sample (in terms of carbon concentration) depends upon three conditions being met:

1) The agitation and pulp characteristics provide a uniform concentration of carbon throughout the tank. If this is not the case then a method of correction must be devised. This usually involves sampling at various vessel locations.

2) The sample methodology must not disturb the agitation conditions beyond an acceptable limit. Holding a sample cup into the pulp for a period of minutes will result in a cupful of carbon, the interior of the cup being a quiescent zone allowing the carbon to settle. A methodology which favores carbon particles of a certain size range or shape would create a bias in gold grade, as discussed in the next section.

3) The sample is of sufficient size to be representative of the vessel. A one litre sample is only about one millionth the volume of a typical CIP/CIL vessel.

Popular sample techniques are a) the surface dip sample, b) a sampler made of a long pipe with a foot valve at the bottom and a ball valve on top, c) sampling spigots along the side of the vessel, and d) an air lift mechanism to lift a sample stream to the surface. If vibrating deck screens are installed as interstage screens it is possible to directly measure the amount of carbon being transferred from stage to stage.

the sample (in concentration) ee conditions

and pulp provide a cation of carbon tank. If this is hen a method of t be devised. volves sampling el locations.

odology must not e agitation nd an acceptable a sample cup for a period of sult in a cupful interior of the quiescent zone arbon to settle. which favores es of a certain or shape would in gold grade, as he next section.

s of sufficient epresentative of one litre sample one millionth the typical CIP/CIL

e techniques are lip sample, b) a a long pipe with the bottom and a top, c) sampling the side of the an air lift t a sample stream If vibrating deck installed as ns it is possible ure the amount of transferred from

From a gold inventory perspective, greater effort should go toward sampling the first and second stages as most of the gold inventory resides at these locations. This may involve larger samples, sample duplication, or an additional sampling technique. If agitation and rheology conditions deteriorate, carbon may settle out of suspension to become dead inventory. Dead inventory carbon can adsorp substantial gold over time, with significant effects upon the production balance. Favorite deposition sites are along the bottom edge of flat bottomed tanks and directly under the impeller shaft.

CARBON GRADE DISTRIBUTIONS

The ability of activated carbon to adsorp gold and silver is a complex matter of many variables, but for a given pulp (or pregnant solution) and agitation conditions, the gold grade of the carbon is a function of 1) the activity of the carbon, 2) the carbon surface area available for adsorption of gold cyanide complexes, and 3) the contact time.

Grade = f(Activity, Surface area, Contact time)

Two important relationships are applied to this equation, that the process flowsheet can determine the relative contact times of carbon particles in the system, and that size and shape factors can influence the surface area to mass ratio of the particles. Both relationships effect the gold grade of individual carbon particles.

Contact times

Carbon columns involve a fixed amount of carbon being contacted with pregnant solution in an ebullated bed, with the contact time of the carbon particles being equal. Assuming adequate mixing, the grade distribution of the particles is dependent upon the first two variables above. This should result in a 'normal' or 'gaussian' grade distribution, as shown by the solid line in Figure 1.

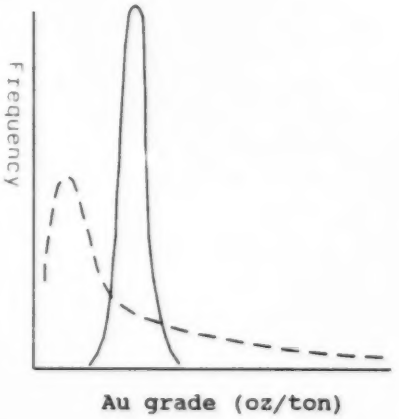

Figure 1. Frequency distribution of carbon particle gold grades.

A countercurrent system such as CIL or CIP with interstage carbon transfer will result in a far different distribution. For example, if a tank with an initial concentration of carbon has a given quantity of pulp pumped across a screen, removing the carbon (the pulp returns to the tank), the concentration of carbon will display an exponential decay over time. Likewise, if gold grade is dependent upon contact time, the carbon particle gold grades will be a highly shewed exponential distribution, with most particles having a low grade but a few having very long contact times resulting in very high grades.

The CIL/CIP circuit situation is more complex because 1) carbon is being transferred in as well as out, 2) the carbon being transferred in has an initial grade distribution, and 3) activity decreases with contact time. Thus the grade distribution of carbon particles from a countercurrent system is approximated as lognormal, shown as the dashed line in Figure 1. Note that both distributions have the same mean grade.

Thus the number of carbon particles required to make a robust estimate of the mean grade will be much greater for the lognormal distribution (CIP/CIL) due to the wide scatter in individual grades. This can effect the sample size requirements and the sample preparation procedures, as discussed in that section.

Size and shape factors

Gold adsorption onto carbon particles is limited by film diffusion as described by Davidson (1974). This means that the gold grade of a carbon particle will be a function of its surface area to mass ratio. Figure 2 illustrates this relationship. Thus smaller, flakier, and irregular shaped particles will have higher grades than their larger, regular shaped cousins. The behavior of such particles in the agitation tanks will be different, possibly resulting in a sample bias. Size and shape factors may cause segregation in sample preparation.

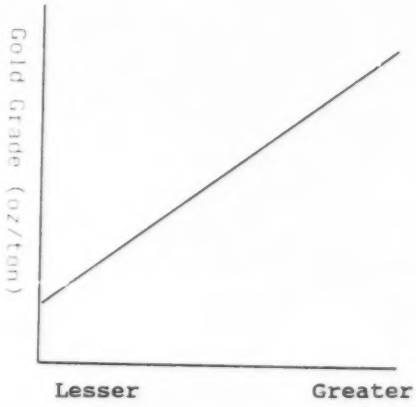

Figure 2. Relationship of surface area / mass ratio to carbon particle gold grades.

SAMPLE PREPARATION AND ASSAY

Having obtained a sample of carbon during our carbon concentration exercise, a subsample can be taken from this for sample preparation and assay.

ted by film
ed by Davidson
that the gold
rticle will be
rface area to
2 illustrates
Thus smaller,
egular shaped
higher grades
regular shaped
vior of such
gitation tanks
nt, possibly
ple bias. Size
s may cause
e preparation.

Greater

ass ratio

nship of surface
atio to carbon
des.

TION AND ASSAY

ied a sample of
our carbon
exercise, a
taken from this
ration and assay.

The size of this subsample should be large enough to contain sufficient carbon particles to provide a robust estimation of the gold grade. As noted in the previous section this will involve a larger sample for the CIL/CIP situation due to its skewed lognormal grade distribution. Segregation will cause the higher grade, smaller particles to separate from the lower grade, larger particles creating a potential sample bias.

Sample weight reduction should be preceded by reduction in sample particle size as outlined by Gy (1979). This is critical for the CIL/CIP case as one high grade particle could bias the results considerably. Thus it is preferable to pulverize the entire sample (dry) prior to splitting to assay charge size. The drawbacks are time, labor, and increased potential for contamination of other samples (loaded carbon may be +200 oz/ton).

Results of 11 round robin carbon assay trials conducted by the Society of Mineral Analysts, Wright (1990), indicates the accuracy of carbon assay repeats to be 7% (standard deviation as a percent of the mean). Thus 32% of the time (one standard deviation) we can expect an error of greater than +/- 7% in the assay.

CASE STUDY

To illustrate the results of 'typical' accuracies from the estimation of carbon inventories a hypothetical gold mine case study is presented. Results of an industry survey, Bruington (1990), show that mill metallurgists estimate the accuracy of estimating carbon concentration to be about +/- 10% to 15%. No correlation of the level of this estimate with sample method, carbon concentration levels, or plant size was detected.

Assume a CIL operation milled 100,000 tons over a one month period with a true head grade of 0.050 oz/ton and a recovery of 86%, resulting from a tailings assay of 0.007 oz/ton. Assume the first stage CIL tank contains 10 tons of carbon at a true grade of 150 oz/ton, and that the true inventory level is unchanged over the month. An error of 10% occurs in estimating carbon concentration, an error of 3% occurs in sample preparation, and an error of 7% occurs in assaying the carbon. If all three sources of error are in the same direction and occur only in the first tank, what are the resulting calculated recoveries and head grades?

VARIABLE	CASE		
	LOW	TRUE	HIGH
FEED (oz)	5000	5000	5000
TAILS (oz)	4300	4300	4300
POURED (oz)	700	700	700
NET TO INVENTORY (calc oz's)	+282	0	-282
RECOVERY (calc)	92%	86%	80%
HEAD GRADE (calc oz/ton)	0.053	0.050	0.047

Table 1. Changes in head grade, net inventory, and recovery by production balance with sampling uncertainty effects.

Table 1 illustrates the impact upon calculated inventory change, head grade, and recovery.

Obviously the errors will not always fall in the same direction, there will be some cancellation of errors. The important point is that the magnitude of the errors can be large and that they are cumulative. Also some of the errors may contain a bias.

CONCLUSIONS

Despite the uniform appearance of activated carbon, significant uncertainties exist for the sampling, sample preparation, and assaying steps of determining carbon (and gold on carbon) inventories. The distribution of carbon particle grades and the surface area to mass ratio of the carbon particles are factors contributing to this uncertainty. Sampling of countercurrent CIL/CIP systems is a complex situation involving pulp rheology, carbon particle shapes, and agitation dynamics. The effect of carbon inventory uncertainties upon a monthly production balance can be substantial.

REFERENCES

Adamson, R. J. "The Chemistry of the Extraction of Gold", Gold Metal. S. Africa.

Bruington, T. S., Unpublished Survey.

Davidson, R. J.,"The Mechanism of Gold Adsorption on Activated Charcoal", J. of S. Afr. Inst. of Min. and Met., 1974, pp 67- 76.

Gy, Pierre, "The Sampling of Particulate Materials", Elsevier.

Wright, P., Private Communication.